2015

Habitat Preferences of Adult Spotted Seatrout, Cynoscion nebulosus, in Lake Pontchartrain, Louisiana

Noelle Marie Bramer
Louisiana State University and Agricultural and Mechanical College

HABITAT PREFERENCES OF ADULT SPOTTED SEATROUT, *CYNOSCION NEBULOSUS*, IN LAKE PONTCHARTRAIN, LOUISIANA

A Thesis

Submitted to the Graduate Faculty of the
Louisiana State University and
Agricultural and Mechanical College
in partial fulfillment of the
requirements for the degree of
Master of Science

in

The Department of Oceanography and Coastal Sciences

by
Noelle Marie Bramer
B.S., University of Vermont, 2011
December 2015

This work is dedicated to my mother, father, sister, brother, and husband-to-be. Each has helped me find my joy in science. From the sands of Cape Cod to the shores I have yet to see, my family has been and always will be there to encourage my love of the sea and support my ambitions to explore it. With the love of my sweetheart, I know I will have the best company to share the views and the patience to tackle the science to fully appreciate them. Thank you.

ACKNOWLEDGEMENTS

First and foremost, I would offer my sincerest thanks to my advisor, Dr. James Cowan, Jr. for his encouragement, enthusiasm, and passion for Louisiana's fisheries. With his guidance, I grew immeasurably as a scientist, but most especially in my critical thinking skills. My future in oceanography will be the better for every bit of advice he has given me. I also thank my committee members, Dr. Sibel Bargu Ates and Dr. Sam Bentley, for their valuable advice and encouragement in my thesis research. I would like to express my heartfelt gratitude to David Nieland for his patience and humor in tackling this project. In addition, I owe a great deal of thanks to Gary Peterson for every boat ride across Lake Pontchartrain and for the best partner in overcoming every complication nature, man, or machine could throw our way. I would like to thank Thomas Blanchard for the compassionate and calm instruction of this graduate student in all water chemistry matters. For everything ArcGIS related, my sincere thanks goes out to Hampton Peele.

For their help, support, and funding for this research initiative, I would like to thank the Louisiana Department of Wildlife and Fisheries as well as the Louisiana Artificial Reef Program. I would also like to extend my thanks to the Lake Pontchartrain Basin Foundation for their invaluable help in understanding Lake Pontchartrain and for their dedication to its health.

I would like to thank every lab mate for taking the time to help me bounce around ideas, reminding me to take time to breathe, enjoy the process of learning with friends, find new viewpoints on my research, and have a real sense of community at LSU. I would especially like to thank Ashley Melancon and Jackie McCool for their energy and partnership. I would like to thank my family for nurturing my inner scientist with trips to the Boston Aquarium, whale watching, Blue Planet marathons, family trips to the

beach every summer, and so much more. Lastly, I'd like to thank my fiancé Nick for being the patient, kind, and caring support I needed to bring my spirits up and my typing fingers down. I cannot wait to celebrate our lives together! I am grateful to every person I have had the pleasure to meet along this journey and am so happy to have worked with this many talented people. My sincerest thanks go out to all of you.

TABLE OF CONTENTS

ABSTRACT

Spotted seatrout (*Cynoscion nebulosus*) are a highly sought after sportfish, making up over 90% of the recreational fishery in Louisiana. As a significant portion of every life history stage is spent within its natal estuary, it is an ideal bio-indicator of estuarine health. As one of the largest estuaries in Louisiana, Lake Pontchartrain represents one such supporting ecosystem. From November 2012 to April 2014 acoustic tagging of individual fish, a lake-wide receiver array, and ArcGIS mapping software were utilized to determine the spatial distribution of spotted seatrout within the lake. Receivers were placed in representative locations including man-made and natural structures. The prevalence of fish "hot spots," between these locations were compared and thus bottom habitat preferences examined. Water quality parameters, including water temperature, dissolved oxygen, salinity, turbidity, colored dissolved organic matter, chlorophyll *a*, and hydrocarbons are biochemical factors with the potential to drive the species' distribution. As such, a flow-through water sampling system was used to obtain monthly "snapshots" of conditions across the lake. Combined with presence/absence receiver data, any water quality preferences were examined. Overall, spotted seatrout showed a distinct preference for the central, central-north, and northeastern areas of the lake. It was also noted, however, that the species showed no distinct preference for a single bottom type, but utilized every habitat in the lake. With respect to water quality, salinity and temperature were determined to be the most important features for the species' distribution. According to the generalized linear model produced, every unit increase in salinity (ppt) improved the odds of observing a spotted seatrout by almost five times while a unit increase in temperature improved the odds by approximately 11 percent. The above results are in agreement with the extensive literature on the species and its

relationship to bottom types and water chemistry, but still leave questions of habitat use/preference in relation to the potential influences of life stage adaptations, availability of food resources, food web dynamics, or major environmental events. Future research in these areas will serve as important additions to the ecosystem-based strategy of management for this valuable Louisiana fishery.

CHAPTER 1: GENERAL INTRODUCTION

FISHERIES AND SUPPORTING ESTUARIES

Fisheries in the Gulf are renowned for their productivity, with Louisiana waters alone accounting for 75% of the annual fishery landings in the US (Cowan et al. 2008). As estuarine-resident and estuarine-dependent species constitute over 50% of this annual yield, estuaries are widely considered the most critical ecosystem for their success (Cowan et al. 2008). Along the US Gulf, there are over 200 such estuaries from the coast of Florida to the Lower Laguna Madre in Texas (Blanchet et al. 2001). According to the Cooperative Gulf of Mexico Estuarine Inventory, over 5.2 million hectares in this region have been designated as estuarine habitat (Blanchet et al. 2001). Lake Pontchartrain, located within a 44,000 km^2 basin, represents one of the largest and most complex fishery-supporting estuaries in Louisiana. Collectively this basin encompasses sixteen Louisiana parishes, four Mississippi counties, five river systems (Amite, Tickfaw, Tchefuncte, Tangipahoa, and Pearl) and three estuaries (Lake Maurepas, Pontchartrain, and Borgne) (Penland et al. 2002; Flocks et al. 2009). Lake Pontchartrain alone supports over 126 species of fish and while it is a highly productive ecosystem, it also exhibits a great deal of variation seasonally and annually in species composition and population sizes due to a unique combination of influences, including physical (bathymetry and geography), chemical (rivers and marine connections), and biological (natural food web and fishing pressures) (Cowan et al. 2008; Hastings 2009; Cowan et al. 2013).

Within its drainage basin, Lake Pontchartrain is surrounded by natural estuarine marshes, cypress swamps, bottomland hardwood forests, and bayous. Natural stressors include wetland loss, subsidence, saltwater intrusion, shoreline erosion, hurricanes, and flooding (Penland et al. 2002). Anthropogenic features include the lake-spanning central

causeway, artificial reefs, powerline structures, train trestle bridge, docks, pipelines and the Bonnet Carré Spillway. Man-made stressors from these sources include Spillway openings as well as runoff from agriculture, industrial, and commercial properties. With a rich assemblage of estuarine species, a primary benefit of the lake has historically been valuable fisheries, particularly for brown shrimp (*Farfantepenaeus aztecus*), white shrimp (*Litopenaeus setiferus*), blue crabs (*Callinectus sapidus*), red drum (*Sciaenops ocellatus*), and especially spotted seatrout (*Cynoscion nebulosus*) (Penland et al. 2002; Hastings 2009). Considering the influential features of the lake's watershed, human population (over 1.5 million people), and valuable estuarine species, concerns over environmental quality and its influence on the fisheries in particular has become important to Louisiana's Department of Wildlife and Fisheries (LDWF), Louisiana State University (LSU), the United States Geological Survey (USGS), and the Lake Pontchartrain Basin Foundation (LPBF) (Penland et al. 2002).

SPOTTED SEATROUT

One of the most important species in Lake Pontchartrain is the spotted seatrout. As the most sought after coastal sportfish in the US, demand by fishermen for this species generates an annual national yield of over 35 million fish with the majority (50-60%) caught in Louisiana (Callihan 2011). In addition to their economic importance, spotted seatrout serve as an indicator species for estuarine health (Bortone 2003). Considered a non-migratory species with a lifespan up to 10 years, population responses to short-term ecological changes are pronounced, making the species an ideal bio-indicator of estuarine conditions (Mazzotti et al. 2008). At each stage of its life, individuals occupy specific zones within their natal estuary (Mazzotti et al. 2008). With each stage's ecological requirements well documented, the distribution and abundance of each can serve as a

marker for habitat quality, water quality, and prey abundance within the ecosystem (Bortone 2003). Generally, adult spotted seatrout prefer shallow, warm estuaries with marsh edges adjacent to open water (Bortone 2003). In general, adults utilize a wide variety of habitats within the estuary, including seagrass beds, oyster reefs, sand/mud bottom, and manmade structures while juveniles are more limited to the marsh edge (Hill 2005).

While adult spotted seatrout are found most often in large regions of shallow (3-6m), brackish (15-28 ppt) water with a stable temperature regime (16-32^{o}C) for successful growth, maturation, spawning, and survival of larvae, they have proven to be remarkably adaptable as a species (Kostecki 1984; Mazzotti et al. 2008). They occupy a wide geographic range, extending south from Cape Cod, MA and across the Gulf Coast to Mexico, exhibiting a highly flexible physiology with respect to the biochemical variables they encounter (Lassuy 1983; Blanchet et al. 2001). As an example, extreme tolerances exhibited by the species have been well documented for both salinity (5 to 45ppt) and temperature (4-33^{o}C) (Lassuy 1983; Kostecki 1984; Blanchet et al. 2001; Hill 2005). In general, the social, economic, and scientific importance of spotted seatrout has produced a great deal of literature covering the life history, physiology, water quality requirements, and habitat preferences in an effort to enhance management (Nieland et al. 2002; Neahr et al. 2010). For effective management of this species and its associated fishery, natural resource managers must focus on building a better understanding of which features represent optimal conditions for the spotted seatrout population within their respective estuary.

STUDY OUTLINE

The following chapters of this thesis provide information about the habitat use patterns exhibited by spotted seatrout through acoustic telemetry and with respect to bottom features and water quality gradients within Lake Pontchartrain. This new study, therefore, is an extension of a previous study that focused on the spatial ecology of spotted seatrout within Lake Calcasieu, another Louisiana estuary. With 90 acoustic receivers placed strategically across a large estuarine system and over 200 tagged individuals, this research initiative represents a unique and complex system for assessing habitat preference for spotted seatrout in Louisiana. For this study, bottom type was determined through literature review, imaging with a Humminbird® system, and physical sampling. Biochemical characteristics were assessed with stationary water sampling stations and monthly sampling transects completed with the Dataflow system, a high resolution water quality data acquisition and mapping instrument (Madden 2013; Stachelek and Madden 2015). Bottom types assessed included man-made and naturally occurring features. Water quality characteristics assessed include salinity, dissolved oxygen, temperature, turbidity, chlorophyll *a* concentration, CDOM, and hydrocarbons. Each chapter discusses how bottom features and water quality, respectively, may be influential forces in the distribution of spotted seatrout in Lake Pontchartrain.

LITERATURE CITED

Baltz, D.M., C. Rakocinski, and J.W. Fleeger. 1993. Microhabitat use by marsh-edge fishes in a Louisiana estuary. Environmental Biology of Fishes 36:109-126.

Beck, M.W., K.L. Heck Jr., K.W. Able, D.L. Childers, D.B. Eggleston, B.W. Gillanders, B. Halpern, C.G. Hays, K. Hoshino, T.J. Minello, R.J. Orth, P.F. Sheridan, and M.P. Weinstein. 2001. The identification, conservation, and management of estuarine and marine nurseries for fish and invertebrates. Bioscience 8:633-341.

Blanchet, H. M.VanHoose, L. McEachron. B. Miller, J. Warren, J. Gill, T. Waldrop, J. Waller, C. Adams, R.B. Ditton, D. Shively, and S. Vanderkooy. 2001. The spotted seatrout fishery of Mexico, United States: A regional management plan. Gulf States Marine Commission.

Bortone, S.A. 2003. Biology of the Spotted Seatrout. CRC Press, Boca Raton, Florida.

Callihan, J.L. 2011. Spatial ecology of adult spotted seatrout, Cynoscion nebulosus, in Louisiana Coastal Waters. Dissertation. Louisiana State University.

Cowan, J.H., C.B. Grimes, and R.F. Shaw. 2008. Life history, history, hysteresis, and habitat changes in Louisiana's coastal ecosystem. Bulletin of Marine Science 83:197-215.

Cowan, J.H., A. Yáñez-Arancibia, P. Sánchez-Gil, and L.A. Deegan. 2013. Estuarine Nekton. Estuarine Ecology Chapter 13. John Wiley & Sons, Inc. Hoboken, New Jersey.

Flocks, J., M. Kulp, J. Smith, and S.J. Williams. 2009. Review of the geologic history of the Pontchartrain Basin, Northern Gulf of Mexico. Journal of Coastal Research. 54: 12-22.

Hastings, R.W. 2009. The Lakes of Pontchartrain. University Press of Mississippi.

Hill, K. 2005. Spotted seatrout (*Cynoscion nebulosus*). Smithsonian Marine Receiver at Fort Pierce. Retrieved from: ‹http://www.sms.si.edu/irlspec/Cynosc_nebulo.htm›

Kostecki, P.T. 1984. Habitat suitability index models: Spotted Seatrout. Washington DC: Fish and Wildlife Service US Department of the Interior.

Lassuy, D.R. 1983. Species profiles: Life histories and environmental requirements (Gulf of Mexico) spotted seatrout. National Coastal Ecosystems Team.

Madden, C. 2013. Personal communication. South Florida Water Management District. West Palm Beach, Florida, cmadden@sfwmd.gov.

Mazzotti, F.J., L.G. Pearlstine, T. Barnes, S.A. Bortone, K. Chartier, A.M. Weintstein, and D. DeAngelis. 2008. Stressor-response model for the spotted seatrout (*Cynoscion nebulosus*). Institute of Food and Agricultural Sciences, University of Florida.

Neahr, T.A., G.W. Stunz, and T.J. Minello. 2010. Habitat use patterns of newly settled spotted seatrout in estuaries of the north-western Gulf of Mexico. Fisheries Management and Ecology 17:404-413.

Nieland, D.L., R.G. Thomas, and C.A. Wilson. 2002. Age, growth, and reproduction of the spotted seatrout in Barataria Bay, Louisiana. Transactions of the American Fisheries Society 131:245-259.

Penland, S., A. Beall, and J. Waters, eds. 2002. Environmental atlas of the Lake Pontchartrain basin. Lake Pontchartrain Basin Foundation, New Orleans.

Stachelek, J. and C.J. Madden. 2015. Application of inverse path distance weighting for high-density spatial mapping of coastal water quality patterns. International Journal of Geographical Information Science. 00:1-11.

CHAPTER 2: HABITAT USE OF ADULT SPOTTED SEATROUT IN RELATION TO BOTTOM TYPE WITHIN LAKE PONTCHARTRAIN, LOUISIANA

INTRODUCTION

The spotted seatrout (*Cynoscion nebulosus*) is a highly sought after sportfish, encompassing an estimated 90% of the total recreational fishery harvest in Louisiana alone (MacRae and Cowan 2010). Landings in Louisiana waters reached over 9 million pounds in 2000, and in Texas spotted seatrout have been listed as the species targeted by the majority of recreational fisherman (Nieland et al. 2002; Bortone 2003; McDonald et al. 2013). In addition to their economic importance, spotted seatrout serve as an indicator species for estuarine health (Bortone 2003). As a non-migratory species, whose ecological requirements are well documented at each life stage and having a lifespan of up to 7-10 years, the distribution and population size can be used as indicators for estuarine health and evidence ecological responses to short-term and long-term ecological stressors on the system (Mazzotti et al. 2008). Understanding the habitat use patterns exhibited by an estuary's spotted seatrout population provides insight into the larger picture of estuarine health and can provide managers with evidence necessary to make informed decisions to protect, enhance, and promote this valuable fishery (Nieland et al. 2002; Neahr et al. 2010).

In assessing habitat use, it was also noted that a matrix of habitats may be more important than the simple presence/absence of any one type (MacRae and Cowan 2010). As coastal systems, estuaries represent a matrix of possible habitats including soft and hard substrates, seagrass beds, marshes (freshwater and saltwater), reefs and in the broadest perspective, the link between the marine waters of the shallow continental shelf and the freshwaters of the rivers/bayous (Cowan et al. 2008; Cowan et al. 2013).

Through the unique combination of physical (bathymetry and geography), chemical (continuum from freshwater rivers to marine connections), and biological (estuarine residents and temporary users) connections each estuary encompasses a highly complex ecosystem (Cowan et al. 2008, Cowan et al. 2013). The scale/region within which one evaluates a species' use of the available habitats must therefore be defined, especially as it has a strong impact on determinations of richness, variability, and any observed patterns (Blanchet et al. 2001). For this purpose, the specific estuarine conditions within Lake Pontchartrain are to be examined.

As one of the largest estuaries in the Gulf of Mexico, Lake Pontchartrain provides habitat for a rich assemblage of estuarine-dependent species, with commercial and recreational fisheries including brown shrimp, white shrimp, blue crabs, red drum, and for the focus of this research, the spotted seatrout (Penland et al. 2002; Hastings 2009). The high productivity of Louisiana's coastal waters is recognized nationally, with annual fishery yields of over 1 billion pounds, accounting for more than 70% of the commercial catch in the US Gulf of Mexico (Bortone 2003). Contributing factors to the health of the lake include the naturally occurring estuarine marshes (salt, brackish, and marine), bottomland hardwood forests, swamps, and bayous. Deleterious impacts on water quality have been a product of pollution by agricultural, urban, and industrial runoff as well as openings of the Bonnet Carré Spillway (Mallin et al. 1999). Concerns over environmental quality have taken center stage for this lake through federal, state, community, and higher education organizations (Penland et al. 2002). Understanding which habitats are most beneficial to spotted seatrout enables managers to more effectively address concerns for the health of both this coastal waterbody and its dependent species.

The waterbodies within the Lake Pontchartrain Basin are very shallow embayments, of which Lake Pontchartrain is the deepest at around 5m and has the largest surface area at 1,630km^2 (Miller et al. 2005). As the centerpiece, Lake Pontchartrain exhibits sediment characteristics typical of shallow coastal waters. Bathymetric surveys show a flat bottom trend with the shorelines encompassing the most relief (Flocks et al. 2009a). The topmost meter of sediment is characterized by brown-grey mud, highly altered through bioturbation and wind-driven resuspension (Flocks et al. 2009a; Reed and FitzGerald 2009). Tidal circulation also acts to deposit more silts on the margins of the lake with clays in the center. In general, bottom sediment contains silt (58%), clay (34%), and organic content (3-9%) (Reed and FitzGerald 2009; Roy and White 2012). Sediment containing ≥50% sand occurs on the northeastern and eastern boundaries of the lake. Sediment composition in tidal channels (Pass Manchac, Chef Menteur, and the Rigolets) and the Bonnet Carré Spillway contain a larger proportion of coarse sediment (Flocks et al. 2009a; Reed and FitzGerald 2009). The resulting character of Lake Pontchartrain's sediment is not limited to natural factors alone. Historically, large shell beds were found along the lake bottom, but dredging has left only very restricted, remnant patches (Flocks et al. 2009a). In addition, hydraulic dredging for fill has left four large holes in the lake's floor along the New Orleans shoreline (Penland et al. 2002, Hastings 2009).

Soft bottom sediments, which make up the majority of the lakebed, provide not only habitat but also food for the various benthic, burrowing, and demersal species inhabiting the lake (Hastings 2009). While this particular bottom type is the most common, it was historically the shell beds, that is, hard substrate, which provided the most dynamic and beneficial bottom habitat (Lopez 2004; Whitmore 2006; Hastings 2009). Past shell reefs were extensive across the lakebed, consisting largely of the clam

Rangia cuneata. Hard substrates like the reefs provide attachment sites for sessile organisms, providing a food base for benthic crustaceans and invertebrates. The availability of hard substrates is assumed to be an ecological food web driver, thus the Lake Pontchartrain Artificial Reef Working Group organized in 2009 to have five artificial reefs built within the lake (Lopez 2004; Whitmore 2006; Hastings 2009). Five former oil and gas drilling sites with remnant shell pads were chosen for the placement of restoration materials (Whitmore 2006). Materials for the restoration included crushed limestone and two forms of concrete ReefBalls^{TM}, 3-ft tall "pallet balls" and 2-ft tall "bay balls" (Lopez 2004; Whitmore 2006). The first site (L1) was completed in 2001 and consisted of 3,200 yards of crushed limestone placed near Lakefront Airport (Lopez 2004). In 2003, three additional sites (H1, H4, and H3) were completed with 180, 208, and 212 reef balls, respectively (Lopez 2004). The final site (N1) was completed in 2004 with 80 reef balls.

While man-made reefs have been used to modestly recreate the historically occurring shell beds, other manmade structures have inadvertently been providing hard substrates around the lake as well (Hastings 2009). Crab traps, posts for docks/piers, and rock piles are such structures, however, the most notable man-made additions to the lake are the Pontchartrain Causeway and Interstate-10 bridges, each with an extensive set of supporting concrete pilings (Hastings 2009). Significant alterations to the shoreline have occurred as well. The extensive Lake Pontchartrain shoreline (125 mi) includes both natural and man-made types (Penland et al. 2002). Natural shorelines include marshes, cypress swamps, and lakeshore camps along the western and eastern boundaries (Hastings 2009). Man-made shoreline protection materials including riprap, bulkhead, and concrete seawalls that have been installed along the southern boundary and mixed with natural shoreline types along the northern boundary (Flocks et al. 2009a; Hastings

2009). Overall, at least 30% of the lake's shoreline has been converted to hard substrate with the development of urban regions (New Orleans, Metairie, Kenner, Slidell, and Mandeville) and 70% remains as natural shoreline (Hastings 2009). Large beds of submerged aquatic vegetation (SAV) were also widespread historically, providing habitat to the same species that utilize the shoreline regions today.

Historically, SAV was abundant along the entire shoreline and largely consisted of native species including American eelgrass (*Vallisneria Americana*), widgeongrass (*Ruppia maritima*), southern naiad (*Najas guadalupensis*), and clasping leaf pondweed (*Potamogeton perfoliatus*) (Duffy and Baltz 1998; Poirrier et al. 2009). The spatial extent available for colonization by these species is largely limited by water clarity, which can change with water depth and wind mixing (Poirrier et al. 2009). With increasing municipal and agricultural runoff, water quality in the lake suffered and the SAV beds declined by 90% from 1950 to 1985 (Duffy and Baltz 1998). In 2000, a lakewide survey from shoreline to the 2-m depth mark was conducted, indicating abundant and continuous beds along the northshore with *R. maritima* and *V. Americana* as the most abundant species and scattered patches from Lincoln beach west to Jahncke Canal along the southshore (Penland et al. 2002). Unlike the simple, soft-bottom type found in most littoral and deeper portions of the lake, grassbeds provide structural complexity, refuge from predators, and food resources to young fish species (Duffy and Baltz 1998). With grassbeds declining, natural resource managers have tried to restore estuarine plants to maintain fisheries production (Cho and Poirrier 2005). Overall, the influence of bottom habitats on estuarine health have been a focal point for developing a better understanding of spotted seatrout and the essential habitat characteristics critical for maintaining this extremely valuable fishery resource. Thus the value of research

focused to this task cannot be understated and the resulting information essential for natural resource managers of Louisiana.

METHODS

Study Area

Lake Pontchartrain is a shallow estuary (4m average depth) covering 1,630 km^2 within the Lake Pontchartrain Basin (Penland et al. 2002; Flocks et al. 2009b). Five river systems, including the Amite, Tickfaw, Tchefuncte, Tangipahoa, and Pearl, feed into Lake Pontchartrain and two additional estuarine waterbodies (Flocks et al. 2009b). West of the lake are Lake Maurepas and the Mississippi River, while to the east is Lake Borgne and the Pearl River. To the north are uplands, and to the southeast are marine connections to Breton, Chandeleur, and Mississippi Sound (Georgiou et al. 2009). With its surrounding watershed, Lake Pontchartrain represents the confluence of two conflicting forces, that is, the human demands for natural resources and the resiliency of an ecologically valuable coastal waterbody (Wu 2005, O'Connell et al. 2013).

Telemetry

Regions within Lake Pontchartrain where spotted seatrout are reported to occur in large numbers as well as waterways connecting to other waterbodies/rivers were chosen for the placement of stationary acoustic receivers. For this study, the lake boundary (visible as a light blue line around the edge of the lake in Figure 2.1) included receivers (75 out of 90 total) for assessing the distribution of spotted seatrout in the lake. Each receiver has a range of 500 to 600 meters under normal lake conditions, but this range can be reduced when turbidity is high (Melancon 2015; Vemco 2015). Acoustic tags were surgically implanted into the peritoneal cavity of adult spotted seatrout in the fall of

2012 (11/15-11/18), spring of 2013 (5/20-5/24), fall of 2013 (11/04-11/08), and spring of 2014 (4/21-4/23). In total, 211 fish were tagged (18 males, 176 females, 17 unknown). Additional data collected included total length (TL in cm), standard length (cm), and total weight (kg). A V9 acoustic tag was implanted in fish with a TL of less than 39.37cm, a V13 tag for fish from 39.37 to 49.53cm, or a V13TP for fish over 49.53cm. Each acoustic tag emits a signal at 69 kHz at random intervals. Expected battery life is 8 months for the V9 tag and 1.5 years for the V13 and V13TP. Each receiver records the time a signal is received, the fish's ID number, and the data pertaining to the fish tagged. The data for fish count (number of fish visiting a receiver) and detections (number of received signals), was then edited to remove the 1st week of movement after tagging, false detections, and continuous detections at a single receiver. The map below shows receiver locations in the lake.

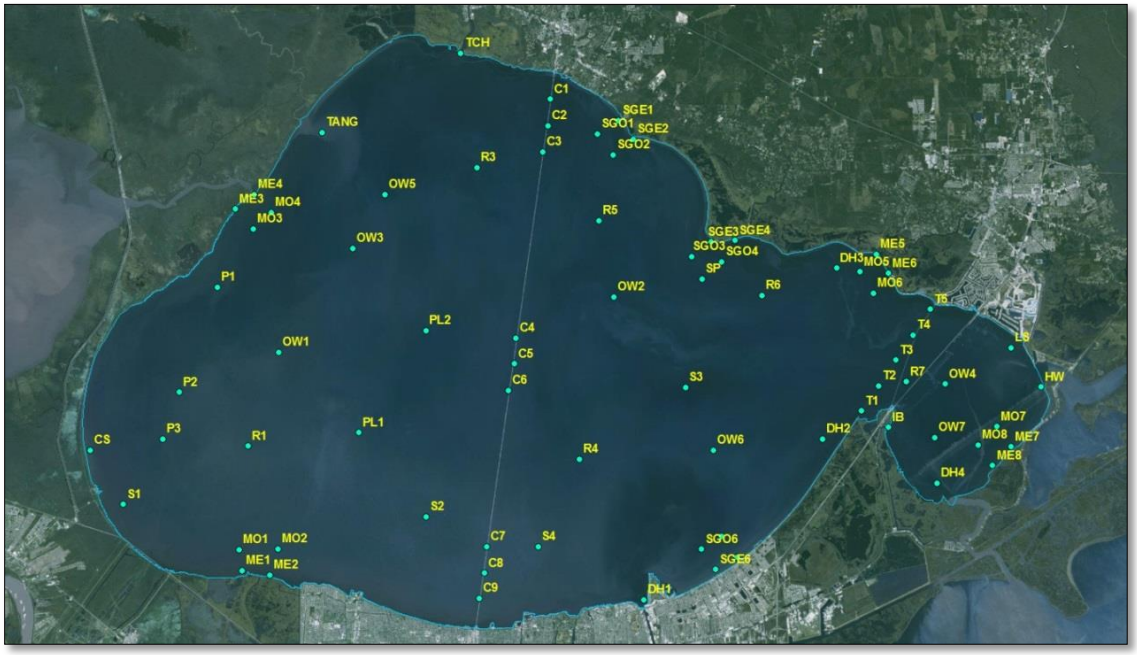

Figure 2.1 Map of receivers within Lake Pontchartrain, noted in yellow, and the study boundary, noted as a pale blue outline.

For the placement of acoustic receivers, locations were chosen to represent a variety of habitat types in the lake. Manmade features include the central causeway (C), reefs (R), powerline structures (P), shell pads (S), single piling (SP), train trestle bridge (T), hospital wall (HW), deep holes (DH), and pipeline (PL). Natural features include cypress swamp (CS), lakeshore (LS), marsh edge (ME), marsh open (MO), seagrass beds edge (SGE), seagrass beds open (SGO), open water (OW), Tangipahoa River entrance (TANG), Tchefuncte River entrance (TCH), and Irish Bayou entrance (IB). These 75 receivers will be included in the analyses for spotted seatrout distribution discussed below.

Monthly Hot Spot Analysis

Fish detections from January 2013 through December 2014 were assessed using ArcGIS. Each dataset included receiver locations and the associated count of individual fish and number of detections. To complete the spatial analyses, points were projected using a Lambert conformal conic projection (LCC), a projection used for the State Plane Coordinate System with the North American Datum 1983 (2011) as its reference point (ArcGIS Resources 2013b, ArcGIS Resources 2013d, and National Geodetic Survey 2015). As the focus of this mapping is Lake Pontchartrain, the State Plane coordinate system designated as Louisiana South was chosen. This transformation allows a curved surface to be portrayed on a flat surface while minimizing distortion between geodetic (curved) and grid (flat) distances (ArcGIS Resources 2013d; National Geodetic Survey 2015).

Analyses were conducted to determine the areas of different spatial distributions of fish in the lake as well as those receivers used most often by spotted seatrout. This analysis uses receiver locations to identify statistically significantly different hot spots

with high fish counts/high use from cold spots (low fish counts/low use) present in the data. For each receiver, this analysis calculates the Getis-Ord Gi* statistic. The Getis-Ord Gi* statistic produces a Z-score and P-value for each receiver by comparing the spatial clustering of values (fish counts and number of detections) to a hypothetical random distribution (ArcGIS Resources 2014). For this tool, the null hypothesis is that values (counts and detections) are randomly distributed. A data point with a high Z-score and low P-value indicates a hot spot while a low Z-score and low P-value indicates a cold spot. The sum of the fish counts/detections for a neighborhood of receivers is compared proportionally to the sum of all receivers' fish counts/detections, and therefore must be significantly higher (hot spot) or lower (cold spot) than the expected sum to determine that the difference is not due to random chance (ArcGIS Resources 2014). The Getis-Ord Gi* statistic as calculated for each receiver is depicted in Figure 2.2 below.

The Getis-Ord local statistic is given as:

$$G_i^* = \frac{\sum_{j=1}^{n} w_{i,j}x_j - \bar{X}\sum_{j=1}^{n} w_{i,j}}{S\sqrt{\frac{\left[n\sum_{j=1}^{n} w_{i,j}^2 - \left(\sum_{j=1}^{n} w_{i,j}\right)^2\right]}{n-1}}} \quad (1)$$

where x_j is the attribute value for feature j, $w_{i,j}$ is the spatial weight between feature i and j, n is equal to the total number of features and:

$$\bar{X} = \frac{\sum_{j=1}^{n} x_j}{n} \quad (2)$$

$$S = \sqrt{\frac{\sum_{j=1}^{n} x_j^2}{n} - \left(\bar{X}\right)^2} \quad (3)$$

The G_i^* statistic is a z-score so no further calculations are required.

Figure 2.2 Computational notes for Hot Spot Analysis Getis-Ord Gi* statistic (ArcGIS Resources 2014).

In order to set an appropriate distance by which to establish the neighborhood of values, an incremental spatial autocorrelation function was utilized (ArcGIS Resources

2013a). In analyzing spatial autocorrelation between the receiver's counts of fish and detections, the tool produces a line graph with Z-scores associated with each distance (ArcGIS Resources 2013a). A peak in the Z-scores indicates a distance wherein the intensity of spatial clustering is most pronounced. The first peak is chosen as the appropriate search distance for establishing the points to be considered within a neighborhood for hot spot analysis (ArcGIS Resources 2013a). As the receivers within the lake are hydrologically connected, the conceptualization of the spatial relationship between each was designated within ArcGIS as a zone of indifference (ArcGIS Resources 2013c). This parameter specifies that once the critical distance for defining a neighborhood is exceeded, the degree of influence by points further away decreases sharply (ArcGIS Resources 2013c). By using this conceptualization, there is a set distance defining a neighborhood, but there are no sharp boundaries eliminating the potential influence of neighboring points (ArcGIS Resources 2013c).

Resulting hot spots are assigned colors associated with the final Z-score for each receiver. Receivers that have been found to be spatially statistically significant at an alpha level of 0.01 are noted in red, at a level of 0.05 in dark orange, and at a level of 0.1 in light orange. Cold spots found significant at the 0.01 level are noted in dark blue, at the level of 0.05 in light blue, and at the level of 0.1 in green. Receivers not found to be spatially statistically significant are noted in yellow. For the purpose of determining the areas used most often by spotted seatrout and those used the least, all receivers categorized as a hot spot or cold spot have been determined using a significance level of 0.1. By utilizing this alpha level, larger areas of use rather than more restrictive areas may be identified as significant. As a highly mobile species, this is a more appropriate significance level to capture regional preferences. In the maps provided for visualizing hot spots and cold spots, the color scheme is maintained for the significance levels

associated with each receiver. In addition, Inverse Distance Weighting (IDW) was utilized so that areas containing hot spots are highlighted in white and greyscale (through interpolation), with cold spots or non-significant areas appearing as black.

Bottom Habitat Characterization Surveys

A Humminbird® 1198C SI imaging system was used to produce a visualization of bottom-type using side-scan sonar imaging across an area covered by each receiver chosen for further evaluation. To image bottom features, transects were oriented North-South at vessel speeds ranging from 3 to 9 km h^{-1}. Each transect was approximately 240m in length, with one line positioned along a centerline over the receiver. Two transects were located on the eastern side and two on the western side of the receiver. The overall area assessed covered approximately 5.76 x 10^4 square meters around each receiver. To ground-truth the visualizations of bottom type, four bottom samples were collected using an Ekman bottom grab sampler (Figure 2.3, A and B) at each chosen receiver. Each sample was taken approximately 60m from the receiver at each cardinal direction. Sediment was photographed and assessed for defining features.

Figure 2.3 (A) Ekman bottom grab sampler pre-deployment and (B) post-deployment.

RESULTS

Hot Spot Analysis-Winter

Hot spots and cold spots were assessed for the winter months (December, January, and February). Images for the results recorded for December 2013 (Figure 2.4, A and B) and December 2014 (Figure 2.4, C and D) are depicted below. In December 2013, hot spots for fish counts occurred in the central, northeastern, and southeastern areas of the lake. Cold spots for fish counts were identified in the western area. Hot spots for detections occurred only in the southeastern area. Cold spots were limited to a single receiver in the northwest. For December 2014, the hot spots were located in the central-north area for both counts and detections.

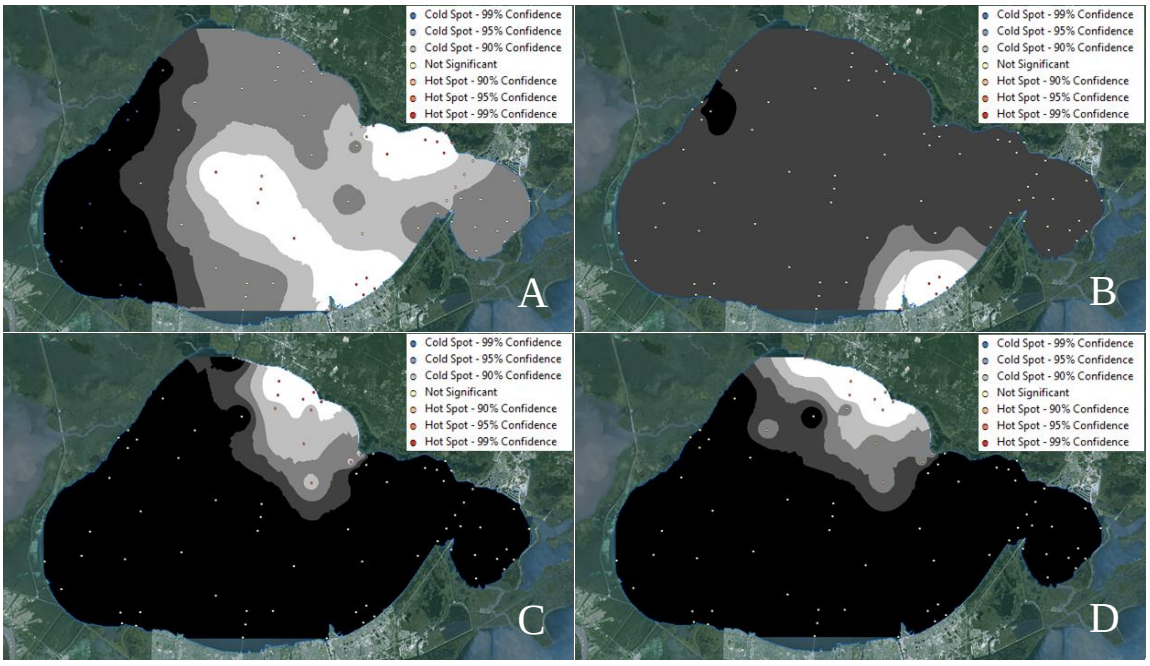

Figure 2.4 Hot spot analysis for (A) fish counts in December 2013, (B) detections in December 2013, (C) fish counts in December 2014 and (D) detections in December 2014.

Images for the results recorded for January 2013 (Figure 2.5, A and B) and January 2014 (Figure 2.5, C and D) are depicted below. For January 2013's fish counts, hot spots occurred in the central-north area, while cold spots occurred in the easternmost

area of the lake, as depicted below. Hot spots for detections were isolated to the center causeway. In January 2014, however, high fish counts occurred in the northeast to the southeast swath of the lake, while cold spots occurred in the eastern and western areas. The hot spots for detections occurred only in the northeastern corner, with cold spots in the east.

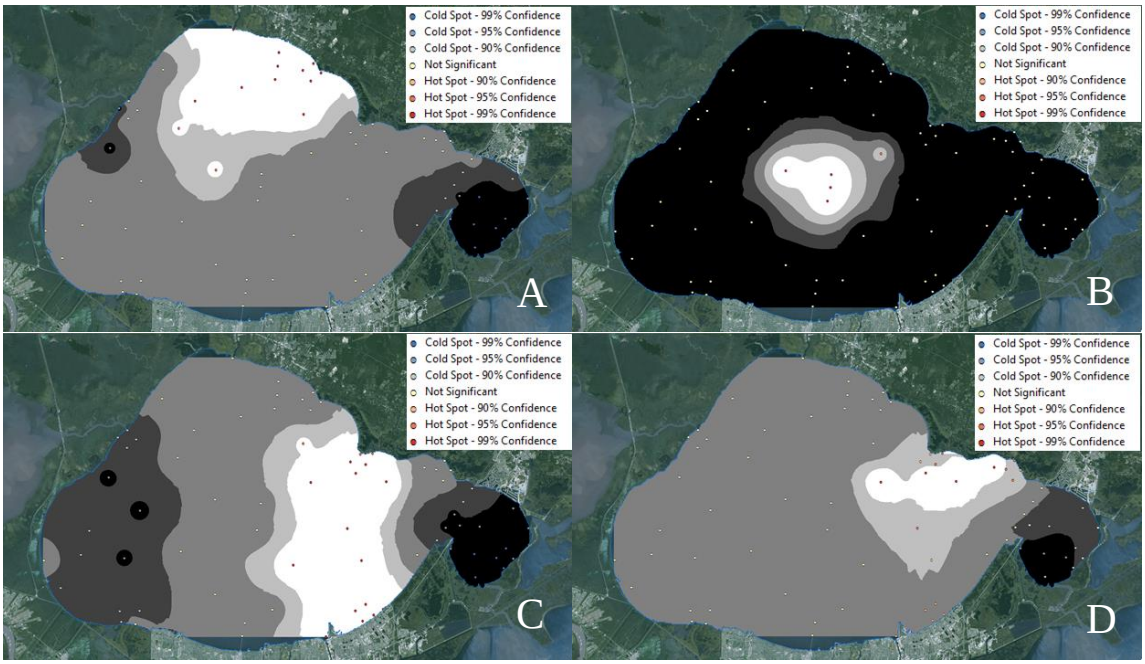

Figure 2.5 Hot Spot Analysis for (A) fish counts in January 2013, (B) detections in January 2013, (C) fish counts in January 2014 and (D) detections in January 2014.

Finally, images for the results recorded for February 2013 (Figure 2.6, A and B) and February 2014 (Figure 2.6, C and D) are depicted below. For February 2013, hot spots for both counts and detections included the central-north area, but cold spots were isolated to the easternmost areas of the lake. An additional area of high fish detections were noted in the northeast corner. For February 2014, the patterns of high counts and detections in the northeast and cold spots in the easternmost area were identified again. Cold spots for fish counts were also identified in the westernmost area of the lake.

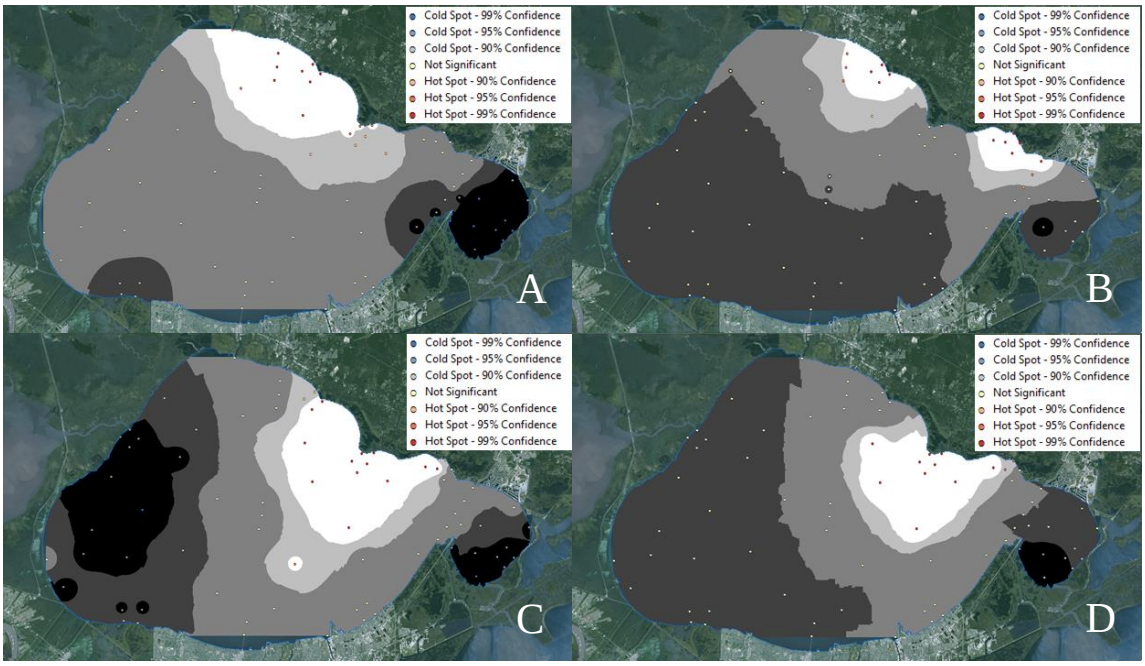

Figure 2.6 Hot Spot Analysis for (A) fish counts in February 2013, (B) detections in February 2013, (C) fish counts in February 2014 and (D) detections in February 2014.

Hot Spot Analysis-Spring

Hot spots were identified for spring months of March, April, and May. For March 2013 (Figure 2.7, A and B) and March 2014 (Figure 2.8, A and B), hot spots for fish counts and detections were identified in the central north and northeastern area of the lake. Cold spots identified for both years included the easternmost area and southwest corner, though for 2013 these were restricted to fish counts. Additionally, the center-south area was identified as a cold spot for fish counts in March 2014.

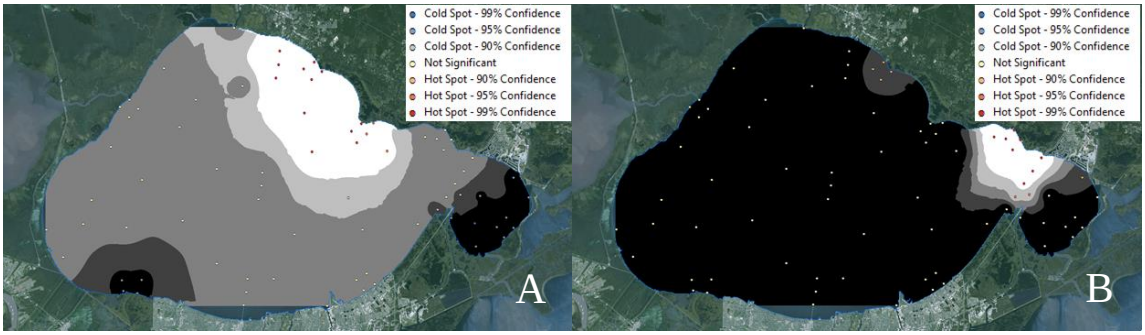

Figure 2.7 Hot Spot Analysis for (A) fish counts in March 2013 and (B) detections in March 2013.

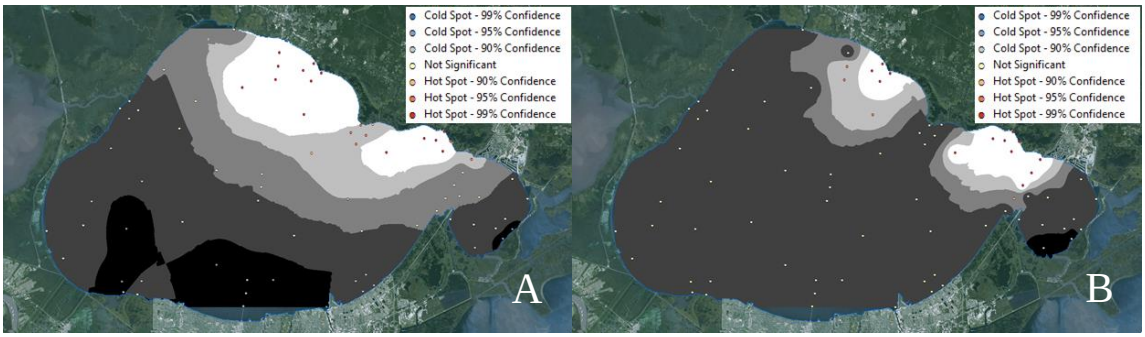

Figure 2.8 Hot Spot Analysis for (A) fish counts in March 2014 and (B) detections in March 2014.

Images for the results recorded for April 2013 (Figure 2.9, A and B) and April 2014 (Figure 2.10, A and B) are depicted below. For April, hot spots for fish counts were found in the eastern and northeastern areas of the lake for both years. These areas were also identified as hot spots for detections in both years, but limited to a smaller area for April 2013. Cold spots for fish counts in 2013 were limited to several isolated areas in the southwest, central, and center-south areas of the lake. For April 2014, the southwest corner contained cold spots for both counts and detections. Additional cold spots for counts occurred in the northwest and southeast areas, while additional cold spots for detections were located only in the southeast area.

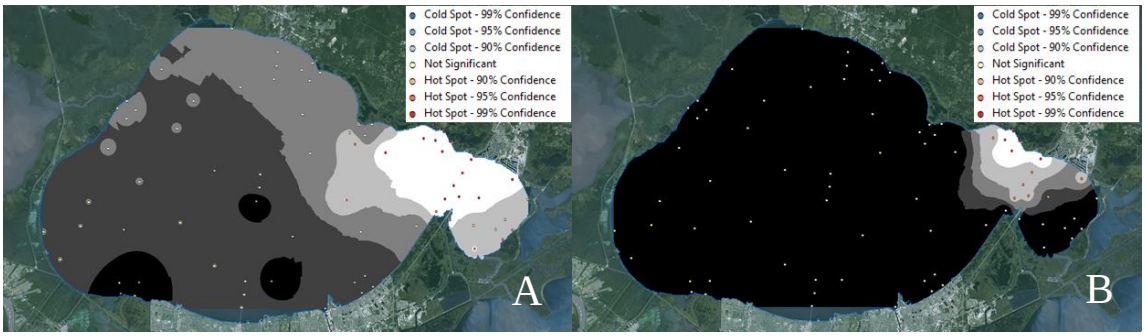

Figure 2.9 Hot Spot Analysis for (A) fish counts in April 2013 and (B) detections in April 2013.

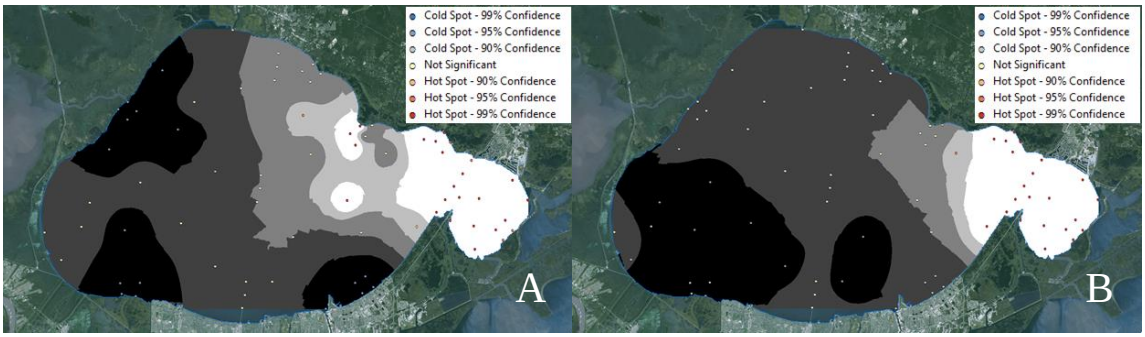

Figure 2.10 Hot Spot Analysis for (A) fish counts in April 2014 and (B) detections in April 2014.

Finally, for May 2013 (Figure 2.11, A and B), hot spots for fish counts occurred in the easternmost area and the northeast corner of the lake, a characteristic shared by fish counts in May 2014. In May 2014 (Figure 2.11, C and D), however, this area of hot spots covers nearly the entire eastern half of the lake. Cold spots for counts in 2013, occurred only in the northwestern area, but in 2014 occurred across the western and central area of the lake. In general, the pattern of hot and cold spots was similar when considering either counts or detections in May of 2014.

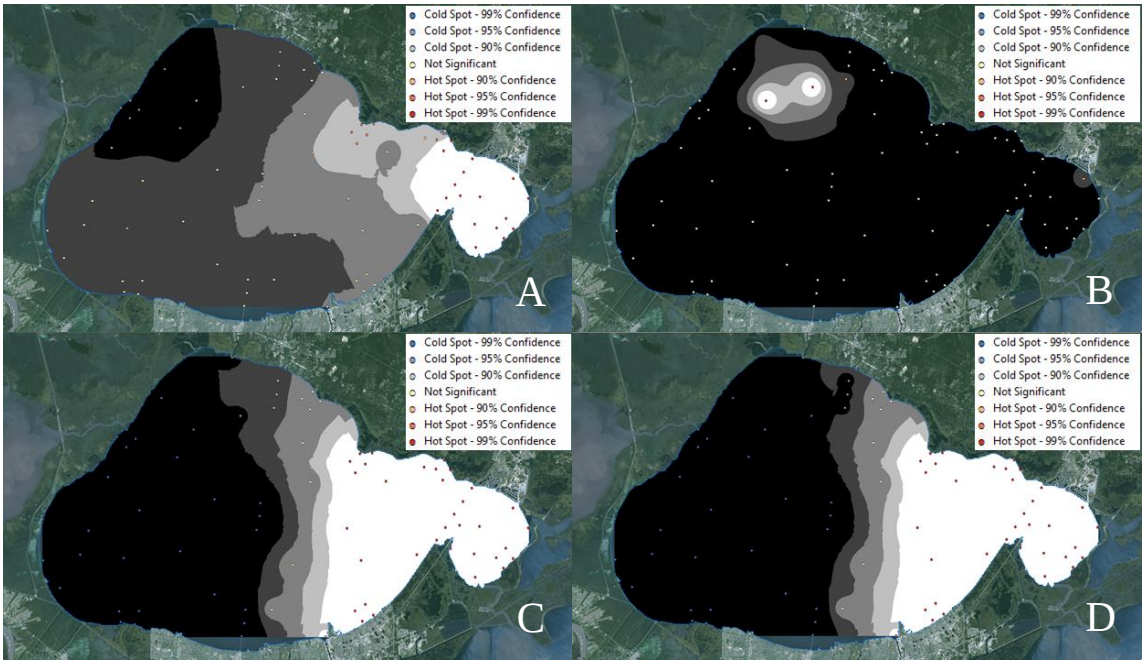

Figure 2.11 Hot Spot Analysis for (A) fish counts in May 2013, (B) detections in May 2013, (C) fish counts in May 2014 and (D) detections in May 2014.

Hot Spot Analysis-Summer

Hot spots overlapped for summer months in 2013 and 2014 (June, July, and August). For June 2013 (Figure 2.12, A and B), hot spots for both fish counts and detections occurred in the eastern and northeastern areas of the lake. No cold spots occurred for either counts or detections. For June 2014 (Figure 2.12, C and D), hot spots occurred in the eastern area for both counts and detections. An additional hot spot for detections was located in the southeast area. Cold spots in June 2014 were limited to counts in the southwest and northwestern areas.

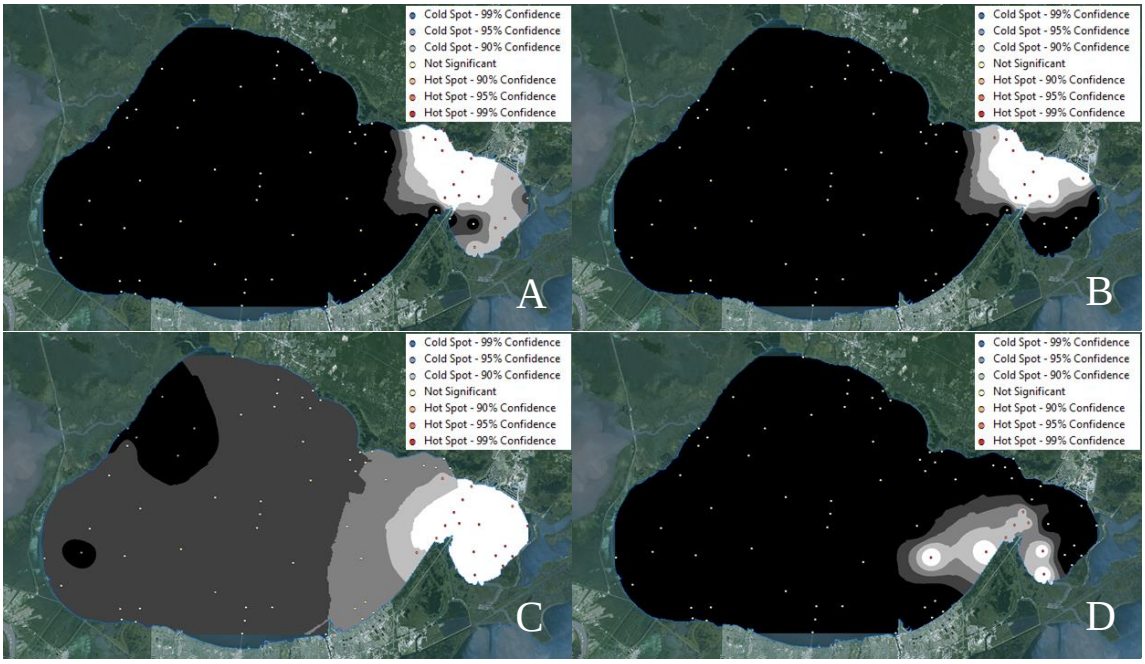

Figure 2.12 Hot Spot Analysis for (A) fish counts in June 2013, (B) detections in June 2013, (C) fish counts in June 2014 and (D) detections in June 2014.

For July 2013 (Figure 2.13, A and B), hot spots for fish counts and detections occurred in the center area of the lake, more specifically around the central causeway. Additional hot spots occurred for counts in a small northeastern area. By comparison, July 2014 (Figure 2.13, C and D) displayed hot spots for counts and detections in the center-north and northeastern areas. No cold spots were identified for either time period.

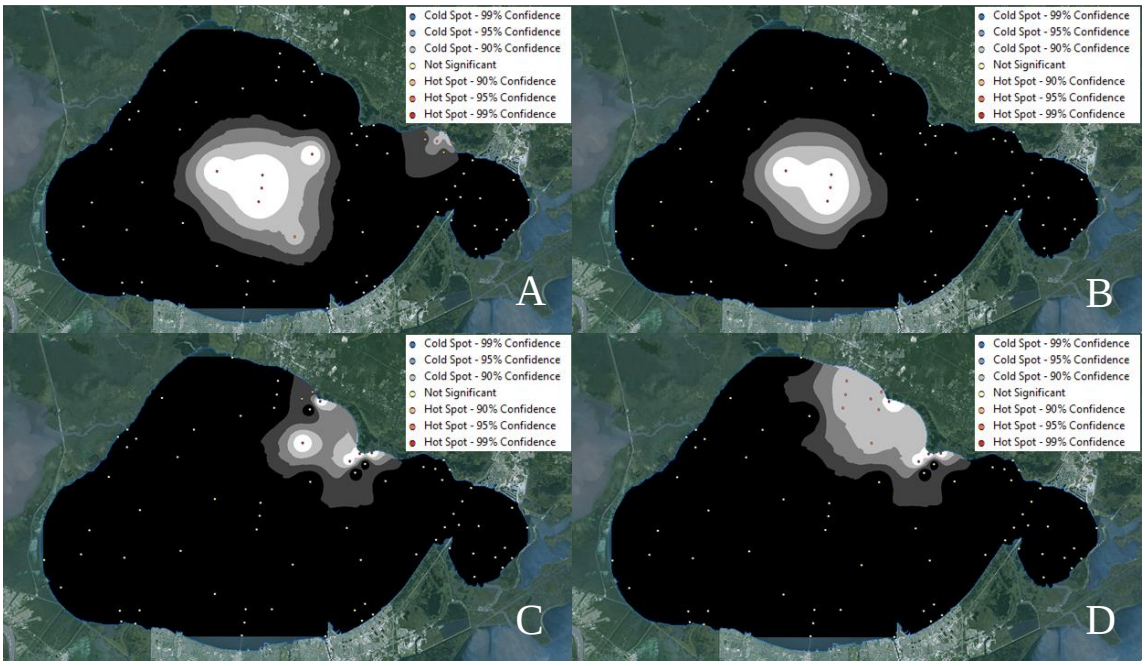

Figure 2.13 Hot Spot Analysis for (A) fish counts in July 2013, (B) detections in July 2013, (C) fish counts in July 2014 and (D) detections in July 2014.

Finally, for August 2013 (Figure 2.14, A and B), hot spots for fish counts and detections occurred in the northeastern and central area of the lake. For the same month in 2014 (Figure 2.15, A and B), however, hot spots for counts occurred in the central-north area, but hot spots for detections were located in the southwestern corner. No cold spots were found for either time period.

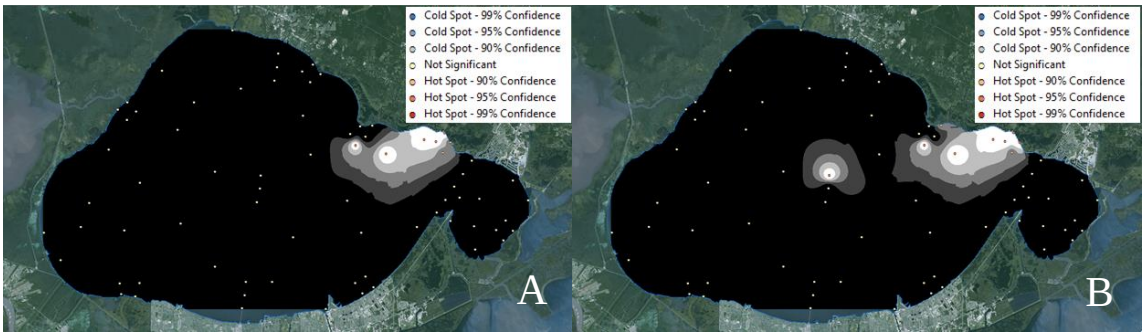

Figure 2.14 Hot Spot Analysis for (A) fish counts in August 2013 and (B) detections in August 2013.

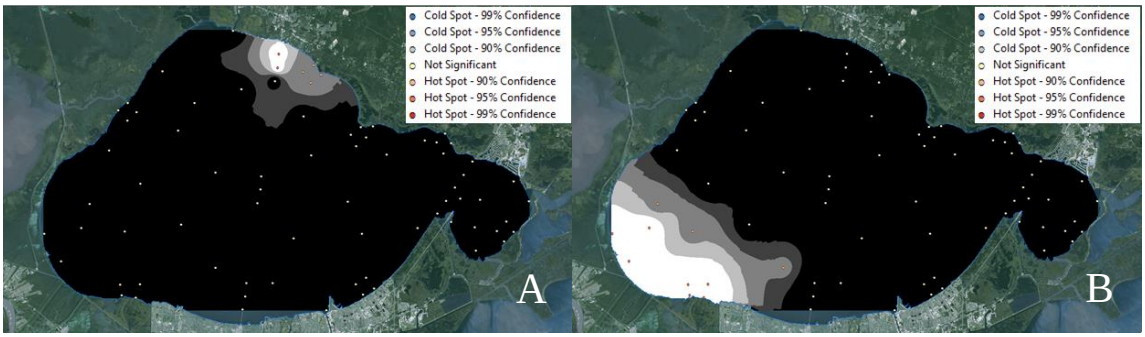

Figure 2.15 Hot Spot Analysis for (A) fish counts in August 2014 and (B) detections in August 2014.

Hot Spot Analysis-Fall

Unfortunately, for September and October of 2013 no fish detections were found to be appropriate for analysis, but for the counterparts in 2014, there were similar use patterns across the months. For September 2014 (Figure 2.16, A and B), high fish counts were identified in the center-north area of the lake. With respect to detections, however, hot spots only occurred in the southwest area. For October 2014 (Figure 2.16, C and D), high fish counts and detections were identified in the center-north area of the lake.

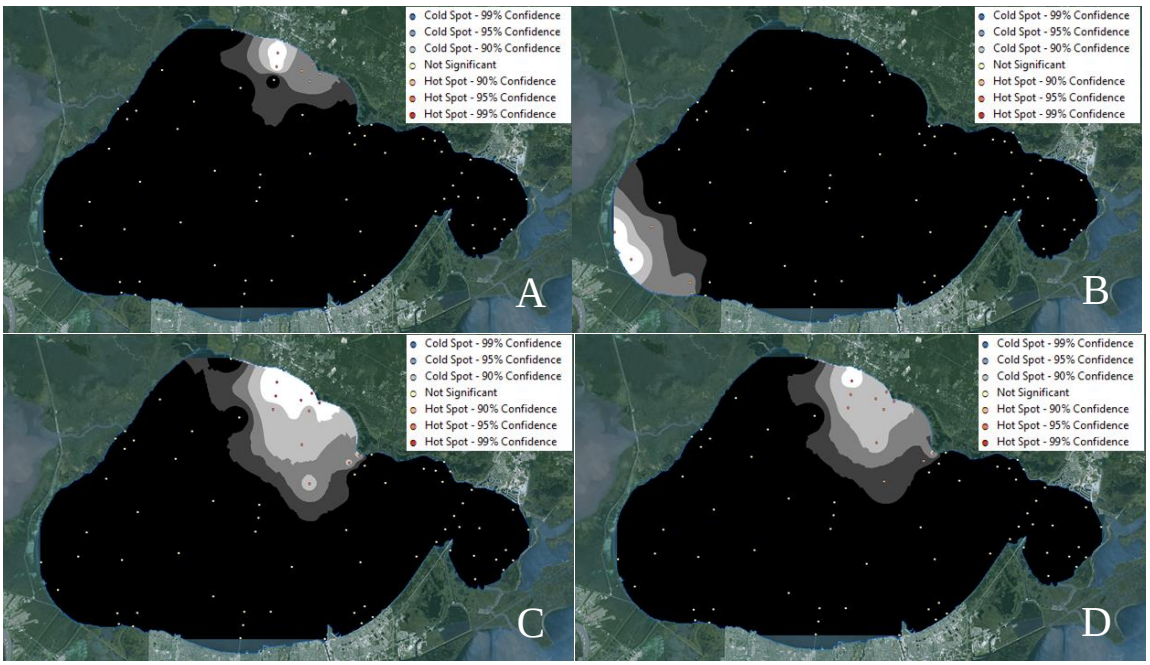

Figure 2.16 Hot Spot Analysis for (A) fish counts in September 2014, (B) detections in September 2014, (C) fish counts in October 2014 and (D) detections in October 2014.

For November 2013 (Figure 2.17, A and B), the patterns were much more varied, with hot spots for counts in the center, southeast, and northeast areas but hot spots for detections isolated to the central area. The only cold spots identified for the fall months occurred in November of 2013 for low fish counts in the southwest area of the lake. For November 2014 (Figure 2.17, C and D), hot spots for high fish counts and detections were located in the central north area of the lake.

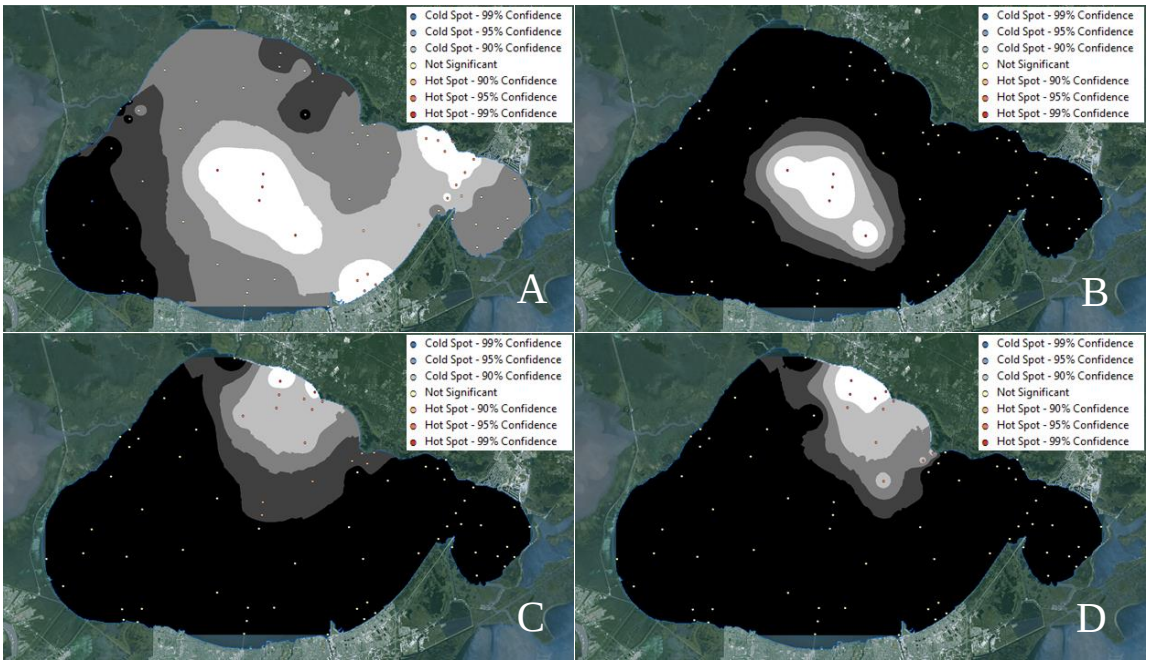

Figure 2.17 Hot Spot Analysis for (A) fish counts in November 2013, (B) detections in November 2013, (C) fish counts in November 2014 and (D) detections in November 2014.

Bottom Habitat Characterization – General Information

Despite the variability seen in the abovementioned figures, some receivers were identified as hot spots more than others. Receivers identified as hot spots for fish counts for ten or more months included ten in the central area, and five in the eastern area. Receivers identified as hot spots for detections for ten months or more only consisted of those within the eastern area of the lake. Cold spots for fish counts were found to be

concentrated in the west. No receivers were identified for more than three months as cold spots for detections. The receivers chosen for further evaluation with the Humminbird® imaging system and an Ekman bottom grab sampler were selected to include prominent hot spots, cold spots, and those designated as both at different times. Figure 2.18 below indicates the chosen hot spots (orange box), cold spots (blue box), and mixed (green box).

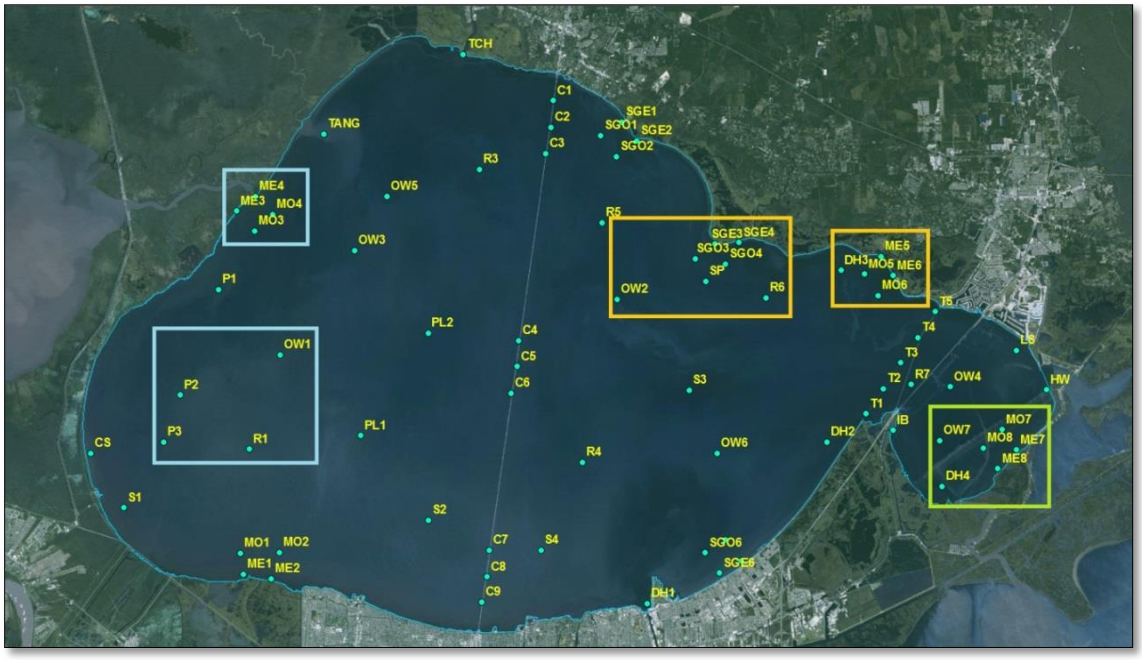

Figure 2.18 Map of receivers chosen for bottom type assessment with the Humminbird® as hot spots (orange box), cold spots (blue box), and mixed (green box).

Bottom Habitat Characterization – Eastern Receivers

The eastern receivers chosen for further assessment include DH4, ME5, ME6, MO5, MO6, MO7, and MO8. Bottom features among these varied. For example, sonar data at ME5 showed what appeared to be soft, vegetated marsh edge, while ME6 included not only this organic marsh bottom, but also a large dock structure (supporting posts), woody debris, and riprap material. Sonar data at DH4, however, showed a steep

drop of 9 meters. None of the sonar data produced at the other receivers contained this level of heterogeneity among bottom types, but rather they were soft sediments without defining features. Images from the Humminbird® system transects are provided below in Figure 2.19, A through D and Figure 2.20, A and B.

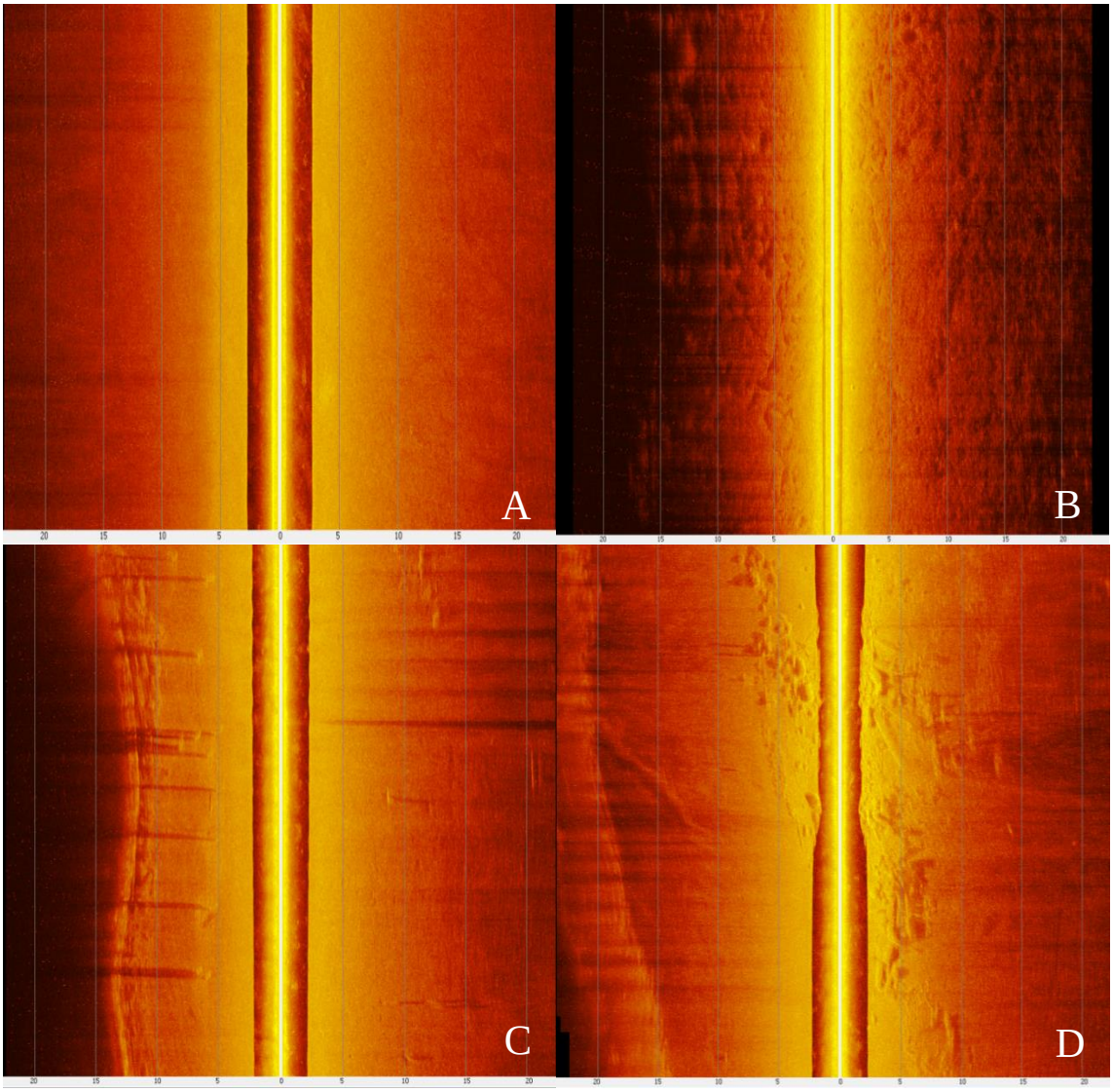

Figure 2.19 (A) Soft, nondescript bottom type (MO6). (B) Highly organic, marsh edge bottom type (ME5). (C) Supporting dock structure (posts) (ME6). (D) Riprap and woody debris (ME6).

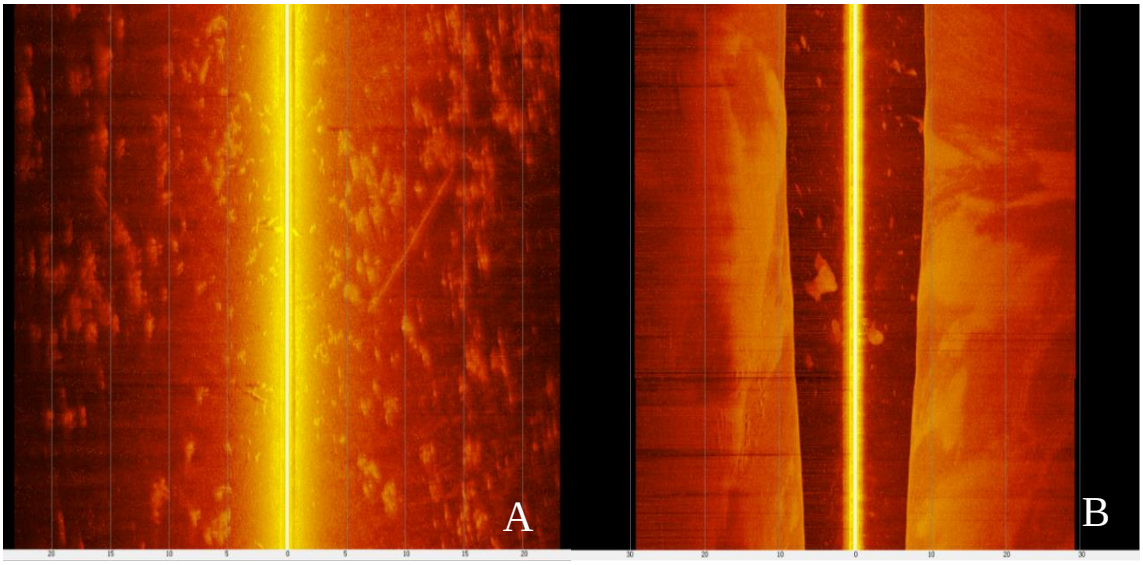

Figure 2.20 (A) Submerged vegetation and woody debris (ME5). (B) Steep drop to 9 meters in depth (DH4).

Images of the Ekman bottom grab samples collected at the eastern receivers are provided below in Figure 2.21, A through D and Figure 2.22, A through D. Using the Ekman bottom grab sampler, it was determined that all the samples taken for DH4 consisted of thick, soft, silty clay. All ME5 samples except the eastern sample consisted of thick, soft clayey silt with shell pieces. The eastern sample contained peat. All ME6 samples contained peat as well as clay in the north, sand in the south, and silty sand in the east. All MO5 samples contained Rangia clams in soft, thick, clayey, sandy, silt. Two samples taken at MO6 consisted of muddy sand with Rangia clams, both the northern sample consisting of clayey silty sand and the western sample consisting of sandy silty clay. MO7 samples all contained Rangia clams or shells, with the north and west consisting of sandy silt and the south and east consisting of clayey silt. Finally all MO8 samples were sandy clayey silt with Rangia clams. Images of the bottom samples are provided below.

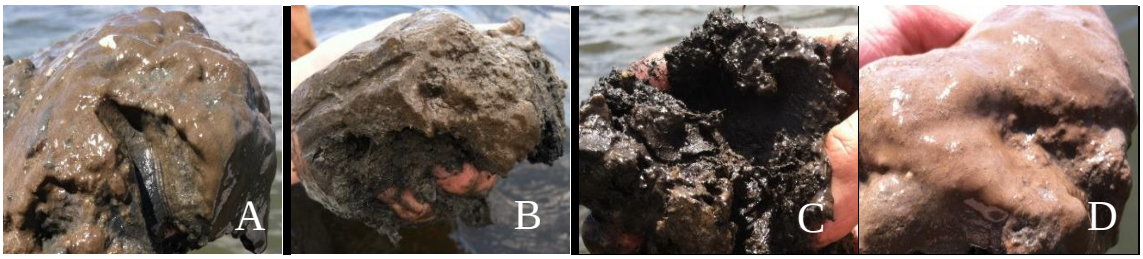

Figure 2.21 (A) Sediment sample (DH4). (B) Sediment sample (ME5). (C) Sediment sample (ME6). (D) Sediment sample (MO5).

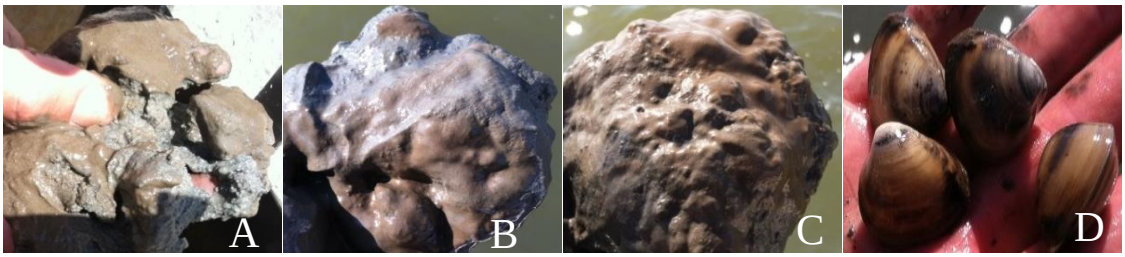

Figure 2.22 (A) Sediment sample (MO6). (B) Sediment sample (MO7). (C) Sediment sample (MO8). (D) Rangia clams found in sediment samples.

Bottom Habitat Characterization – Central Receivers

The central receivers assessed for bottom type included OW2, R6, SGE3, SGE4, SGO3, SGO4, and SP. Sonar data for R6 showed what appeared to be large limestone reefballs immediately beneath the receiver. For both seagrass edge receivers (SGE3 and SGE4), soft sandy sediment and patches of thick *Ruppia maritima* (seagrass) characterized the area. The single post (SP) receiver contained a small pile of shells and a wooden post. None of the sonar data produced at the other receivers contained heterogeneity among bottom types, but appeared as soft sediments without defining features. Images produced at these stations are provided below in Figure 2.23, A through F.

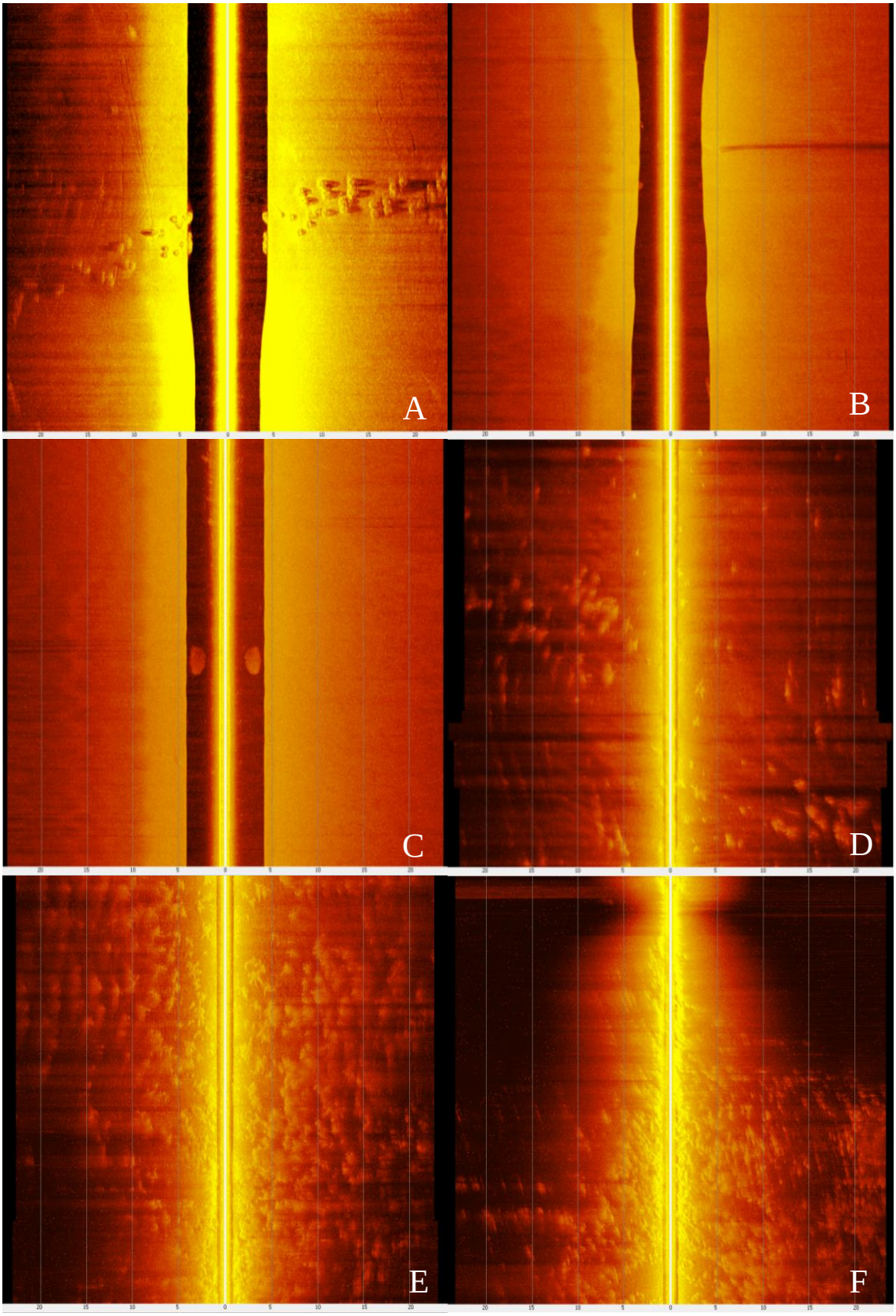

Figure 2.23 (A) Reefball structures (R6). (B) Single piling (SP). (C) Shell pile (SP). (D) Patchy seagrass (SGE3). (E) Dense seagrass patches (SGE4). (F) Seagrass beds too thick for sonar imaging (SGE4).

Images of the Ekman bottom grab samples collected at the central receivers are provided below in Figure 2.24, A through D and Figure 2.25, A through C. Using the Ekman bottom grab sampler it was determined that all samples for OW2 consisted of soft, thick clayey silt, and all but the east sample had shell pieces. R6 samples were identical to those collected for OW2. SGE3 samples were all silty sandy clay. Sand and Rangia clams defined the samples taken at SGE4, with grass in the western sample. Thick beds of *Ruppia maritima* were observed in the vicinity of both seagrass receivers (Figure 2.26, A). Soft, clayey silt was found in all samples from SGO3, but the western sample consisted of sandy, clayey silt with Rangia clams. SGO4 samples consisted of soft, clayey silt with Rangia clams. Finally, sandy silt with Rangia clams and shell pieces were found in all the samples collected around SP (Figure 2.26, B).

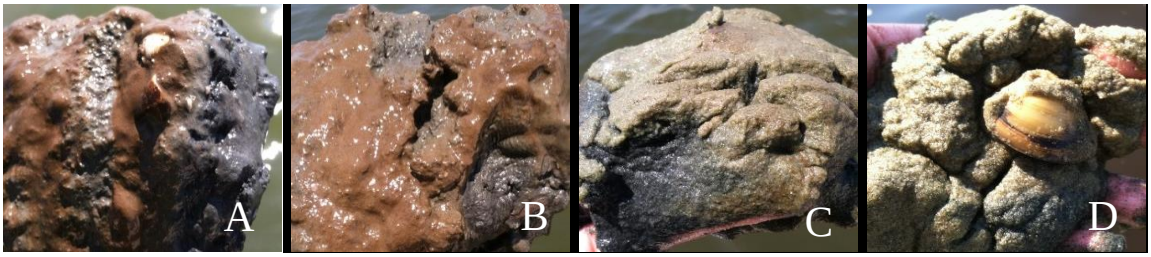

Figure 2.24 (A) Sediment sample (OW2). (B) Sediment sample (R6). (C) Sediment sample (SGE3). (D) Sediment sample (SGE4).

Figure 2.25 (A) Sediment sample (SGO3). (B) Sediment sample (SGO4). (C) Sediment sample (SP).

Figure 2.26 (A) Seagrass beds (SGE4). (B) Shell pieces (SP).

Bottom Habitat Characterization – Western Receivers

The western receivers assessed for bottom type include ME3, ME4, MO3, MO4, OW1, P2, P3, and R1. Features appearing in sonar data included woody debris at MO3, solid supporting concrete beams for the powerline structures by P2 and P3, and limestone reefballs at R1. Dense, scattered woody and organic debris on and within soft sediment appeared to characterize the bottom types of ME3 and ME4. None of the sonar data produced at the other receivers contained heterogeneity among bottom types, but appeared as soft sediments without defining features. Images detailing bottom features are provided in Figure 2.27, A and B, and Figure 2.28, A through D.

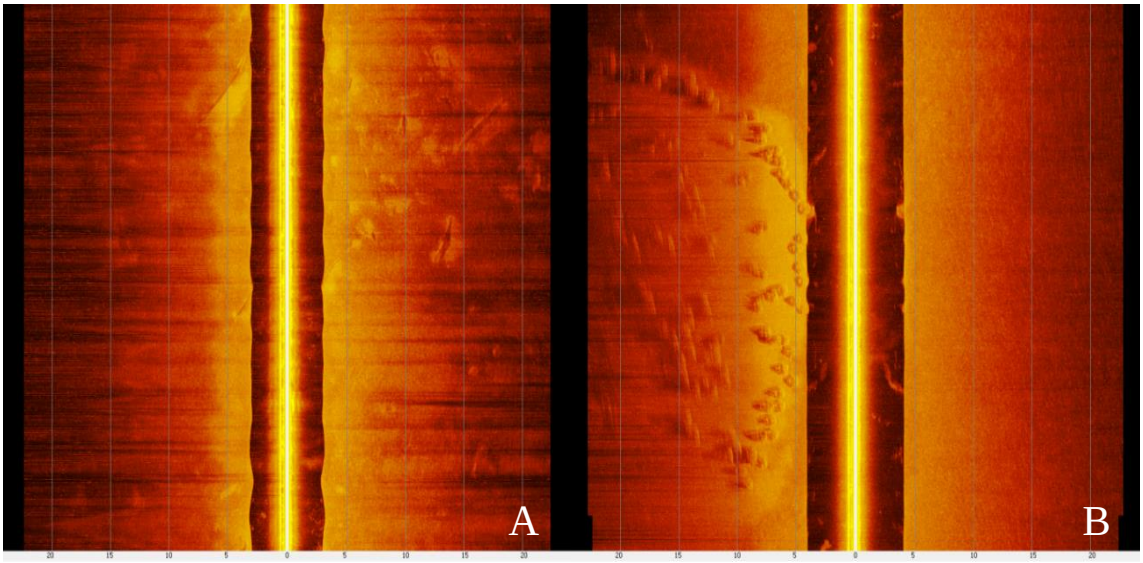

Figure 2.27 (A) Scattered woody debris over soft sediment (MO3). (B) Reef ball formation (R1).

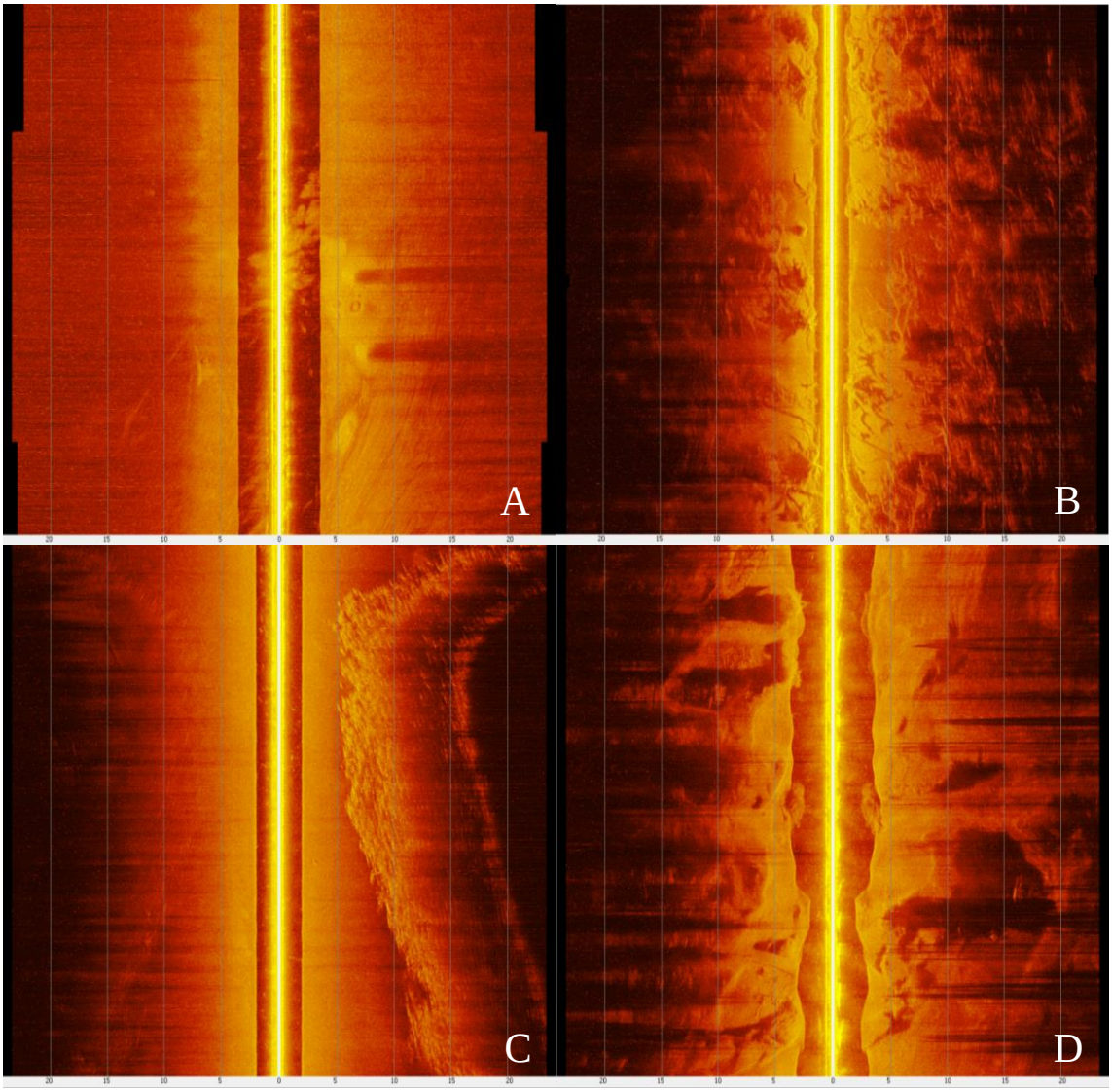

Figure 2.28 (A) Supporting powerline structure beams (P2). (B) Dense woody/organic debris (ME3). (C) Rock wall feature (ME3). (D) Soft sediment with organic detritus (ME4).

Images of the Ekman bottom grab samples collected at the western receivers are provided below in Figure 2.29, A through D and Figure 2.30, A through D. Using the Ekman bottom grab sampler, it was determined that ME3 samples varied greatly, with sandy, clayey silt in the east, silt and organic matter (peat) in the north, layers of silty clay and peat in the west, and clayey silt in the south. Soft clayey silt with Rangia clams/shell pieces defined all the samples from ME4, MO3, MO4, OW1, P2, P3, and R1. In

addition, thick woody debris was noted at ME3 and the powerline structures at P2 and P3. Images of these features are provided below in Figure 2.31, A through C.

Figure 2.29 (A) Sediment sample (ME3). (B) Sediment sample (ME4). (C) Sediment sample (MO3). (D) Sediment sample (MO4).

Figure 2.30 (A) Sediment sample (OW1). (B) Sediment sample (P2). (C) Sediment sample (P3). (D) Sediment sample (R1).

Figure 2.31 (A) Woody debris/stumps (ME3). (B) Rangia clams (ME4). (C) Powerline structures (P2 and P3).

DISCUSSION

My results indicate that hot spots of spotted seatrout were persistent in the center, center-north, and northeastern areas of Lake Pontchartrain in terms of both fish counts and detections. The western edge of the lake contained the majority of cold spots for

both fish counts and detections. Receivers representing every bottom type were designated as both hot spots and cold spots over the time period considered. Interestingly, the easternmost area, specifically, contained receivers categorized as hot spots and cold spots in both categories at different times.

In the eastern area, hot spots for both fish counts and detections for a period of six months or more included receivers on the train trestle (T2, T3, T4, T5), over a reef (R7), and along the lakeshore (LS). In addition, DH3 (deep hole feature) came up as a top hot spot with the designation for 11 months for fish counts and 10 months for detections. For the central area, receivers identified as hot spots for six months or more included central causeway receivers (C1, C2, and C3) and one over a shell pad (S3). Hot spots for ten months or more with respect to fish counts included a receiver over a reef (R5) and four within seagrass beds (SGE1, SGE2, SGO1, SGO2). In the western areas, cold spots were much more prevalent. Those identified as cold spots for fish counts, for six months or more, were near a marsh (ME2), powerline (P1), open water (OW3), and the entrance to the Tangipahoa River (TANG). Cold spots for ten months or more were limited to three near marshes (ME1, MO1, and MO2). Considering the abovementioned receivers and those addressed in detail through the habitat characterization surveys, there are representative receivers from each bottom type (and even in some instances the same receiver), found to be both hot spots and cold spots for fish count and detections.

Bottom habitat characterization revealed that most bottom sediments consisted of silty clay or clayey silt. Sand was noted to be a minor component of the sediment (when present) except for one receiver by a marsh (MO6) and two near seagrass beds (SGE3 and SGE4). The geological history of the lake provides further evidence of clay and silt being the dominant sediment components. Since the Pleistocene (approximately 22,000-18,000 years ago), the majority of sediments accumulating within the lake are

predominantly silts and clays, with approximately 70% of recent sediment samples having grain sizes <63 µm (Flocks et al. 2009a; Hastings 2009). The accumulation of such fine sediment deposits is due in large part to the shallow nature and low-energy environment of the lake (Flocks et al. 2009a; Hastings 2009). Lacking a major river's influence/sediment load, the sediment reaching the lake is from lower-energy riverine sources or from overland flow (Flocks et al. 2009a). The commonality of sediment type across the lake is further evidenced in the maps depicted in Figure 2.32 and Figure 2.33 provided below. The classification system used for defining sediment types is provided in Figure 2.34.

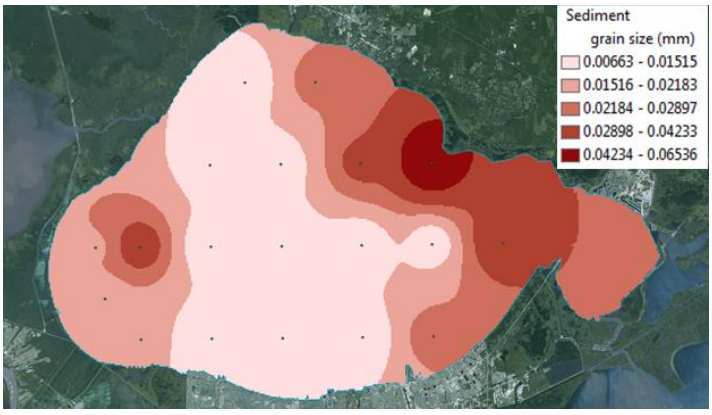

Figure 2.32 Sediment cores including small grain sizes, from 0.007mm to 0.065 mm (clays to very fine sand) (Fabre 2012).

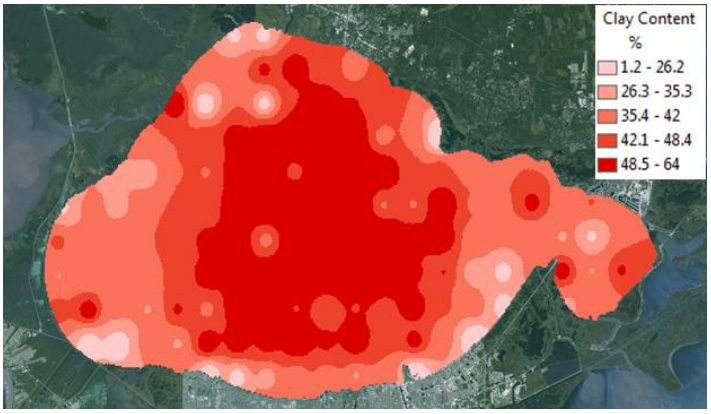

Figure 2.33 Clay content of bottom samples which range from 1.2 to 63.97 percent (DeLaune et al. 2004).

Wentworth classification	Size range (mm)
Boulder	>256
Cobble	64 to 256
Pebble[a]	4 to 64
Granule (very fine gravel)	2 to 4
Very coarse sand	1 to 2
Coarse sand	0.5 to 1
Medium sand	0.25 to 0.5
Fine sand	0.125 to 0.25
Very fine sand	0.063 to 0.125
Silt	0.004 to 0.063
Clay	<0.004

[a] The USGS has subdivided this category as follows:

Very coarse gravel	32 to 64 mm
Coarse gravel	16 to 32 mm
Medium gravel	8 to 16 mm
Fine gravel	4 to 8 mm

Figure 2.34 Sediment grain size classification guide (Assad et al. 2004).

In predicting species distribution and abundances related to habitat preferences, there appears to be a pattern of higher use in the central, central-north, and northeastern areas of the lake. However, when it comes to assessing bottom type preference as a determining factor, there appears to be mixed results. While background literature, Humminbird® images, and Ekman bottom sample grabs showed little variation in bottom sediments across the lake, bottom habitats (designated by the special features) did not significantly shift overall hot spot or cold spot distribution. Some receivers were even designated as both hot and cold spots for fish counts and detections. It is therefore useful to determine if this pattern is specific to the spotted seatrout of Lake Pontchartrain. For this purpose, Habitat Suitability Models (HSM) have been developed by leading researchers and natural resource managers, including the Center for Coastal Monitoring and Assessment Biogeography Program, US Fish and Wildlife Services Habitat Evaluation Procedures Program, and BP's Estuarine Living Marine Resources Database Program (Bortone 2003). HSMs incorporate past research into the habitat requirements/preferences of a species in order to generate an assessment model for areas

of interest. Researchers working in Pensacola Bay, FL, developed a qualitative model specific to spotted seatrout, with suitability index values (Bortone 2003). According to the values for adult spotted seatrout, optimal suitability is found with the presence of submerged aquatic vegetation, but a high suitability is noted even in its absence. The same was determined by the researchers for the presence/absence of wetlands, three potential bottom types (clay, silt/mud, and sand), and all depths (0-50m) (Bortone 2003). A similar HSM developed by the Florida Department of Environmental Protection revealed similar measures of suitability for spotted seatrout in Tampa Bay and Charlotte Harbor in Florida (Bortone 2003).

Preferences for bottom type, however, have been noted under certain conditions. Spawning sites used by adults are most often situated between barrier islands and in deep water channels adjacent to marsh edges or seagrass beds (Neahr et al. 2010). Seagrass beds provide a complex habitat of various submerged aquatic plant species, where both larval and juvenile spotted seatrout are found in close association with the bottom (Lassuy 1983). Adults also show a preference for deep holes/channels with seasonal changes in temperature. For spotted seatrout in Louisiana's coastal waters, the post spawning period (September) and overwintering season (October-March) are when adult spotted seatrout contend with cooling temperatures and are prompted to occupy more thermally stable deep channels or holes in the estuary, and in extreme shifts to emigrate into the deeper waters of the coastal shelf (Lassuy 1983, Bortone 2003). This preference was evidenced in Lake Calcasieu, Louisiana, wherein during extreme heat or cold events, deeper bay channels, specifically Calcasieu Pass and Calcasieu Ship Channel, were utilized by the species as a direct shift in distribution in response to seasonal temperature changes (Arnoldi 1984).

Overall, the lack of distinct bottom type preference for adult spotted seatrout is not unusual. Mark-recapture and acoustic telemetry studies conducted within Lake Calcasieu in Louisiana assessed the distribution of spotted seatrout designated as large (>500 mm TL), medium (400-499 mm TL), or small (<400 mm TL) (Callihan 2011) (Callihan et al. 2013). Being a highly mobile species, all size classes and both genders were found in every habitat, which included channel, marsh, mud, natural reef, and artificial reef. Adult spotted seatrout were also found by researchers from LDWF in cooperation with LSU in Barataria Bay to display little habitat selection. Adults in the bay chose to spawn over rubble, sand/shell reefs, pilings, and soft bottom uniformly (Bortone 2003). In addition, once spawning was complete, adult spotted seatrout showed little physical habitat preference (MacRae and Cowan 2010). Data clearly indicated that adult spotted seatrout displayed no consistent pattern of selection even between marsh edge, soft-bottom, and oyster shell reef areas (MacRae and Cowan 2010).

CONCLUSION

Bottom habitat preferences exhibited by spotted seatrout in Lake Pontchartrain during 2013 and 2014, in agreement with the previous studies' findings, appeared to be conditional and temporary. The use of every bottom type in the lake indicates a flexibility exhibited by most species adapted to estuarine environments, strengthening the conclusion that the value of any one habitat type is more likely tied to its connectivity with other habitats (Cowan et al. 2008, Cowan et al. 2013). The heterogeneity in bottom types is especially important when one considers that each one in turn (and often at the same time) is critical for a life stage of the species (Cowan et al. 2008, Cowan et al. 2013). While the adults do utilize a wide variety of habitats within the estuary, the distribution of this species within the lake is considered to be driven more by water

quality parameters, specifically those which are beneficial to a species' relative fitness (Neahr et al. 2010). The third chapter of this thesis will therefore address habitat use patterns exhibited by spotted seatrout along water quality gradients within Lake Pontchartrain and as determined utilizing the Dataflow Water Sampling System.

LITERATURE CITED

ArcGIS Resources. 2013a. Incremental Spatial Autocorrelation. ArcGIS Tool Reference. Retrieved from: ‹http://resources.arcgis.com/EN/HELP/MAIN/10.1/index.html#//005p0000004z000000›

ArcGIS Resources. 2013b. Lambert Conformal Conic. ArcGIS Guide Books. Retrieved from: ‹http://resources.arcgis.com/en/help/main/10.1/index.html#/Lambert_Conformal_Conic/003r00000034000000/›

ArcGIS Resources. 2013c. Modeling Spatial Relationships. ArcGIS Tool Reference. Retrieved from: ‹http://resources.arcgis.com/en/help/main/10.1/index.html#/Modeling_spatial_relationships/005p00000005000000/›

ArcGIS Resources. 2013d. State Plane Coordinate System. ArcGIS Guide Books. Retrieved from: ‹http://resources.arcgis.com/en/help/main/10.1/index.html#//003r00000043000000›

ArcGIS Resources. 2014. How Hot Spot Analysis Works. ArcGIS Tool Reference. Retrieved from: ‹http://resources.arcgis.com/en/help/main/10.2/index.html#/How_Hot_Spot_Analysis_Getis_Ord_Gi_works/005p00000011000000/›

Arnoldi, D.C. 1984. Aspects of the biology of spotted seatrout (*Cynoscion nebulosus*) in Calcasieu Lake, Louisiana, with management implications. Louisiana Department of Wildlife and Fisheries.

Assad F.A., J.W. LaMoreaux, and T. Hughes (Eds.). 2004. Field methods for geologists and hydrogeologists. Springer-Verlag, Berlin, Germany.

Blanchet, H., M. V. Hoose, L. McEachron, B. Miller, J. Warren, J. Gill, T. Waldrop, J. Waller, C. Adams, R.B. Ditton, D. Shively, and S. Vanderkooy. 2001. The spotted seatrout fishery of Mexico, United States: A regional management plan. Gulf States Marine Commission.

Bortone, S.A. 2003. Biology of the Spotted Seatrout. CRC Press, Boca Raton, Florida.

Callihan, J.L. 2011. Spatial ecology of adult spotted seatrout, *Cynoscion nebulosus*, in Louisiana Coastal Waters. Dissertation. Louisiana State University. Baton Rouge.

Callihan, J.L., J.H. Cowan, Jr., and M.D. Harbison. 2013. Sex differences in residence of adult spotted seatrout in a Louisiana estuary. Marine and Coastal Fisheries: Dynamics, Management, and Ecosystem Science 5:79-92.

Cho, H.J. and M.A. Poirrier. 2005. Seasonal growth and reproduction of Ruppia Maritima in Lake Pontchartrain, Louisiana, USA. Aquatic Botany. 81:37-49.

Cowan, J.H., C.B. Grimes, and R.F. Shaw. 2008. Life history, history, hysteresis, and habitat changes in Louisiana's coastal ecosystem. Bulletin of Marine Science 83:197-215.

Cowan, J.H., A. Yáñez-Arancibia, P. Sánchez-Gil, and L.A. Deegan. 2013. Estuarine Nekton. Estuarine Ecology Chapter 13. John Wiley & Sons, Inc. Hoboken, New Jersey.

DeLaune R.D., I. Devai, and W.H. Patrick Jr. 2004. Total mercury, methylmercury and other toxic heavy metals in Lake Pontchartrain Basin. Lake Pontchartrain Basin Foundation.

Duffy, K.C., and D.M. Baltz. 1998. Comparison of fish assemblages associated with native and exotic submerged macrophytes in the Lake Pontchartrain estuary, USA. Journal of Experimental Marine Biology and Ecology. 223: 199-221.

Fabre J.B. 2012. Sediment flux and fate for a large-scale diversion: The 2011Mississippi River flood, the Bonnet Carre Spillway, and the implications for coastal restoration in South Louisiana. Thesis. Louisiana State University.

Flocks, J., J. Kindinger, M. Marot, and C. Holmes. 2009a. Sediment characterization and dynamics in Lake Pontchartrain, Louisiana. Journal of Coastal Research. 54:113-126.

Flocks, J., M. Kulp, J. Smith, and S.J. Williams. 2009b. Review of the geologic history of the Pontchartrain Basin, Northern Gulf of Mexico. Journal of Coastal Research. 54: 12-22.

Georgiou, I., J.A. McCorquodale, J. Schindler, A.G. Retana, D.M. FitzGerald, Z. Hughes, and N. Howes. 2009. Impact of multiple freshwater diversions on the salinity distribution in the Pontchartrain estuary under tidal forcing. Journal of Coastal Research. 54: 59-70.

Hastings, R.W. 2009. The Lakes of Pontchartrain. University Press of Mississippi, Jackson, Mississippi.

Lassuy, D.R. 1983. Species profiles: Life histories and environmental requirements (Gulf of Mexico) spotted seatrout. National Coastal Ecosystems Team.

Lopez, J. 2004. The Lake Pontchartrain artificial reef program. Lake Pontchartrain Basin Foundation with the Louisiana Department of Wildlife and Fisheries.

MacRae, P.S.D. and J.H. Cowan, Jr. 2010. Habitat preferences of spotted seatrout, *Cynoscion nebulosus*, in coastal Louisiana: A step towards informing spatial management in estuarine ecosystems. The Open Fish Science Journal 3:154-163.

Mallin, M.A., M.H. Posey, G.C. Shank, M.R. McIver, S.H. Ensign, and T.D. Alphin. 1999. Hurricane effects on water quality and benthos in the Cape Fear watershed: natural and anthropogenic impacts. Ecological Applications 9:350-362.

Mazzotti, F.J., L.G. Pearlstine, T. Barnes, S.A. Bortone, K. Chartier, A.M. Weintstein, and D. DeAngelis. 2008. Stressor-response model for the spotted seatrout (*Cynoscion nebulosus*). Institute of Food and Agricultural Sciences, University of Florida.

McDonald, D.L., P.D. Cason, B.W. Bumguardner, and S. Bonnot. 2013. Critical thermal maximum of juveniles spotted seatrout (*Cynoscion nebulosus*) reared for summer stocking in Texas. Journal of Applied Aquaculture 25:308-319.

Melancon, A. 2015. Personal Communication. Department of Oceanography and Coastal Sciences, Louisiana State University, Baton Rouge, LA, amela22@lsu.edu.

Miller, R.L., C.E. del Castillo, and K.A. McKee. 2005. Remote sensing of coastal aquatic environments: Technologies, Techniques and Applications. Springer, Dordrecht.

National Geodetic Survey. 2015. State Plane Coordinate (SPC) Utilities. Retrieved from: ‹http://www.ngs.noaa.gov/TOOLS/spc.shtml›

Neahr, T.A., G.W. Stunz, and T.J. Minello. 2010. Habitat use patterns of newly settled spotted seatrout in estuaries of the north-western Gulf of Mexico. Fisheries Management and Ecology 17:404-413.

Nieland, D.L., R.G. Thomas, and C.A. Wilson. 2002. Age, growth, and reproduction of the spotted seatrout in Barataria Bay, Louisiana. Transactions of the American Fisheries Society 131:245-259.

O'Connell, M.T., A.M.U. O'Connell, and C.S. Schieble. 2013. Response of Lake Pontchartrain fish assemblages to Hurricanes Katrina and Rita. Estuaries and Coasts. 37: 461-475.

Penland, S., A. Beall, and J. Waters (Eds.). 2002. Environmental atlas of the Lake Pontchartrain basin. Lake Pontchartrain Basin Foundation, New Orleans.

Poirrier, M.A., E.A. Spalding, and C.D. Franze. 2009. Lessons learned from a decade of assessment and restoration studies of benthic invertebrates and submerged aquatic vegetation in Lake Pontchartrain. Journal of Coastal Research. 54: 88-100.

Reed, D.J., and D. FitzGerald. 2009. Introduction. Journal of Coastal Research, 54: vii-xi.

Roy, E.D., and J.R. White. 2012. Nitrate flux into the sediments of a shallow oligohaline estuary during large flood pulses of Mississippi River water. Journal of Environmental Quality. Technical Report.

Vemco. 2015. Range calculator. Retrieved from: ‹http://vemco.com/range-calculator/›

Whitmore, K.A. 2006. Artificial reef performance in Lake Pontchartrain, Louisiana. Thesis. University of New Orleans.

Wu, K. 2005. Long-term freshwater input and sediment from three tributaries to Lake Pontchartrain, Louisiana. Dissertation. Louisiana State University.

CHAPTER 3: HABITAT USE OF ADULT SPOTTED SEATROUT IN RELATION TO WATER QUALITY WITHIN LAKE PONTCHARTRAIN, LOUISIANA

INTRODUCTION

Spotted seatrout is a valuable estuarine fish species in Louisiana. At all life stages, spotted seatrout in this state and elsewhere are closely associated with the estuarine environment (Bortone and Wilzbach 1997). Rapid growth in the early stages allow the young to reach a total length (TL) of 200-350mm during the first year, with females often exhibiting faster growth than males across their geographic range (Nieland et al. 2002; Bortone 2003). Spotted seatrout reach maturity at or just before age-1, which occurs prior to the first spawning season following hatching (Nieland et al. 2002). The maximum ages reported for this species range from 7 to 10 years (Nieland et al. 2002, Bortone 2003). In general, adult spotted seatrout prefer large regions of shallow, brackish (15-28 ppt) water with an abundance of crustaceans and fish of a suitable size for consumption and a stable temperature regime (16-32^{o}C) for successful growth, maturation, and spawning (Kostecki 1984, Mazzotti et al. 2008).

Adult spotted seatrout, which utilize less energy for growth than any earlier life stages, are capable of leaving an environment where stressful conditions are present (Blanchet et al. 2001). With respect to dissolved oxygen, adult spotted seatrout are considered moderately susceptible to hypoxia (2-3 mgL^{-1}) in estuarine habitats, but younger juvenile and larval stages are more susceptible (Blanchet et al. 2001). With respect to salinity tolerances, the species as a whole is capable of adapting to salinities as low as 0.2 ppt and as high as 70 ppt through the processes of osmoregulation, but as a result have a decreased capacity to meet metabolic energy demands (Banks et al. 1991, Wuenschel et al. 2004). Salinities below 10 ppt or above 45 ppt leave little available

energy for any activities beyond basic biological maintenance (Lassuy 1983). Salinities below 5 ppt are noted by researchers as intolerable and likely to lead to mass mortalities, especially if such conditions result from a rapid freshening (Lassuy 1983; Blanchet et al. 2001; Hill 2005). With respect to temperature, spotted seatrout in Louisiana waters are most frequently found in a temperature range of 20-32^{o}C (Kostecki 1984; MacRae and Cowan 2010). When annual cool temperatures occur in the post spawning period (September) and overwintering season (October-March), adult spotted seatrout emigrate from their estuaries and into the deeper waters of the shallow continental shelf (Lassuy 1983; Bortone 2003). However, sudden and extreme temperature drops, have been recorded and linked with winterkills of the species (623,000 in 1993 and 759,000 in 1989) (Blanchet et al. 2001). With Mississippi River water entering Louisiana's estuaries ranging in temperature from 5-34.9^{o}C (with the range of 7-10^{o}C specifically identified as adverse to spotted seatrout) a winterkill event is certainly possible (Blanchet et al. 2001).

The least detailed feature of the estuarine conditions preferred by spotted seatrout is turbidity (Bortone 2003). It is considered beneficial to early life stages as it enhances survival by providing physical cover to the smallest and most vulnerable life stages. With the shallow, microtidal (<2 m) estuaries of Louisiana dominated by storm events and fine sediments from the Mississippi River, the abundance of small fish is estimated to be higher in those nearshore shallow environments with a turbidity over 10 nephlometer turbidity units (NTU) (Bortone 2003). Typical turbidity values for the surface waters of the lake are between 5.8 and 9.3 nephelometric turbidity units (NTU**)** (Xu and Wu 2006).

A final consideration is the influence of algal blooms in Lake Pontchartrain. Phytoplankton species in Lake Pontchartrain are the most widespread of the autotrophs. Green algae (*Chlorophyceae*: e.g. *Chlamydomonas*, *Phacotus*, and *Sphaerocystis*) and diatoms (*Chrysophyceae*: e.g. *Chaetoceros*, and *Coscinodiscus*) typically dominate the

phytoplankton community in the early spring, however, it is the blue green algae species (cyanobacteria) that are often responsible for blooms appearing in late summer/early autumn in the western half of the lake (Hastings 2009; Bargu et al. 2011; Smith 2014). Potentially toxic cyanobacteria species of *Oscillatoria*, *Microcystis*, *Lyngbya*, and *Anabaena* dominate this group (Hastings 2009). Eutrophication defines the conditions wherein waterbodies receive a high supply of organic matter, typically enriching the supply of phosphorus and/or nitrogen and producing seasonal blooms of these species (Roy et al. 2012; Smith 2014). The danger to the spotted seatrout lies in their resulting toxin production, particularly as the blooms form during their spawning season (Moffatt and Nichol Engineers 2010; Smith 2014). The primary toxin producing blue-green algae in Lake Pontchartrain include *Anabaena*, *Aphanizomenon*, *Microcystis*, *Cylindrospermopsis*, *Planktothrix* and *Nodularia* which can in turn produce hepatotoxins that block protein synthesis in the fish and neurotoxins that attack the nervous system (Moffatt and Nichol Engineers 2010).

While highly adaptable to a wide range of water quality conditions within estuaries, spotted seatrout appear to be locally adapted to their natal estuary, characterized by unique water quality regimes (Bortone 2003). It is the seasonal/event-driven variability in dissolved oxygen (DO), salinity, and temperature that appear to be the most influential physiochemical variables on spotted seatrout distribution. Secondary/complicating variables, specifically turbidity and algal blooms are also important features in determining the suitability of estuarine ecosystems for spotted seatrout (Bortone 2003). With the confluence of both natural and man-made influences on the water quality of Lake Pontchartrain, knowledge of the biochemical variability in the lake is a priority for understanding fisheries production and sustainability.

METHODS

Study Area

Lake Pontchartrain is a shallow estuary (0.5-5m deep) covering 1,630 km^2 within the Lake Pontchartrain Basin (Penland et al. 2002; Flocks et al. 2009). Within the basin lie five river systems, including the Amite, Tickfaw, Tchefuncte, Tangipahoa, and Pearl (Flocks et al. 2009). In general, the tidal range within the lake is microtidal, only 10-20 cm, so tides are mainly meteorological, with easterly and southerly winds driving water into the estuary (Cho 2007). Winds from the west and north push waters from the lake (Cho 2007). In addition, there are two narrow tidal channels (Rigolets Pass and Chef Menteur Pass) located along the eastern edge of the lake that allow the inflow of higher salinity water to the lake (Penland et al. 2002; Wu 2005). Direct sources of freshwater, nutrient, and sediment includes the aforementioned river systems as well as a direct connection from Lake Maurepas to Lake Pontchartrain by way of Pass Manchac (Xiaobo and Azad Hossain 2013). The lake thus exhibits a rather narrow salinity range, typically from 0-8 ppt, with lower values (1.2 ppt) in the west and higher values (up to 15.2 ppt) in the east (Hastings 2009). Due to the lake's wide fetch (surface area) and shallow depths, it only requires a wind speed of 6.8 ms^{-1} (15 mph) to mix the bottom sediments throughout the water column (Cho 2007). Typical turbidity values for the surface waters of the lake are between 5.8 and 9.3 NTU (Xu and Wu 2006). Overall, the estuary is considered to be well-mixed, with its major hydrologic connections depicted in Figure 3.1 below.

Figure 3.1 Geographic map of Lake Pontchartrain with connecting waterways (Pass Manchac, Pass Rigolets, Pass Chef Menteur), rivers (Tangipahoa and Tchefuncte River), and waterbodies (Lake Maurepas and Lake Borgne).

Telemetry

Regions within Lake Pontchartrain where spotted seatrout are reported to occur in large numbers as well as waterways connecting to other waterbodies/rivers were chosen for the placement of stationary acoustic receivers. For this study, the lake boundary (visible as a light blue line around the edge of the lake in Figure 3.2) included receivers (75 out of 90 total) for assessing the distribution of spotted seatrout in the lake. Each receiver has a range of 500 to 600 meters under normal lake conditions, but this range can be reduced when turbidity is high (Melancon 2015; Vemco 2015). Acoustic tags were surgically implanted into the peritoneal cavity of adult spotted seatrout in the fall of 2012 (11/15-11/18), spring of 2013 (5/20-5/24), fall of 2013 (11/04-11/08), and spring of 2014 (4/21-4/23). In total, 211 fish were tagged (18 males, 176 females, 17 unknown). Additional data collected included total length (cm), standard length (cm), and total weight (kg). A V9 acoustic tag was implanted in fish with a TL of less than 39.37cm, a V13 tag for fish from 39.37 to 49.53cm, or a V13TP for fish over 49.53cm. Each acoustic tag emits a signal at 69 kHz at random intervals. Expected battery life is 8

months for the V9 tag and 1.5 years for the V13 and V13TP. Each receiver records the time a signal is received, the fish's ID number, and the data pertaining to the fish tagged. This data was then edited to remove the 1st week of movement after tagging, false detections, and continuous detections at a single receiver. Figure 3.2 below shows receiver locations throughout the lake.

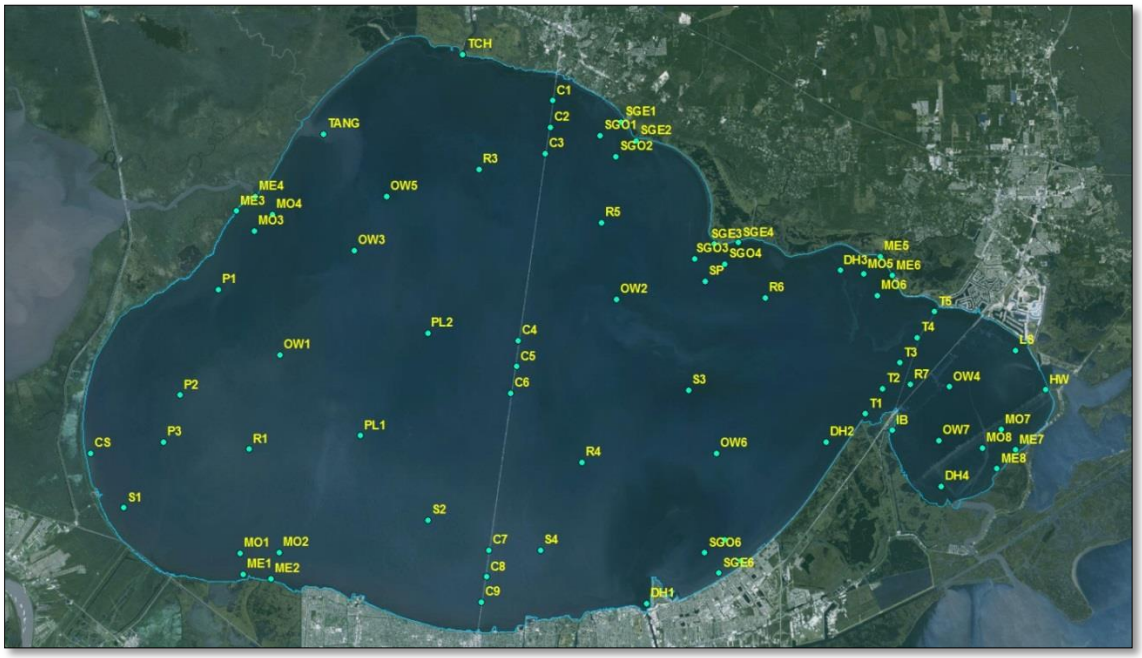

Figure 3.2 Map of receivers within Lake Pontchartrain and lake boundary (light blue).

For the placement of acoustic receivers, locations were chosen to represent a variety of habitat types in the lake. Manmade features include the central causeway (C), reefs (R), powerline structures (P), shell pads (S), single piling (SP), train trestle bridge (T), hospital wall (HW), deep holes (DH), and pipeline (PL). Natural features include cypress swamp (CS), lakeshore (LS), marsh edge (ME), marsh open (MO), seagrass beds edge (SGE), seagrass beds open (SGO), open water (OW), Tangipahoa River entrance (TANG), Tchefuncte River entrance (TCH), and Irish Bayou entrance (IB). These 75

receivers will be included in the analyses for spotted seatrout distribution discussed in more detail below.

Monthly Water Quality Analysis

To determine long term water quality trends, two YSI 6600 V2 multi-parameter sondes were placed in the westernmost (30°17'34.38" N, 90°17'54.2" W) and easternmost (30° 11' 23.64"N, -89° 46' 13.4394"W) regions of the lake; the sondes recorded water temperature (^{o}C), dissolved oxygen (mgL^{-1}), turbidity (NTU), and salinity (ppt) every thirty minutes. To determine water quality parameters with higher spatial resolution, a Dataflow system was used for the collection of field measurements during shipboard cruises. As a portable flow-through system consisting of a YSI 600XL and Turner Designs C6 fluorometer unit, it is capable of collecting high quality and high resolution biogeochemical data, including water temperature (^{o}C), dissolved oxygen (mgL^{-1}), pH, salinity (ppt), chlorophyll *a* (μgL^{-1}), hydrocarbons (ppb), turbidity (NTU), and CDOM (ppb). In addition, an integrated global positioning system (GPS) provided georeferencing information at each sample point. A transect was designed to provide adequate coverage across Lake Pontchartrain when weather (winds $<5ms^{-1}$, wave height $\leq$1m) and scheduling allowed the use of the laboratory boat. Sampling cruises were completed and the data combined with long term sampling station results to generate monthly maps representing the spatial distribution of each parameter across the lake. The complete sampling transect across Lake Pontchartrain, as well as the locations of long-term sampling stations are presented in Figure 3.3 below.

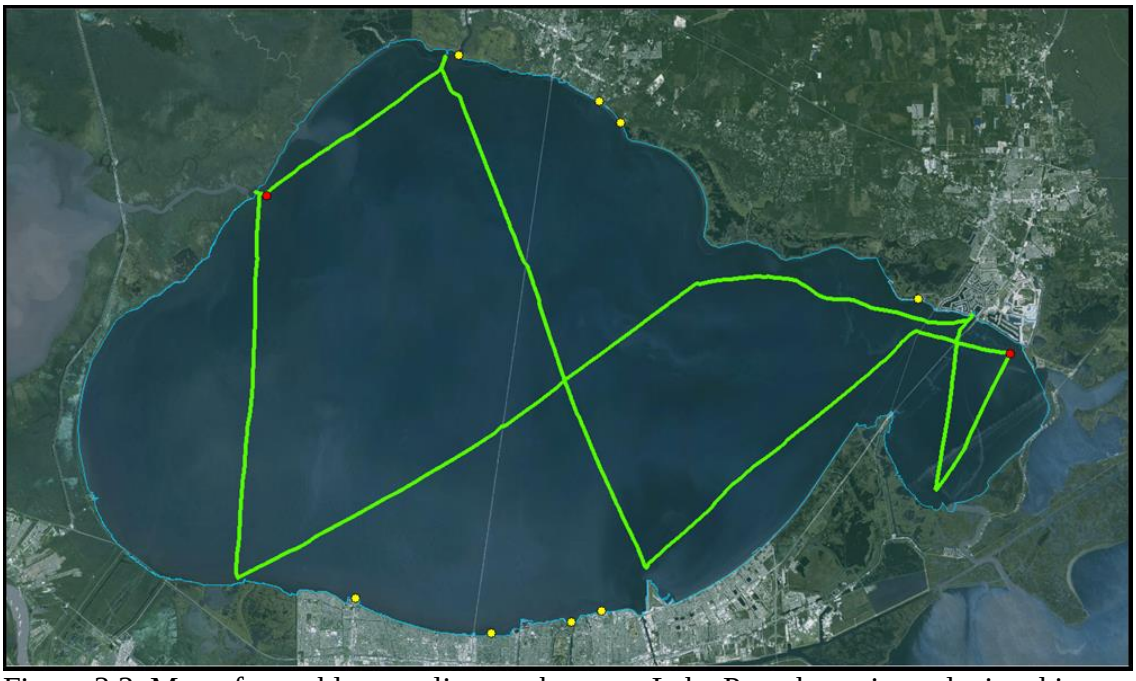

Figure 3.3 Map of monthly sampling track across Lake Pontchartrain as depicted in green, two stationary YSI 6600 V2 locations as depicted in red, and eight LPBF long-term water quality monitoring stations as depicted in yellow.

Data collected from 2013 (October), 2014 (February, March, June-December), and 2015 (January, March, April) were assessed using ArcGIS. For proper spatial analyses to be completed, the points were projected using a Lambert conformal conic projection (LCC), a projection used for the State Plane Coordinate System with the North American Datum 1983 (2011) as its reference point (ArcGIS Resource Center 2013b; ArcGIS Resources Center 2013c; National Geodetic Survey 2015). As the focus of this mapping is Lake Pontchartrain, the State Plane coordinate system designated as Louisiana South was chosen. Converting the data in this manner utilizes a mathematical transformation, allowing a curved surface to be portrayed on a flat surface while minimizing distortion between geodetic (curved) and grid (flat) distances (ArcGIS Resources Center 2013c; National Geodetic Survey 2015). Continuous water quality data collected from the stationary YSI units as well as receivers maintained by the LPBF were

combined with Dataflow water quality mapping to produce maps that represent average lake conditions for the months sampled.

Water quality data collected along the sampling transects was analyzed with ArcGIS 10.3, to interpolate between data points and provide an approximation of the true chemical conditions of the surface water (Stachelek and Madden 2015). The interpolation method chosen is the Euclidean IDW, which is a deterministic method. The process assigns cell values using a linearly weighted combination of sample points, wherein cell weight, or influence, is inversely related to distance from the point to be determined; thus the interpolation surface is dependent on neighborhood values (Stachelek and Madden 2015). This interpolation method operates on the assumption that for the variable being mapped, influence is reduced with increasing distance from the sample location. The estimated value at a prediction point (V) is therefore determined through the following equation:

$$V = \frac{\sum_{i=1}^{n} v_i \frac{1}{d_i^p}}{\sum_{i=1}^{n} \frac{1}{d_i^p}}$$

Where: p= a power parameter, d= the distance between prediction and measurement points, and VI= the measured parameter value (Stachelek and Madden 2015). The inverse of the distance is raised to a power (p) (ArcGIS Resource Center 2013a). Higher values for power increase the influence of the points nearest the sample location. The default power value of two was used for this research. Interpolation accuracy is determined using a cross-validation procedure incorporated into the IDW procedure in ArcGIS (ArcGIS Resource Center 2013a). Through this process, a data location is removed individually, its value predicted, and then the predicted value is compared to the actual value (ArcGIS 9.2 Desktop Help 2007). By comparing interpolated predictions

against the validation data set, one can assess how well the model predicts values for sampled locations and therefore how well it predicts un-sampled locations. Once completed, a scatterplot of predicted values and true values are displayed with a fitted line (regression function) and the root-mean-square prediction error (RMSPE) (ArcGIS 9.2 Desktop Help 2007; ArcGIS Resource Center 2013a). The RMSPE effectively quantifies the error in the prediction surface produced, with higher values indicating higher errors in predictions (ArcGIS Resource Center 2013a). As a well-mixed estuary with major gyres in the center, a smoothing method (factor of 0.2) was utilized and positioned in the center of the lake for the interpolation (ArcGIS Resource Center 2012).

Within ArcGIS, monthly water quality was combined with data collected from the stationary receivers. A final dataset was completed and included month, receiver ID, fish count, detections, and the biochemical variables given previously. The relationships between water quality variables were assessed using SAS 10.3 using a Pearson product-moment correlation. In using the Pearson product-moment correlation, it is assumed that the sets of variables to be examined for a relationship are continuous in nature, not categorical (Salkind 2008). In addition, it is assumed that the relationship between the paired variables is linear in nature (Salkind 2008). A resulting correlation value less than -0.6 or greater than 0.6 indicates a strong relationship between the variables compared, and as such one of the pair will be removed from consideration for further analysis to reduce error incurred through this relationship (Salkind 2008).

Generalized Linear Model of Water Quality

A generalized linear model was constructed to describe the association and interaction between water quality parameters and fish counts. Each monthly fish count was treated as a series of Bernoulli Trials, wherein a zero value was recorded for a

failure/no fish observed and a value of one recorded for a success/at least one fish observed (Agresti 2007). Trials were assumed to be identical (same probability for success) and independent (observing a fish was random event) (Agresti 2007). For this assessment, a multiple logistic regression was utilized. Equation A below mathematically defines this regression with explanatory variables and the probability of success (Y=1). Equation B provides the method to directly calculate the probability for observing a spotted seatrout. The β values determined for each explanatory variable determine the rate of increasing (if positive) or decreasing (if negative) probability of observing a spotted seatrout (Agresti 2007). To assess the significance of each component of the model, a Wald test, Likelihood Ratio, and Score test were completed. To test the Goodness of Fit, a full model (all parameters and cross products) were compared to sequentially simpler models through Deviance, a likelihood ratio statistic (Agresti 2007). Once a final model was achieved, it was assessed through the Hosmer-Lemeshow Test, which compared the observed number of successes and failures to those predicted by the model, and the Akaike Information Criterion (AIC), which assess how closely fitted values are to expected values (Agresti 2007).

A. $$\text{logit}[P(Y=1)] = \alpha + \beta_1 x_1 + \beta_2 x_2 + \cdots + \beta_k x_k$$

B. $$\pi(x) = \frac{\exp(\alpha+\beta x)}{1+\exp(\alpha+\beta x)} = \frac{e^{\alpha+\beta x}}{1+e^{\alpha+\beta x}}$$

RESULTS

High Fish Counts and Detections

To determine if water quality is a main driver in spotted seatrout distribution in Lake Pontchartrain, the months assessed were limited to those during which the weather

permitted the use of the Dataflow. Fish counts and detections for these months are discussed below, followed by their associated water quality maps.

The winter months assessed included December and February 2014, as depicted in Figure 3.4, A through D below. Fish detections were limited in December to only two individuals, recorded at the central receivers C1 and SGE3. For February, however, counts were significantly higher. The number of fish recorded at a single receiver ranged from zero to seven. Receivers that recorded four fish or more were located in the northeast area (SGO3, SGO4, SGE3, SGE4, and R6) and the central east area (S3, OW6). In December, C1 had four times the number of detections as SGE3. In February, receivers with 100 detections or more were limited to central and eastern areas. Receivers with 300 detections or more included those previously noted for high fish counts, with the exception of OW6 and the addition of receivers in the north east area (SP, DH3, MO6, MO5, OW2, and SGO1).

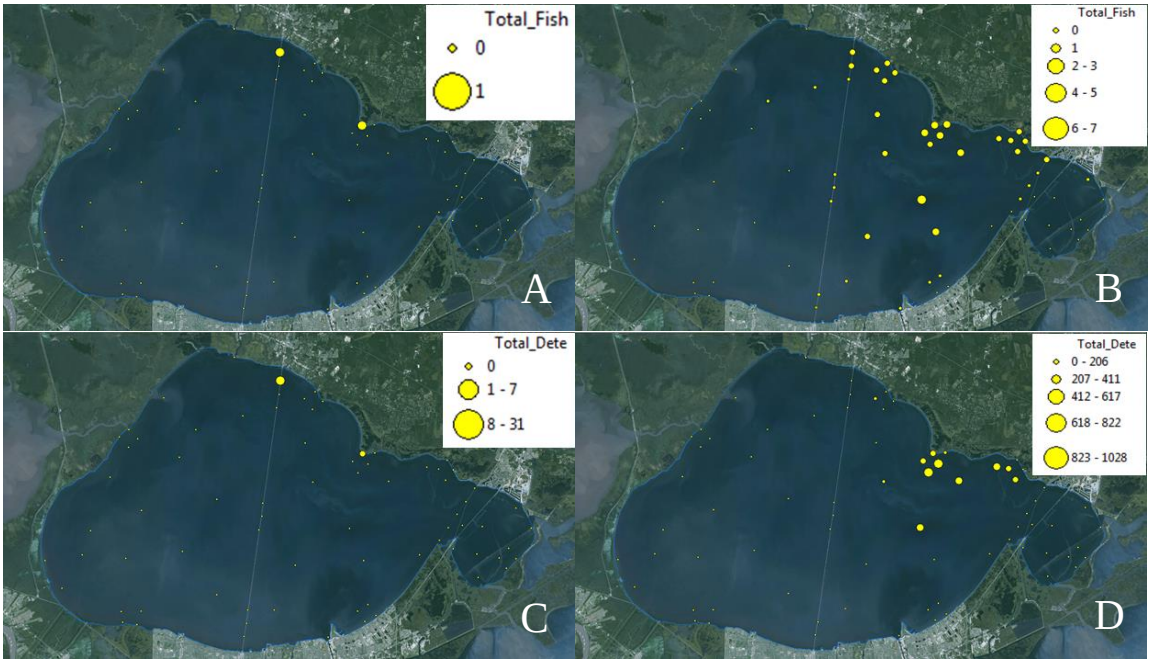

Figure 3.4 (A) Total fish count in December 2014. (B) Total fish count in February 2014. (C) Total detections in December 2014. (D) Total detections in February 2014.

With respect to the spring months (March, April, and May), fish count data concurrent to Dataflow cruises was limited to March 2014 (Figure 3.5, A and B). In March 2014, fish counts at each receiver ranged from zero to five. Receivers that recorded four fish or more were located in the central-north area (SGO1, SGO2, SGE2, and C3). Receivers with 100 detections consisted largely of receivers in the central and eastern areas. Receivers with 300 detections or more included those in the central-north area (SGE1, SGO1, C1, OW5, and R5) and northeastern area (DH3, ME6, MO6, MO5, and T4).

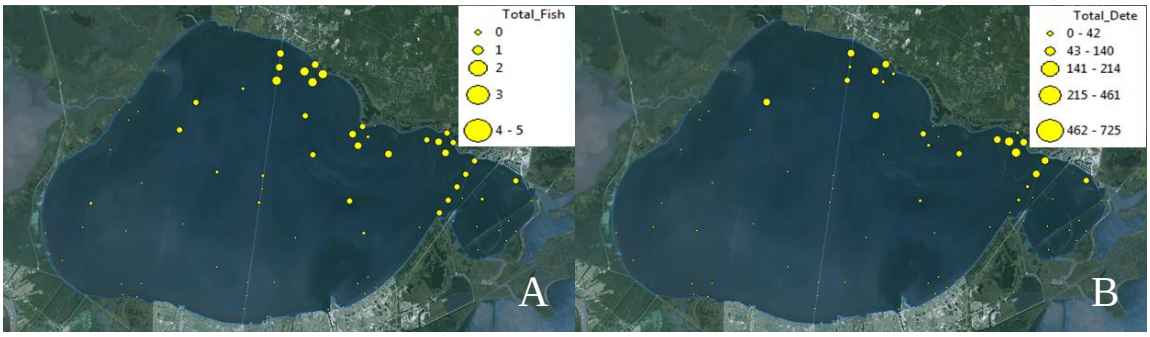

Figure 3.5 (A) Total fish count in March 2014. (B) Total detections in March 2014.

The summer months assessed included June, July, and August of 2014, as depicted in Figure 3.6, A through F below. In June, fish counts ranged from zero to two. Receivers with two or more fish include those in the northeast (ME5, MO6), east (MO7, ME7, MO8, T1, and T2), north (C1), west (OW3), and southeast (SGE6) areas. In July, only two receivers were found to have a fish recorded, one in the central north (SGE2) and one in the northeast (SGE4) area. In August, a single fish was recorded in the central north (C1), northeast (SGE3), and southwest (MO1) areas. With respect to detections in June, receivers with 60 detections or more were located in eastern and western areas. Receivers with 100 or more detections were limited to two receivers in the eastern area (LS, and DH2). In July, each receiver had five or fewer detections. In August, the

number of detections for C1 and SGE3 were no higher than six, but significantly higher (172) for MO1.

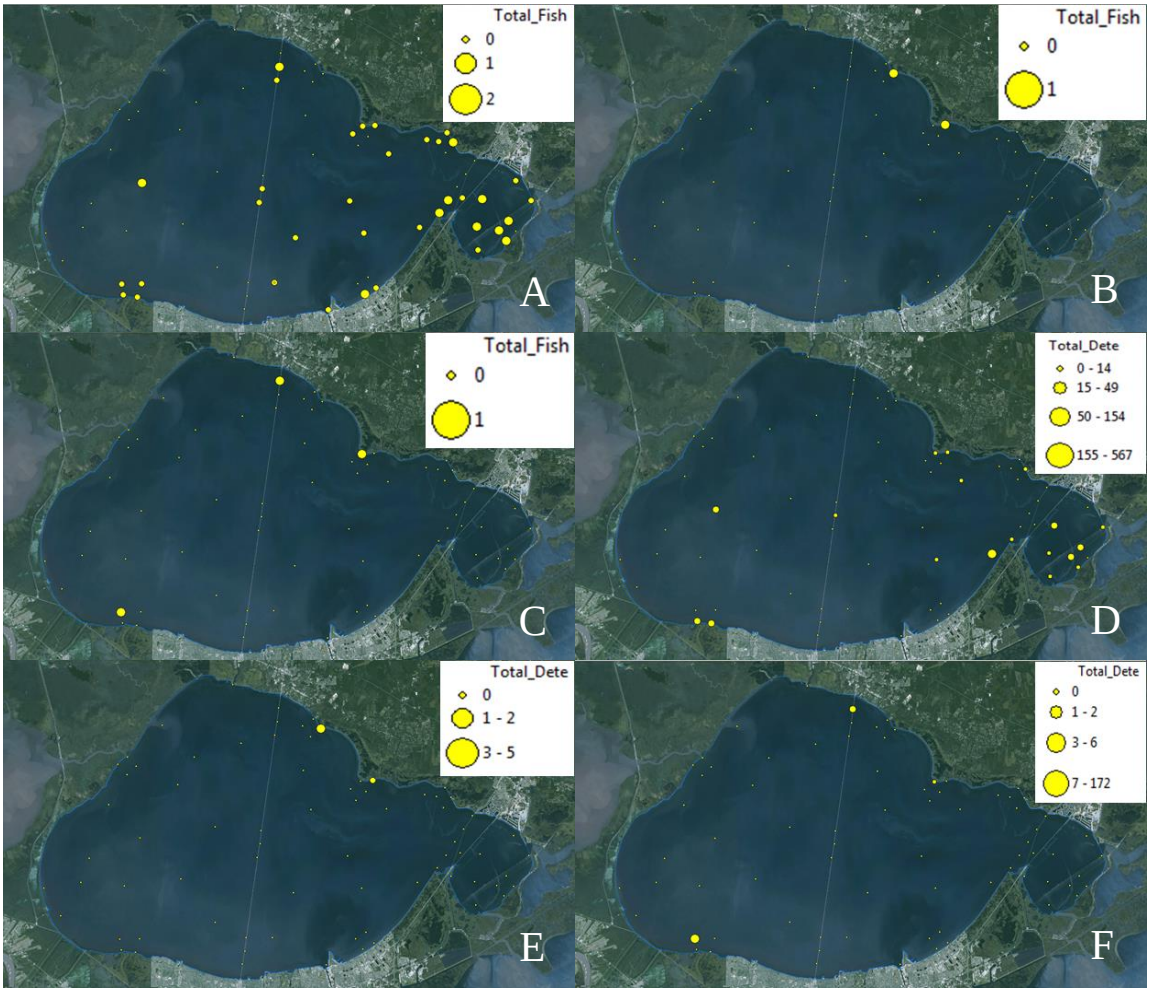

Figure 3.6 (A) Total fish count in June 2014. (B) Total fish count in July 2014. (C) Total fish count in August 2014. (D) Total detections in June 2014. (E) Total detections in July 2014. (F) Total detections in August 2014.

The fall months assessed included September, October, and November of 2014, as depicted in Figure 3.7, A through F below. The count of individual fish at a single receiver was limited to a single fish for every month within this season. In September the receivers visited included one in the central north (C1), northeast (SGE3), and southwestern (MO1) areas. In October the receivers visited also included C1 and SGE3. In November, these two receivers also registered a single individual fish. Receiver C5

(located in the central area) also registered a single individual fish. With respect to detections in September, the highest number (152) was recorded at MO1, 63 at C1, and seven at SGE3. In October, the highest count (30) was recorded at SGE3 and the lower count (10) was recorded at C1. This detection pattern was similar in November, with 48 detections at SGE3 and 28 at C1. Just two detections were recorded at C5.

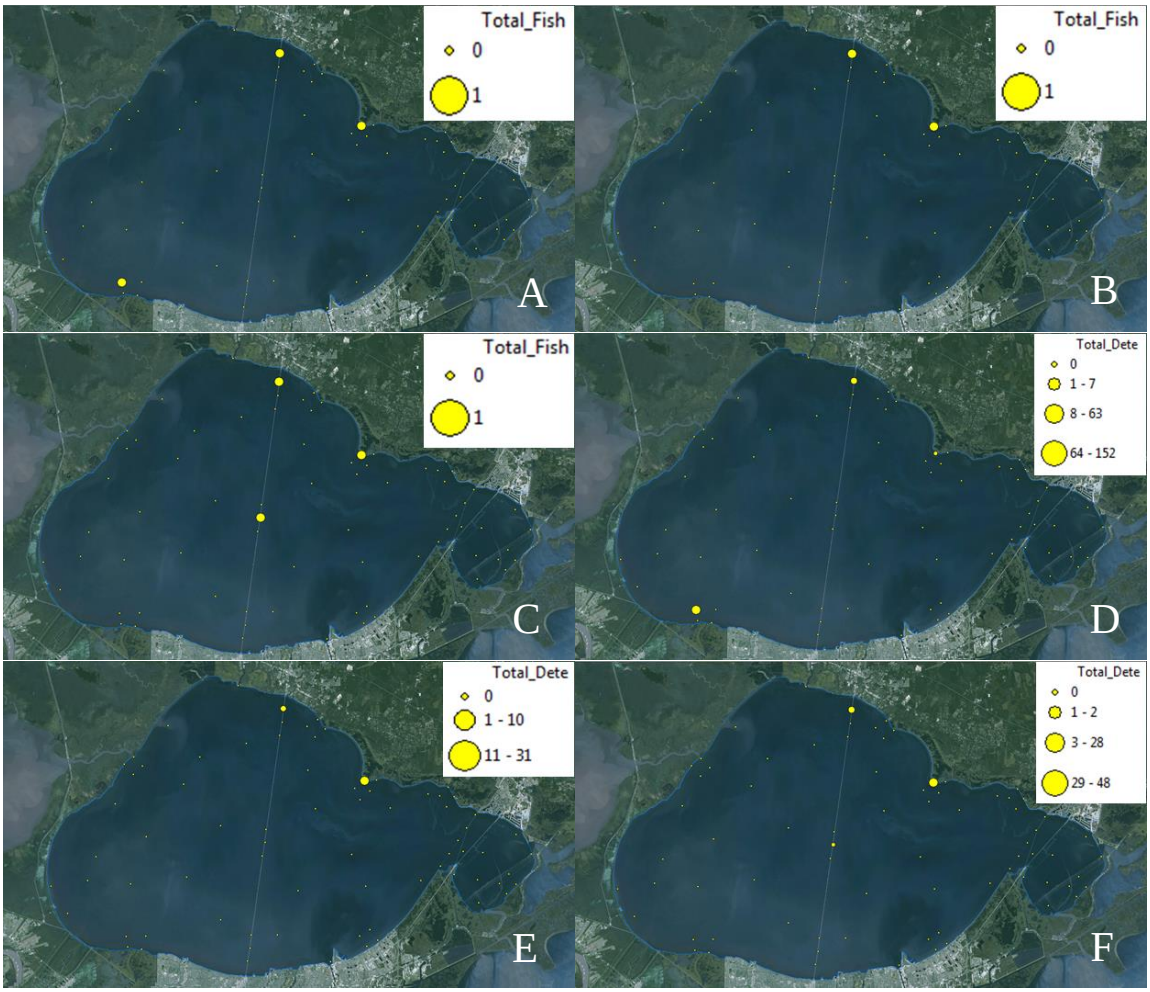

Figure 3.7 (A) Total Fish count in September 2014. (B) Total fish count in October 2014. (C) Total fish count in November 2014. (D) Total detections in September 2014. (E) Total detections in October 2014. (F) Total detections in November 2014.

Monthly Water Quality Analysis- CDOM

CDOM, or colored dissolved organic matter, consists of naturally-occurring humic acids from the decomposition of detritus (Turner Designs 2015). Chromophores contained in this material absorb sunlight and therefore fluoresce after absorbing the light (Turner Designs 2015). CDOM ranges in the lake for the winter and spring months (Figure 3.8, A through F), were very similar, from 26.4 to 86.17 ppb overall. The highest concentrations in the winter were identified in the vicinity of Pass Manchac in the northwest, and extended to the central north area (Tchefuncte River) for both seasons. In the spring, however, high readings were also found in the southwest and northeastern areas. The majority of the lake in the winter was characterized by the lowest CDOM levels, from 26.40 to 38.93 ppb. In the spring, the area characterized by low CDOM concentrations was smaller in extent but with a similar range, from 26.92 to 41.77 ppb.

In the summer months (Figure 3.8, G through I), CDOM concentrations ranged from 25.70 to 76.13 ppb. In the fall (Figure 3.8, J), the minimum value was similar, but maximum value only reached 55.93 ppb. Areas with the highest concentrations were located extending from the northwest (Pass Manchac) to the central north area for both seasons, but the spatial extent was reduced in the fall. The southwest area had the lowest CDOM readings for the summer (25.7 to 38.13 ppb) but the highest readings in the fall (39.42 to 55.94 ppb). In general, the largest area of the lake was dominated by the relatively lower readings in the summer and fall, from 25.7 to 47.63 ppb. It should be noted that due to equipment complications in the fall, CDOM mapping was limited to September 2014. With the highest RMSPE of 0.64 in March 2015, the maps below are good representations of the spatial distribution of CDOM in the lake.

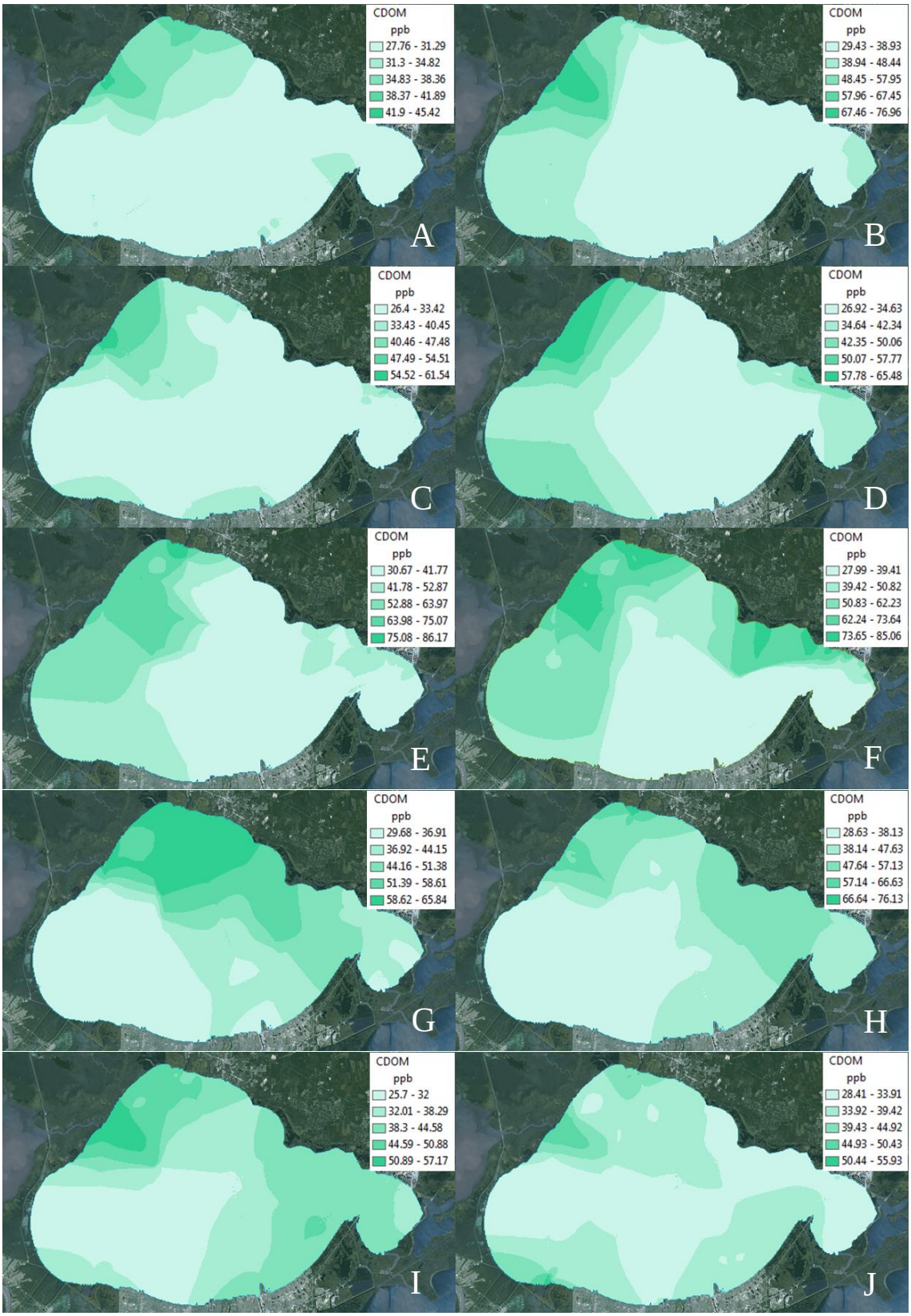

Figure 3.8 CDOM distribution in (A) December 2014, (B) January 2015, (C) February 2014, (D) March 2014, (E) March 2015, (F) April 2015, (G) June 2014, (H) July 2014, (I) August 2014 and (J) September 2014.

Monthly Water Quality Analysis- Hydrocarbons

Hydrocarbons are highly fluorescent and their concentration is often used as an indicator of contamination by crude oil, gasoline, or motor oil (Turner Designs 2015). Thus the concentration of hydrocarbons was assessed in Lake Pontchartrain's surface waters in the winter (Figure 3.9, A through C), spring (Figure 3.9, D through F), summer (Figure 3.9, G through I), and fall seasons (Figure 3.9, J) . Hydrocarbon ranges for December, February, and March 2014 were comparable, ranging from 131.8 to 369.5 ppb. The range for January (239.2 to 628.4 ppb) and the spring months of March and April 2015 (225.6 to 706.1 ppb) represented higher hydrocarbon concentrations. The areas characterized by these high values extended from the northwest area (Pass Manchac) to the central north area (near Tchefuncte River) for both the winter and spring seasons. In the spring, additional areas in the southwest and the northeast were also categorized by relatively high hydrocarbon concentrations. The majority of the lake remained in the lowest range of hydrocarbon concentrations for these two seasons. The range in this area was from 131.8 to 254.1 ppb for December, February and March 2014. For January and the remaining spring months, it ranged from 225.6 to 338.3 ppb.

Hydrocarbon concentrations for the summer (June, July, and August) shared a similar range, from 120.7 to 380.8 ppb. The fall (September) displayed a range from 133.7 to 278.6 ppb. The area with the highest concentrations of hydrocarbons were the same in these seasons as noted in the winter and spring months. In addition, the eastern area of the lake was characterized by relatively high hydrocarbon readings for the summer. The largest area of the lake, however, was noted to have the lowest readings, with an overall range from 120.7 to 184.7 ppb. With the highest RMSPE of 5.11 in March 2015, the maps below are good representations of the spatial distribution of hydrocarbons in the lake.

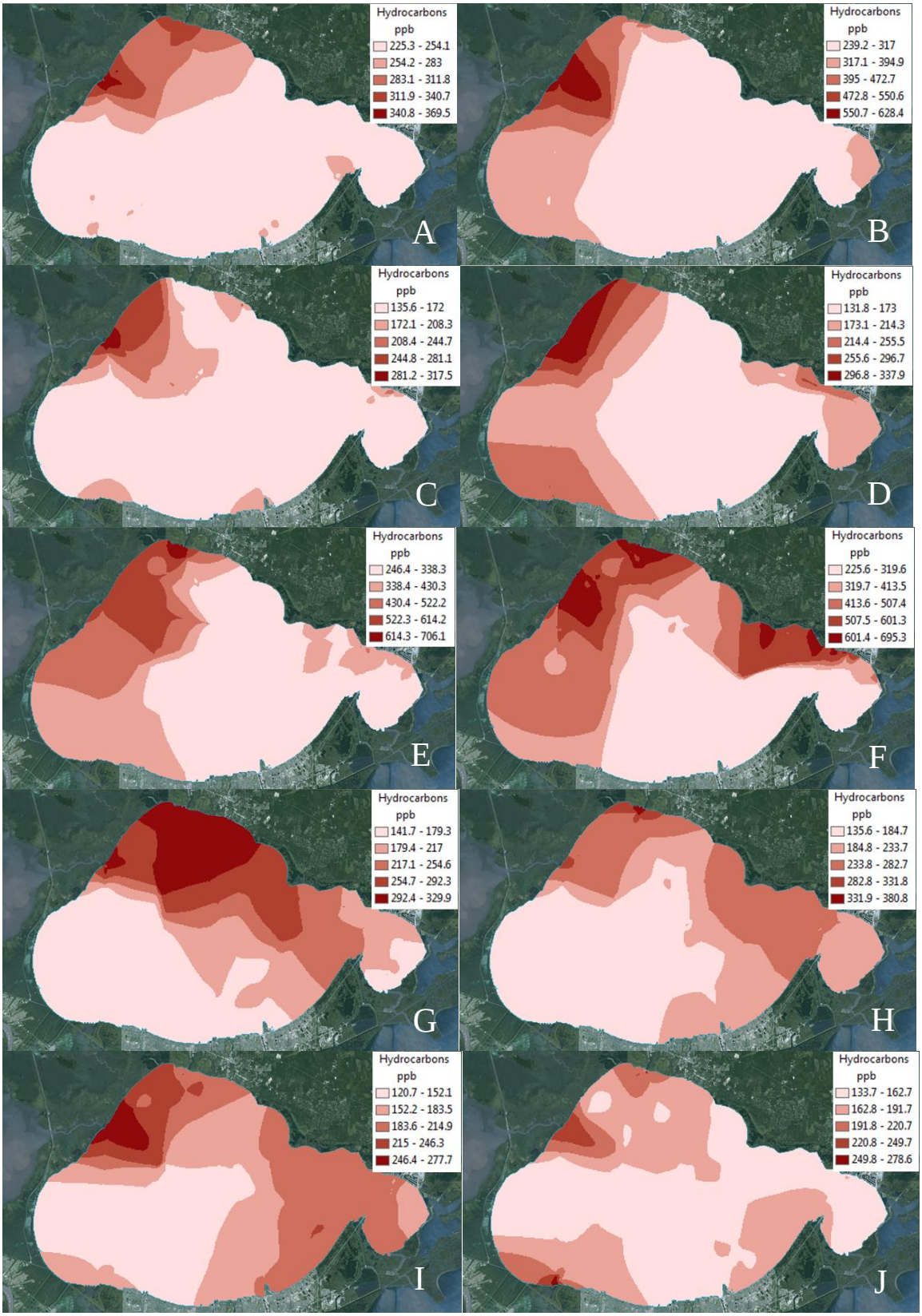

Figure 3.9 Hydrocarbon distribution in (A) December 2014, (B) January 2015 (C) February 2014, (D) March 2014, (E) March 2015, (F) April 2015, (G) June 2014, (H) July 2014, (I) August 2014, and (J) September 2014.

Monthly Water Quality Analysis- Turbidity

Lake Pontchartrain is far more turbid than freshwater lakes or marine waters due primarily to continual re-suspension of sediments produced through wind stress (Flocks et al. 2009b). In the winter months of December 2014, February 2014, and January 2015, turbidity values ranged from 0.56 to 25.99 NTU (Figure 3.10, A through C). This range was comparable for March 2014 and 2015 (Figure 3.10, D and E), but the widest range (6.16 to 58.10 NTU) was detailed in April 2015 (Figure 3.10, F). For both seasons, an area of high turbidity was located in the northwest (Pass Manchac) and southwest areas. Additional areas characterized by high turbidity values were detailed in the easternmost area in January, in the central-south area in April, and extending from the southeast to the northeast in February. The majority of the lake, however, consisted of low turbidity conditions for both seasons, ranging from 0.75 to 16.55 NTU overall.

Turbidity values in the summer (Figure 3.10, G through I) were most similar between June and July, ranging from 1.68 to 24.93 NTU. This range was reduced in August (1.74 to 12.14 NTU) and September (0.77 to 17.86NTU). Areas of high concentration were detailed in the central-north area in June, in the easternmost area in July and August, in the northwest (by Pass Manchac) for August, and very small areas along the southern shoreline in September (Figure 3.10, J). The largest area of the lake for these two seasons was characterized by the lowest turbidity readings, from 0.77 to 6.33 NTU overall. With the highest RMSPE of 0.996 in April 2015, the maps below are good representations of the spatial distribution of turbidity in the lake.

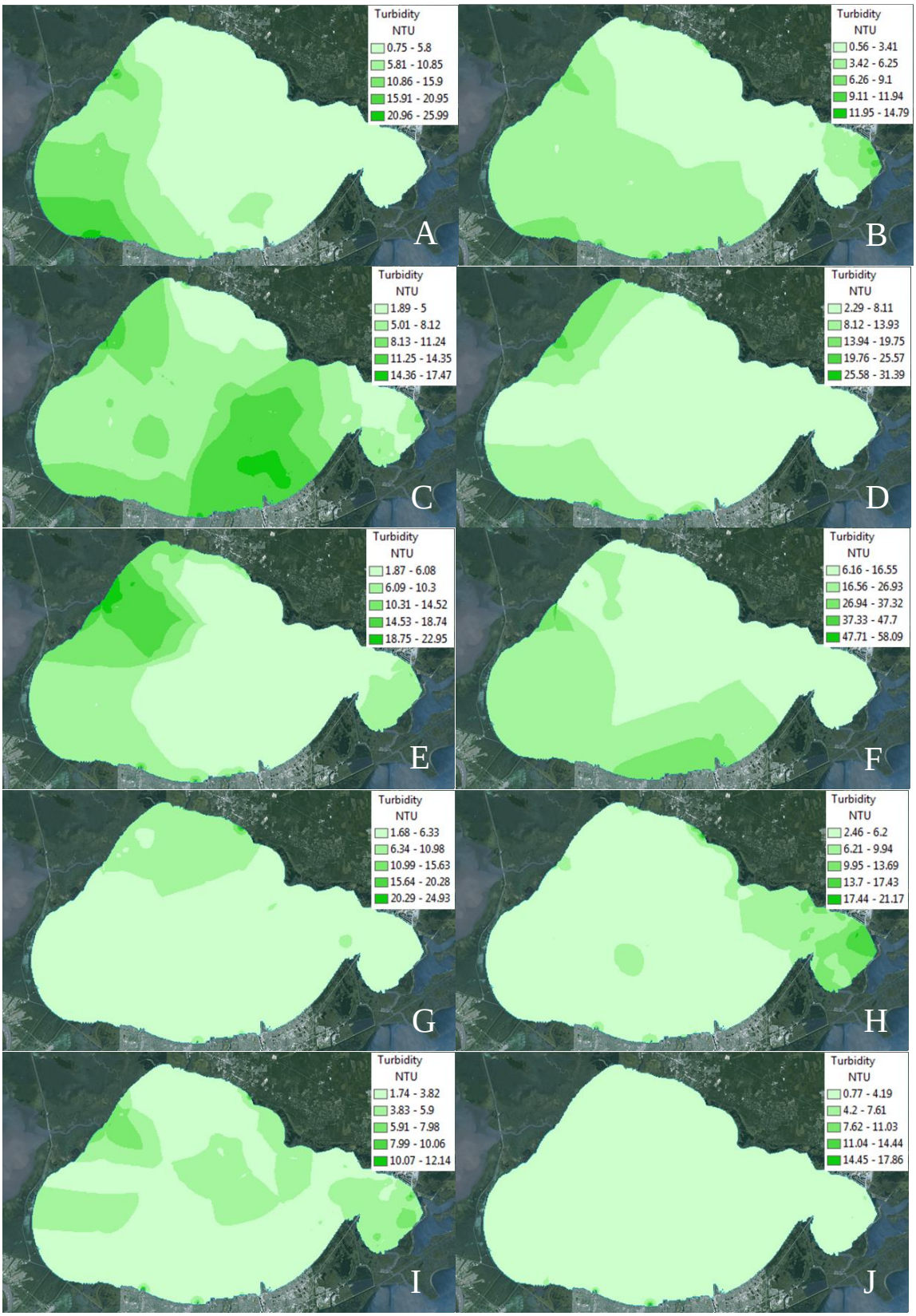

Figure 3.10 Turbidity distribution in (A) December 2014 (B) January 2015, (C) February 2014, (D) March 2014, (E) March 2015, (F) April 2015, (G) June 2014, (H) July 2014, (I) August 2014 and (J) September 2014.

Monthly Water Quality Analysis- Dissolved Oxygen

Surface dissolved oxygen (DO) for the lake typically ranges from 5.6 to 10.3 mgL^{-1} (Hastings 2009). While the long term average air temperature is 19^{o}C, colder winter temperatures (12^{o}C) can allow higher levels of DO while warmer summer temperatures (28^{o}C) can exceptionally reduce levels of DO in the lake (Xu and Wu 2006; Kansheng and Xu 2007). Accordingly, DO ranges were found to be very similar and very high when assessing the winter months, ranging from 8.42 to 14.08 mgL^{-1}. For all of the winter months (Figure 3.11, A through C), the largest area of the lake consisted of the highest levels of DO, ranging from 12.35 to 14.08 mgL^{-1}. In the spring the DO range (5.27 to 14.08 mgL^{-1}) was similar. In the spring months (Figure 3.11, D through F), the largest area of the lake also consisted of the highest DO values, but for March 2014 and 2015 the high range was from 10.12 to 14.08 mgL^{-1} while the range for April the DO in this area ranged from 8.64 to 10.86 mgL^{-1}.

In the summer months (Figure 3.11, G through I), DO values appeared to decline from June (5.07 to 10 mgL^{-1}) through August (1.91 to 7.29 mgL^{-1}). For June, the largest area of the lake was characterized by high DO levels (8.04 to 10.01 mgL^{-1}) but in July and August the majority of the lake had far lower values (1.91 to 5.19 mgL^{-1}). DO values in the fall (Figure 3.11, J and Figure 3.12, A through C) followed an opposite trend, with low values (3.75 to 7.52 mgL^{-1}) in September, higher levels (6.06 to 11.75mgL^{-1}) in October 2013 and 2014, and the highest readings (9.33 to11.26 mgL^{-1}) in November 2014. Following this pattern, the largest area in the lake in September was determined to have the lowest readings (6.02 to 7.52 mgL^{-1}) while the other fall months this area was characterized by higher values (7.90 to 11.75 mgL^{-1}). With the highest RMSPE of 0.909 in September 2014, the maps below are good representations of the spatial distribution of dissolved oxygen in the lake.

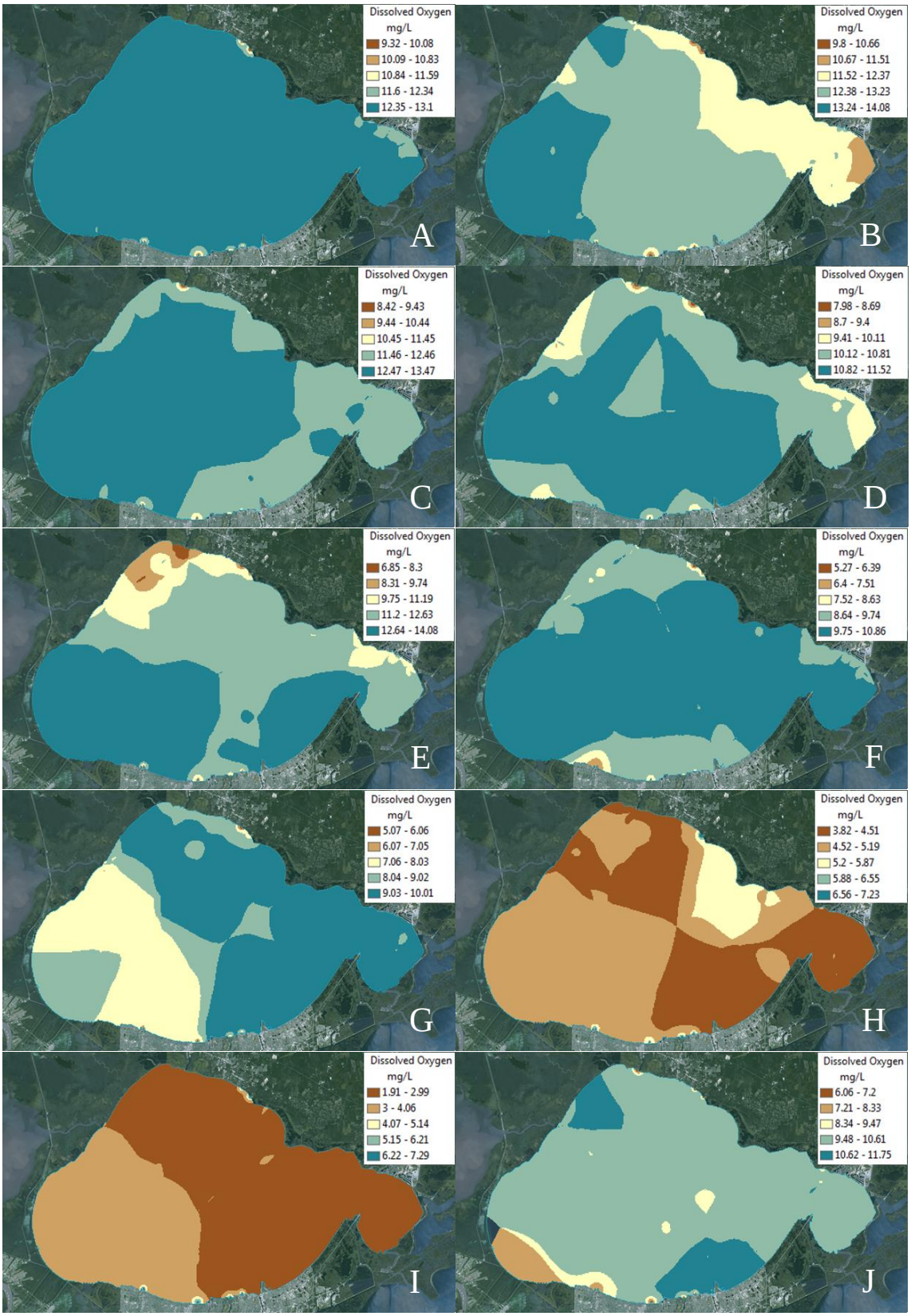

Figure 3.11 Dissolved oxygen distribution in (A) December 2014, (B) January 2015, (C) February 2014, (D) March 2014, (E) March 2015, (F) April 2015, (G) June 2014, (H) July 2014, (I) August 2014, and (J) October 2013.

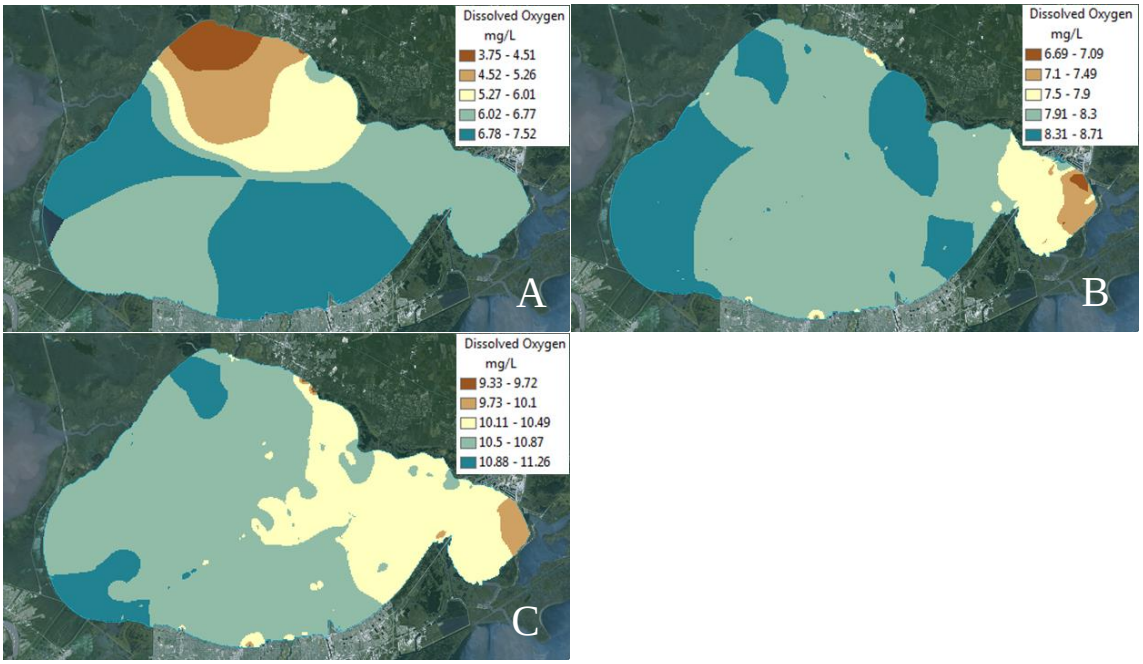

Figure 3.12 Dissolved oxygen distribution in (A) September 2014, (B) October 2014 and (C) November 2014.

Monthly Water Quality Analysis- Temperature

As noted previously, seasonal air temperature variation (which translates to water temperature variations) observed for Lake Pontchartrain include low values (12^{o}C) in the winter months and higher values (28^{o}C) in the summer months. In the winter months (Figure 3.13, A and B and Figure 3.14, A), the water temperature range was low, from 9.91^{o}C to 15.58^{o}C. While the temperature ranges were limited, the patterns of highs and lows varied by month and by the time of day an area was assessed. Areas noted for higher temperatures (13.84^{o}C to 15.58^{o}C overall) were located in the southwest area in December and January but in the southeast and central north areas in February. An additional area of relatively high temperature was noted in the along the northeastern shoreline in December. Cold temperatures remained for the spring months (Figure 3.14, B through D), ranging from 13.44^{o}C to 22.35^{o}C in March 2014 and 2015. A slightly warmer temperature range (21.36^{o}C to 25^{o}C) was present in April. Similarly, the largest

area of the lake was colder in March 2014 and 2015 (17.08°C to 21.11°C) when compared with April (22.83°C to 23.55°C).

The range of water temperatures across the lake increased throughout the summer months (Figure 3.14, E through G), from 27.81°C to 35.29°C. Again, the temperature range was limited and the patterns of highs and lows varied by the time of day an area was assessed. The areas with the highest temperatures for June, July, and August were consistently located in the southwest area of the lake and a smaller area of the northeast. For June, an additional area in the central north was also characterized by high water temperatures. Water temperatures in the fall (Figure 3.14, H through J and Figure 3.15), ranged from 22.98°C to 31.40°C in October 2013, October 2014, and September 2014. For these months, the highest temperatures were noted in the west, central north, and easternmost areas. For these months, the largest area of the lake was characterized by temperatures from 23.31°C to 31.40°C. In November, however, the temperature range declined significantly, ranging from 11.59°C to 15.94°C. The largest area of the lake in November was noted to be much colder than the other fall months, ranging from 11.59°C to 14.20°C, with warmer areas limited to small patches along the northern shoreline. With the highest RMSPE of 0.21 in March 2015, the maps below are good representations of the spatial distribution of temperature in the lake.

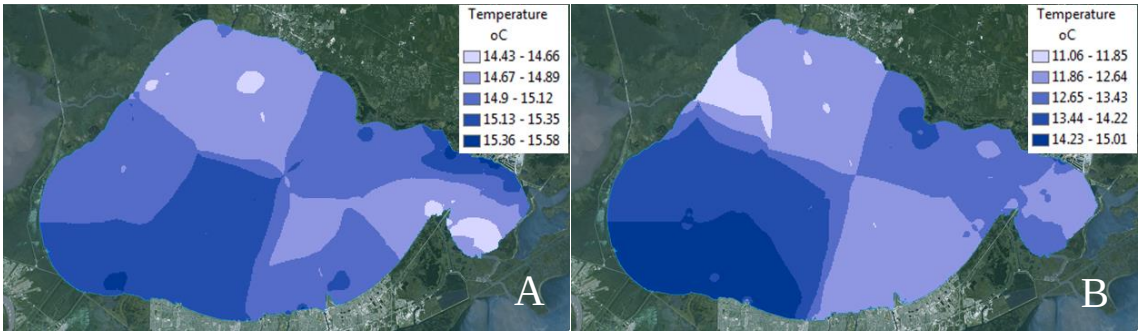

Figure 3.13 Temperature distribution in (A) December 2014 and (B) January 2015.

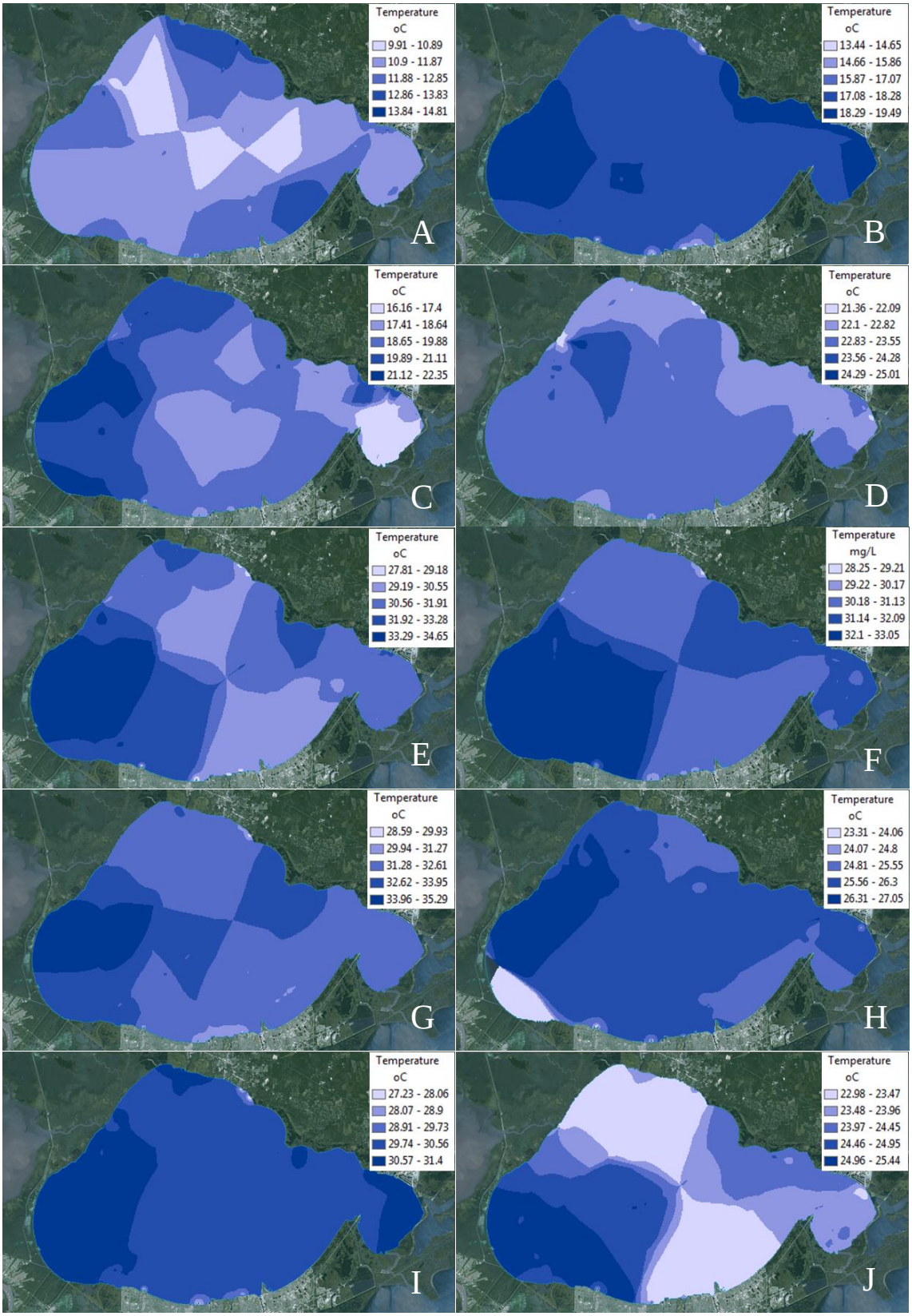

Figure 3.14 Temperature distribution in (A) February 2014, (B) March 2014, (C) March 2015, (D) April 2015, (E) June 2014, (F) July 2014, (G) August 2014, (H) October 2013, (I) September 2014, and (J) October 2014.

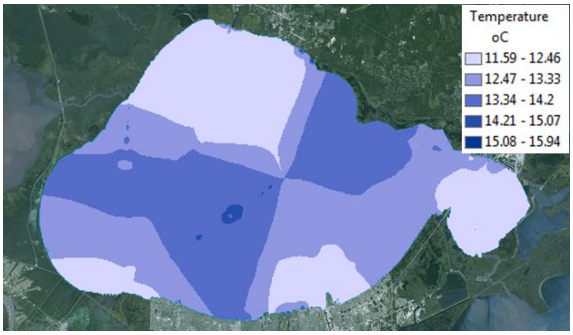

Figure 3.15 Temperature distribution in November 2014.

Monthly Water Quality Analysis- Salinity

With the influences of the freshwater rivers as well as hydrologic connections to Lake Maurepas and Lake Borgne, Lake Pontchartrain has a unique salinity regime. In the winter and spring, salinity ranges varied by month, but all were relatively low. During the winter months (Figure 3.16, A through C), salinities reached a low of 0.88 ppt and highs of 3.35 ppt in February, 5.10 ppt in January, and 7.27 ppt in December. Spring salinities peaked at 3 ppt (Figure 3.16, D through F). In December and January high salinity values were limited to the easternmost and northeastern edge of the lake, with a larger central area having mid-range salinity values from 2.65 to 4.73 ppt. The largest area of the lake for February and the spring months consisted of very low salinities, from 1.79 to 3.35 ppt overall.

Low salinity values continued to characterize the lake in the summer months (Figure 3.17, A through C), with June and July, ranging from 0.12 to 2.03 ppt. In August, however, the maximum salinity was recorded at 6.92 ppt. Nevertheless, the largest area of the lake was characterized as having very low salinities for all three months, reaching only a maximum of 2.87 ppt. In the fall months (Figure 3.17, D through G), the salinity range (0.89 to 6.59 ppt) was very similar for October 2013 and November 2014. In September and October of 2014 the lowest salinity reading was similar (0.7 ppt) but the highest value in September (8.11 ppt) was far below the 11.02

ppt reading for October 2014. Overall, the highest salinities were located in the easternmost area of the lake and the lowest readings were located in the western side. The salinity ranges that dominated the largest area of the lake in all of the fall months were very close in value, from 0.7 to 4.87 ppt. With the highest RMSPE of 0.065 in October 2014, the maps below are good representations of the spatial distribution of salinity in the lake.

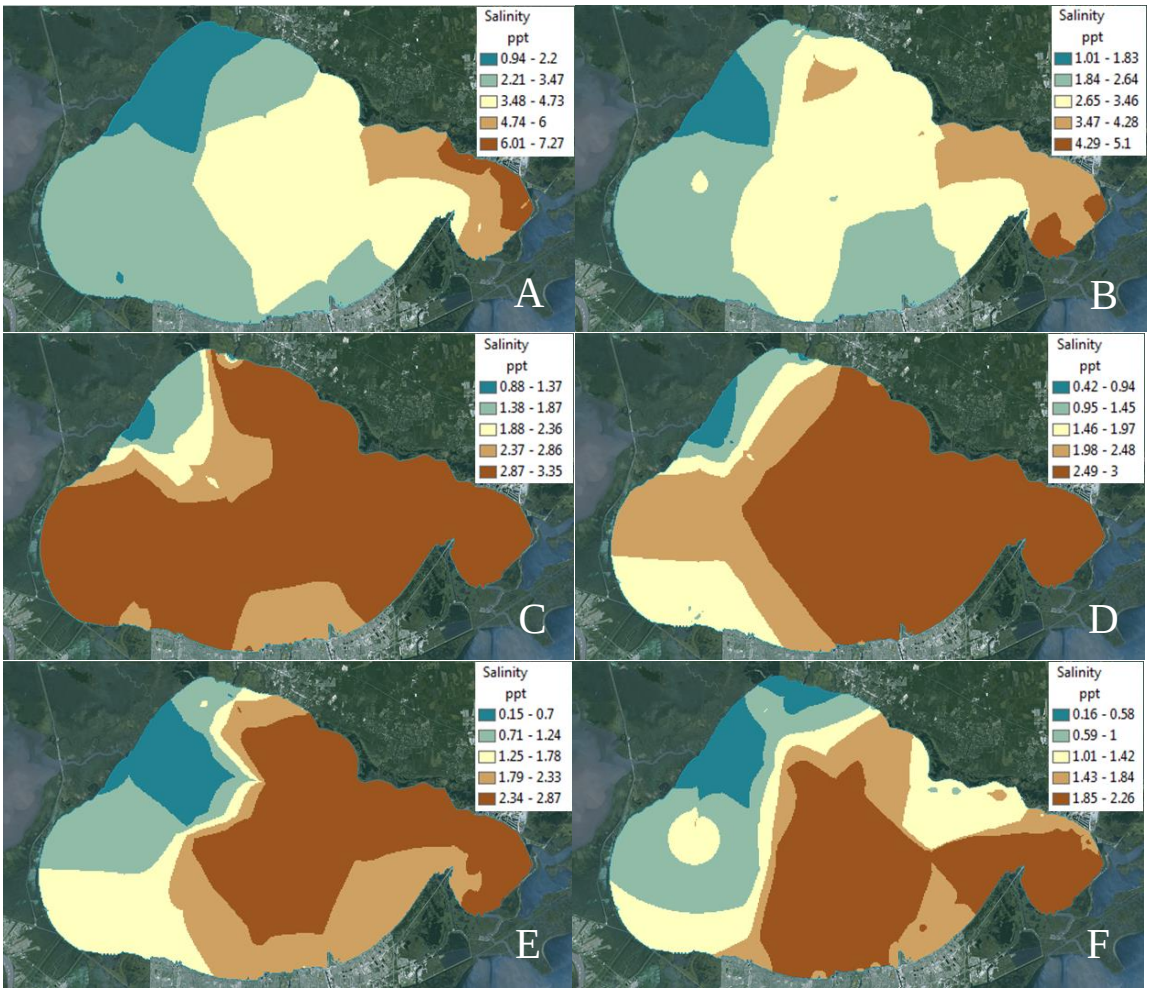

Figure 3.16 Salinity distribution in (A) December 2014, (B) January 2015, (C) February 2014, (D) March 2014, (E) March 2015, and (F) April 2015.

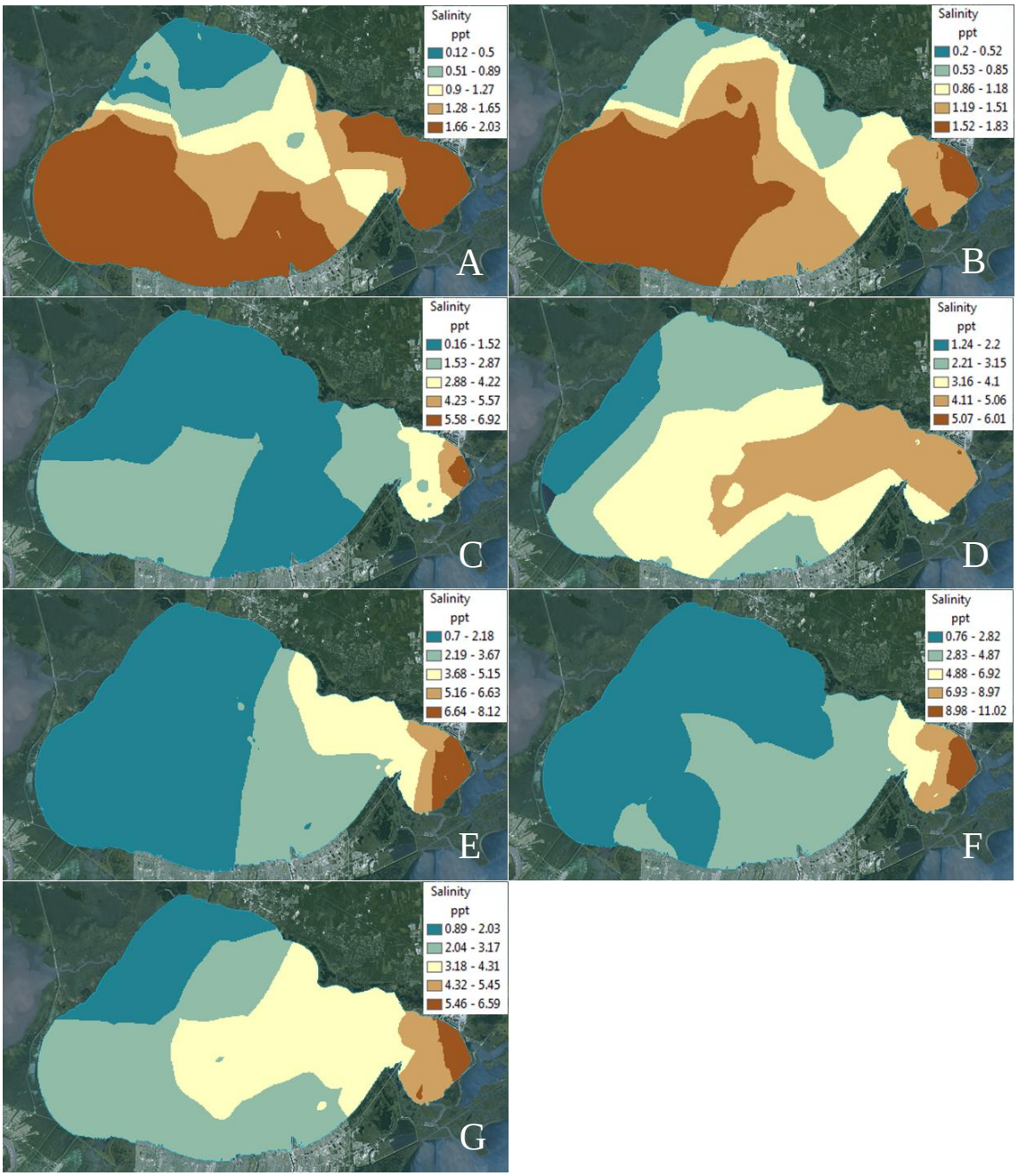

Figure 3.17 Salinity distribution in (A) June 2014, (B) July 2014, (C) August 2014, (D) October 2013, (E) September 2014, (F) October 2014 and (G) November 2014.

Monthly Water Quality Analysis- Chlorophyll *a*

Chlorophyll *a* concentrations are a tool largely used to assess the distribution and abundance of photosynthetic microorganisms as this pigment is found in all species of algae and can be read *in-vivo* (within living organisms) (Turner Designs 2015). In the winter months (Figure 3.18, A and B and Figure 3.19, A), the concentrations of this

pigment were very low, ranging from 0 to 6.94 μgL^{-1}. In the spring months (Figure 3.19, B through D), March 2014 and 2015 had a similar range to the winter months, but in April chlorophyll *a* concentrations reached a maximum of 16.24 μgL^{-1}. The areas with the highest readings were located in the northwest area (Pass Manchac) for both seasons. Additional areas of relatively high readings occurred in the southwest area in December as well as March 2014 and 2015, the easternmost corner in January, the central south area in April, and a large swathe from the southeastern area to the northeastern area in February. The largest area of the lake was characterized by low values, from 0 to 4.64 μgL^{-1}, for both seasons.

Chlorophyll *a* concentrations remained low throughout the summer and fall months (Figure 3.19 E through H), from 0 to 5.66 μgL^{-1} overall. An area of relatively high chlorophyll *a* concentrations was located in the northwest area in most months. In September 2014, however, only a small patch of high concentration (2.47 to 3.09 μgL^{-1}) was identified in the southwest area. Additional areas of relatively high readings occurred in the central-north area in June and the easternmost area in July and August. The largest area of the lake's surface waters was noted as having the lowest chlorophyll readings (0 to 2.5 μgL^{-1}) for both seasons. With the highest RMSPE of 0.21 in April 2015, the maps below are good representations of the spatial distribution of chlorophyll *a* in the lake.

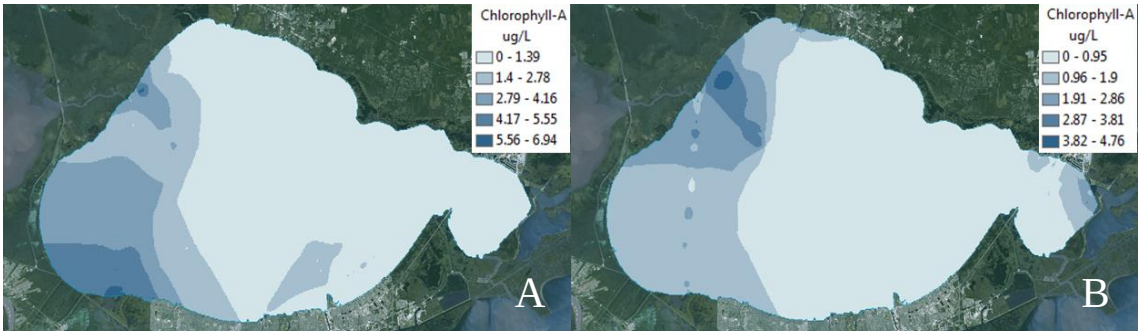

Figure 3.18 Chlorophyll *a* distribution in (A) December 2014 and (B) January 2015.

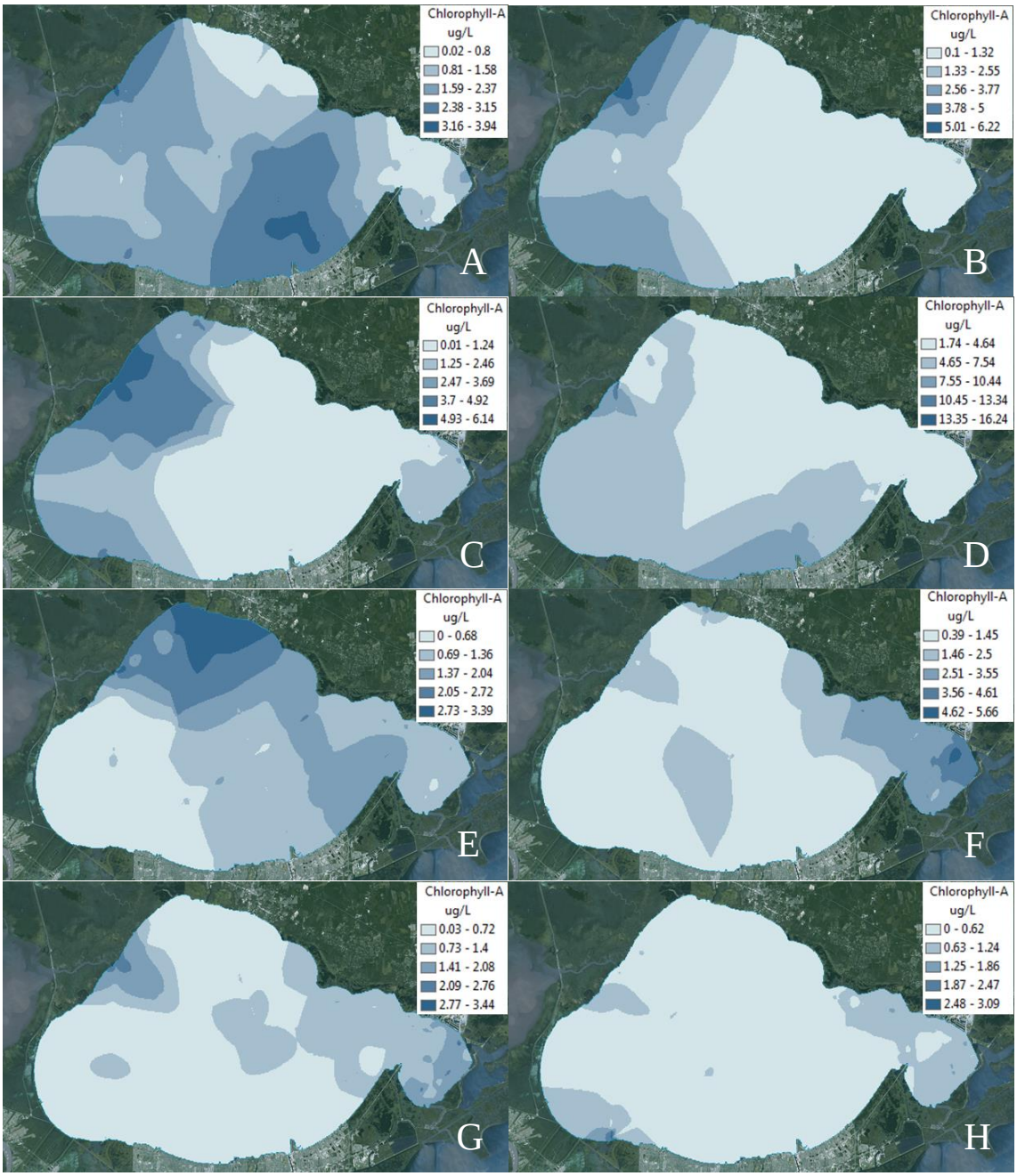

Figure 3.19 Chlorophyll *a* distribution in (A) February 2014, (B) March 2014, (C) March 2015, (D) April 2015, (E) June 2014, (F) July 2014, (G) August 2014, and (H) September 2014.

Monthly Water Quality Analysis- Correlations

Due to technical complications, the months of October and November in 2014, have a limited scope with respect to water quality parameters. For these months, only data collected with the YSI unit was available (dissolved oxygen, temperature, and

salinity). As such, they were assessed separately from the remaining months, which have data collected by the Dataflow unit and include all seven water quality parameters. For these two months, a strong negative correlation (-0.96) was determined between dissolved oxygen and temperature. No strong correlation was found between temperature and salinity, or salinity and dissolved oxygen.

For February, March, June, July, August, September, and December of 2014, strong positive correlations were found between hydrocarbons and CDOM (0.68) and between turbidity and chlorophyll *a* (0.93). In addition, strong negative correlations were observed between salinity and CDOM (-0.62) and between temperature and dissolved oxygen (-0.87). Since correlated data can introduce significant error into subsequent statistical analyses, one of the two parameters determined to have a strong relationship are removed from further consideration. CDOM and turbidity were kept from the positive correlations, but CDOM was then dropped due to a strong relationship with salinity. Temperature was chosen for further consideration in place of dissolved oxygen from the negative correlations. The final set of water quality parameters used for additional assessments included salinity, temperature, and turbidity. Table 3.1 below provides the results of the Pearson product-moment correlation analysis.

Table 3.1 Results of Pearson product-moment correlation between seven water quality parameters, including CDOM, Chlorophyll *a*, dissolved oxygen (DO), hydrocarbons, salinity, temperature (temp), and turbidity.

	CDOM	Chlorophyll a	DO	Hydro-carbons	Salinity	Temp
CDOM						
Chlorophyll a	0.45					
DO	-0.31	0.11				
Hydrocarbons	0.68	0.43	0.16			
Salinity	-0.62	-0.29	0.41	-0.25		
Temp	0.38	-0.13	-0.87	-0.08	-0.45	
Turbidity	0.29	0.93	0.22	0.31	-0.26	-0.3

Generalized Linear Model of Water Quality

Due to the high error induced when building a binomial model where there are very few successes/failures, it was determined those months with three or fewer fish detected in the entire lake would be removed from the process of model building. Months with scarce data do not provide enough information about conditions that affect the probability of observing a spotted seatrout, and highly skew the data. Due to the limited area covered by the 75 selected receivers (at a range of 500m, they would cover approximately 59.25 km^2 out of a possible 1630km^2, ~3.6% of the total lake area), such conditions were possible. With these considerations, the months used in model building included February, March, and June of 2014. Each month represented a different season. A full model (all parameters and cross products) was compared to sequentially simpler models (backward elimination) for the best fit, as detailed in Table 3.2 below.

Table 3.2 Backward elimination of variables from a full model incorporating the influences of salinity (Sa), temperature (Te), and turbidity (Tu) on the probability of observing a spotted seatrout.

Model	Predictors	Deviance	Df	AIC	Models Compared	Difference
(1)	$Sa * Te + Sa * Tu + Te * Tu$	281.1723	218	295.1723	Full Model	
(2)	$Sa + Te + Tu$	282.0002	221	290.0002	$(2) - (1)$	0.8279 (df=3)
(3)	$Sa + Te$	282.0242	222	288.0242	$(3) - (2)$	0.024 (df=1)
(4)	Sa	296.0718	223	300.0718	$(4) - (3)$	14.0476 (df=1)
(5)	Te	311.3035	223	315.3035	$(5) - (3)$	29.2793 (df=1)
(6)	None	311.6984	224	313.6984	$(6) - (3)$	29.6742 (df=2)

Using a Chi-squared distribution, the differences in the deviance between each model as well as the degrees of freedom were compared, progressing from the most complex (full) model to sequentially simpler models. If these differences were not more extreme than the critical value, the two models being compared were not considered statistically significantly different and the simpler model could be used to appropriately model the data (Agresti 2007). When compared to the full model, the main effects model (Sa +Te +Tu) was not significantly different. Thus the interactions were removed. When turbidity was removed, the two-parameter model (containing only salinity and temperature), was not significantly different from the main effects model. As such, turbidity was removed. When salinity or temperature was removed from the two-parameter model, however, the single-parameter model was significantly different. Thus both parameters were important to the model's results. As a final step, the two-parameter model was tested against one including only the intercept and was found to be significantly different, indicating that salinity and temperature are necessary components in the model for determining the likelihood of observing spotted seatrout.

To test model fit, the AIC value determined for the two-parameter model (288.02) was found to be the lowest among those tested and therefore represented the best fitting model. The results from the Hosmer-Lemeshow Test also indicated that the two-parameter model was adequately fitting the data (Agresti 2007). With a test value of 9.33 (8 df) and a p-value of 0.32, the null hypothesis of adequate model fit could not be rejected. Finally, when addressing the number of explanatory variables, a rule of thumb is at least ten outcomes (at least ten successes or failures) for each predictor, especially if the data is unbalanced (Agresti 2007). With Y=1 (successes) occurring 109 times and Y=0 (failures) occurring 116 times, the model is well balanced and two predictors are appropriate.

Once the model was found to adequately fit the data, another consideration was the β values assigned by the model to each water quality parameter. For both salinity and temperature, their respective β values indicated a strong positive effect on the probability of observing a spotted seatrout (Table 3.3). According to the Wald test results, the β value for each parameter is statistically significantly different from zero, and therefore both salinity ($p<0.0001$) and temperature ($p =0.0006$) have a significant positive effect in the model (Agresti 2007). In testing the global null hypothesis (all β values are equal to zero), the Wald Test, Score Test, and Likelihood Ratio test all provide strong evidence of the effects of these variables and the intercept on the distribution of spotted seatrout in the lake (all p-values <0.0001) (Agresti 2007).

Analysis of Maximum Likelihood Estimates					
Parameter	DF	Estimate	Standard Error	Wald Chi-Square	Pr > ChiSq
Intercept	1	-5.8730	1.4069	17.4249	<.0001
sal	1	1.5680	0.3462	20.5175	<.0001
temp	1	0.1062	0.0310	11.7193	0.0006

Figure 3.20 SAS output for final, two-parameter model providing the significant β values for the intercept, salinity, and temperature components.

The final model for the spotted seatrout distribution is as follows:

Logit [P(Y=1)] = -5.8730 + 1.5680 (salinity) + 0.1062 (temperature). In looking at each parameter separately, exp(β) provides the multiplicative effect on the odds of observing a spotted seatrout when that parameter is increased by one unit and all other parameters are held equal (Agresti 2007). With this consideration for salinity, exp(1.5680) comes to a value of 4.80, indicating that the odds of observing a spotted seatrout are nearly five times greater with every one unit increase in salinity (ppt). With respect to temperature,

exp(0.1062) comes to a value of 1.11, indicating that the odds of observing a spotted seatrout increase by 11% with every degree increase in temperature (^{o}C). Using the 95% confidence intervals (Table 3.4), the odds of observing a spotted seatrout increase as little as 2.43 times and as much as 9.46 times with every increase in salinity (ppt). For temperature changes, the odds of success increase as little as 4.6% and as high as 18% for every unit increase. The probability of observing a spotted seatrout with increasing salinity (temperature held constant to the seasonal means) reaches 100% probability between 2.5 and 3.5 ppt for all temperatures considered (winter -13.26^{o}C, spring- 20.04^{o}C, summer- 31.80^{o}C, fall- 22.38^{o}C). The probability of observing a spotted seatrout with increasing temperature (salinity held constant to the seasonal means) reaches 100% probability at very different points. This point occurred at 17^{o}C in the winter (3.23 ppt), 35^{o}C in the spring (2.0 ppt), 42^{o}C in the summer (1.52 ppt), and 16^{o}C in the fall (3.28 ppt). It should be noted that these results are specific to the period of time considered for the lake and the conditions determined therein. Other years/seasons may provide different patterns of water quality across the lake and, therefore, different patterns of use by the spotted seatrout.

Odds Ratio Estimates			
Effect	Point Estimate	95% Wald Confidence Limits	
sal	4.797	2.434	9.455
temp	1.112	1.046	1.182

Figure 3.21 SAS output for odds ratios determined for salinity and temperature

DISCUSSION

By using acoustic receivers placed in strategic locations across the lake, it was possible to assess the number of individual fish (fish count) that were recorded within

range of a receiver as well as the overall use of this area through the total number of detections. For the months which were concurrent with Dataflow cruises, most consisted of very limited fish counts (≤1 individual per receiver per month and ≤ 3 fish total detected in the lake). Only during February, March, and June of 2014 did receivers record more than one individual per receiver per month. Receivers in March recorded up to five individuals, in February up to four individuals, and in June up to two individuals. Receivers in June registered over 100 detections collectively in the northeast, east, north, west, and southeastern areas. In February, receivers detected spotted seatrout across the eastern half of the lake, and in March detections were registered in the central north and northeastern areas of the lake. With over 300 detections recorded in February and March, it is clear that spotted seatrout were actively using and allocating a significant amount of time to many receivers across the lake. Due to the limited range of counts (0-5 fish) across these three months, it was most appropriate to address receiver data on a presence/absence basis for the purpose of assessing the influence of water quality parameters on the likelihood of observing a spotted seatrout.

In evaluating the water quality patterns and relationships in Lake Pontchartrain, it is clear that there are distinct patterns occurring across the months evaluated. Across all the seasons considered, CDOM concentrations were very similar and only reached a maximum value of 86.17 ppb. Areas with predominantly higher values were in the northwest, by Pass Manchac, the Tangipahoa River, and the Tchefuncte River. Hydrocarbon concentrations followed an almost identical distribution across the lake when compared with CDOM. Hydrocarbon concentrations were very similar except in January and the spring months, reaching a high value of 706.13 ppb. With the distribution of CDOM and hydrocarbons being so similar, it appears that the sources are

from freshwater waterways and overland flow from the developed shoreline cities. It was therefore reasonable that these parameters were highly positively correlated (0.68).

Chlorophyll *a* concentrations found in Lake Pontchartrain were similar for all of the seasons except spring, which exhibited the highest reading of 16.24 μgL^{-1}. With the influx of nutrients in the spring, this pattern is reasonable. The distribution of high chlorophyll *a* readings varied by month and by season, but predominantly high areas were in the western areas of the lake and along the southern shoreline. Areas of high turbidity were very similar to those found for chlorophyll *a*. While turbidity exhibited the most variability in its distribution, its concentrations were very similar for all of the seasons except spring, which exhibited the highest reading of 58.10 NTU. In addition to sharing areas of high concentration, chlorophyll *a* and turbidity were found to have a strong positive correlation (0.93). This is reasonable considering both the distribution of these parameters, and the necessary correction of chlorophyll *a* readings to account for the influence of turbidity.

With the sources for higher saline waters located in the east and rivers in the west, the resulting pattern of higher salinities in the east, lower salinities in the west, and a well-mixed central area was expected. Low salinity readings characterized the majority of the lake area and all of the seasons except one fall month with a limited area of higher salinity water (11.02 ppt) in the easternmost area. With high influxes of freshwater from the previously mentioned waterways, the salinity in the lake can shift fresher waters eastward and force out the high salinity water. With little riverine/freshwater input, the higher salinities can move westward from the marine sources. It was therefore not unexpected that CDOM (linked to freshwater inflows) and salinity (linked to marine water flux) would have a strong, negative correlation (-0.62).

For temperature, the lake showed clear seasonal patterns with the coldest temperatures in the late fall/winter months (9.91^{o}C) and highest temperatures in the summer and early fall (35.29 ^{o}C). The amount of dissolved oxygen showed a strong, inverse relationship to these seasonal changes with the highest values (14.08 mgL^{-1}) in the winter, spring, and fall. Lowest values for DO (1.91 mgL^{-1}) clearly begin in the early summer and progressively decline through the late summer. With these patterns and the fact that the solubility of oxygen is inversely related to water temperature, the strongly negative Pearson correlation value of -0.87 between these two parameters met expectations.

The generalized linear model fit the data adequately and allowed me to isolate the water quality parameters to be used for predicting the presence/absence of a spotted seatrout to temperature and salinity. Salinity and temperature have often been attributed the largest amount of influence over habitat preferences for spotted seatrout, and are dominant features in many professional Habitat Suitability Models developed for the species (Bortone 2003). While adult spotted seatrout have a wide temperature tolerance (4-33^{o}C), they typically have a specific range dependent on their native region (Bortone 2003). The temperature range for Lake Pontchartrain (9.91^{o}C to 35.29^{o}C) certainly falls within these tolerance limits, extending to warmer temperatures by only 2.29^{o}C. In addition, the range most beneficial for spotted seatrout in the Gulf region (16-32^{o}C) was present in the lake from March through October (Kostecki 1984, (MacRae and Cowan 2010). Perhaps for this reason, temperature was an influence on spotted seatrout distribution, but not with the same magnitude as salinity. According to literature on the species, the biological limits for this parameter range from 5 ppt to 45 ppt, and yet spotted seatrout counts used to build the model were noted in February, March, and June, when salinities within the lake ranged from 0.12 ppt to 3.35 ppt (Lassuy 1983, Blanchet

et al. 2001, and Hill 2005). In addition, salinities for the lake only reached as high as the lower end of the species' tolerance range in August (6.92 ppt), September (8.12 ppt), November (6.59 ppt), and December (7.27 ppt). October had the highest salinity reading at 11.02 ppt. For these months, only areas nearest the marine water sources had salinities that would have been categorized as being within the appropriate range for the species. Overall the model fits well and describes the expected relationship between salinity, temperature, and spotted seatrout distribution in this estuary, but leaves questions around the native population's adaptability to a low salinity environment.

What is most unusual for this species is the adaptation to what, according to the literature, would be classified as extremely stressful salinities. With salinities in the lake generally remaining at the lower limits of the species' tolerance and well below the conditions most beneficial to metabolic processes or for spawning, it is unclear why spotted seatrout are present in the lake for any portion of their life history. With the potential for temperature and salinity to act synergistically as stressors, perhaps the presence of a beneficial temperature regime allows the species to have an increased ability to adapt physiologically to a low-salinity environment (Cowan et al. 2013). Literature on the species does evidence to its extensive geographic range, highly adaptable physiology, and specialization in adaptation to the water quality regimes of natal estuaries. It may be that the spotted seatrout in Lake Pontchartrain are either highly adapted to the unique water chemistry present in the lake or make use of the habitat despite its salinity range due to other metabolically beneficial conditions.

CONCLUSION

In assessing water quality across Lake Pontchartrain, seven parameters were initially assessed. After similar seasonal distribution patterns and strong correlations

were determined, the influences of salinity, temperature, and turbidity became the focus for assessing which factor is most influential on spotted seatrout distribution in the estuary. The generalized linear model developed for assessing the influence of these water quality parameters on spotted seatrout presence was built on a balanced model. Through model testing, a final model was produced, indicating not only good fit for the data, but illuminating the very strong influence of salinity. As a result of this model, the odds of observing a spotted seatrout increase as little as 2.43 times and as much as 9.46 times with every increase in salinity (ppt), and the odds increase as little as 4.6% and as high as 18% for every unit increase in temperature (^{o}C). The model, however, still leaves many questions for fisheries managers. While it is beyond the scope of this research to determine if additional dynamics (life history stage adaptations, food web dynamics, responses to event-driven changes) in Lake Pontchartrain are a significant driving force for the species' use of the waterbody, they are certainly areas that should be considered in order to build a more complete understanding of the spotted seatrout population and thus strengthen ecological management strategies for this fishery.

LITERATURE CITED

Agresti, A. 2007. An introduction to categorical data analysis. John Wiley and Sons, Inc., Hoboken, New Jersey.

ArcGIS 9.2 Desktop Help. 2007. How inverse distance weighted (IDW) interpolation works. ArcGIS Help Library. Retrieved from: ‹http://webhelp.esri.com/arcgisdesktop/9.2/index.cfm?TopicName=How_Inverse_%20Distance_Weighted_(IDW)_interpolation_works›

ArcGIS Resource Center. 2012. Smooth interpolation. ArcGIS Help Library. Retrieved from: ‹http://resources.arcgis.com/en/help/main/10.1/index.html#//003100000020000000›

ArcGIS Resource Center. 2013a. How inverse distance weighting works. ArcGIS Help Library. Retrieved from: ‹http://help.arcgis.com/EN/arcgisdesktop/10.0/help/index.html#//00310000002m000000›

ArcGIS Resource Center. 2013b. Lambert Conformal Conic. ArcGIS Help Library. Retrieved from: ‹http://resources.arcgis.com/en/help/main/10.1/index.html#//003r00000034000000›

ArcGIS Resource Center. 2013c. State Plane Coordinate System. ArcGIS Help Library. Retrieved from: ‹http://resources.arcgis.com/en/help/main/10.1/index.html#//003r00000043000000›

Banks, M.A., G.J. Holt, and J.M. Wakeman. 1991. Age-linked changes in salinity tolerance of larval spotted seatrout (*Cynoscion nebulosus*). Journal of Fish Biology 39:505-514.

Bargu, S., J.R. White, C. Li, J. Czubakowski, and R.W. Fulweiler. 2011. Effects of freshwater input on nutrient loading, phytoplankton biomass, and cyanotoxin production in an oligohaline estuarine lake. Hydrobiologia. 661: 377-389.

Blanchet, H. M.VanHoose, L. McEachron. B. Miller, J. Warren, J. Gill, T. Waldrop, J. Waller, C. Adams, R.B. Ditton, D. Shively, and S. Vanderkooy. 2001. The spotted seatrout fishery of the of Mexico, United States: A regional management plan. Gulf States Marine Commission.

Bortone, S.A. and M.A. Wilzbach. 1997. Status and trends of the commercial and recreational landings of spotted seatrout (*Cynoscion nebulosus*) South Florida. Florida Center for Environmental Studies. Technical Series 2:1-47.

Bortone, S.A. 2003. Biology of the Spotted Seatrout. CRC Press, Boca Raton, Florida.

Cho, H.J. 2007. Effects of prevailing winds on turbidity of a shallow estuary. International Journal of Environmental Research and Public Health. 4: 185-192.

Cowan, J.H., A. Yáñez-Arancibia, P. Sánchez-Gil, and L.A. Deegan. 2013. Estuarine Nekton. Estuarine Ecology Chapter 13. John Wiley & Sons, Inc. Hoboken, New Jersey.

Flocks, J., M. Kulp, J. Smith, and S.J. Williams. 2009. Review of the geologic history of the Pontchartrain Basin, Northern Gulf of Mexico. Journal of Coastal Research. 54: 12-22.

Hastings, R.W. 2009. The Lakes of Pontchartrain. University Press of Mississippi.

Hill, K. 2005. Spotted seatrout (*Cynoscion nebulosus*). Smithsonian Marine Receiver at Fort Pierce. Retrieved from: ‹http://www.sms.si.edu/irlspec/Cynosc_nebulo.htm›

Kostecki, P.T. 1984. Habitat suitability index models: Spotted Seatrout. Washington DC: Fish and Wildlife Service US Department of the Interior.

Lassuy, D.R. 1983. Species profiles: Life histories and environmental requirements (Gulf of Mexico) spotted seatrout. National Coastal Ecosystems Team.

MacRae, P.S.D. and J.H. Cowan, Jr. 2010. Habitat preferences of spotted seatrout, *Cynoscion nebulosus*, in coastal Louisiana: A step towards informing spatial management in estuarine ecosystems. The Open Fish Science Journal 3:154-163.

Mazzotti, F.J., L.G. Pearlstine, T. Barnes, S.A. Bortone, K. Chartier, A.M. Weintstein, and D. DeAngelis. 2008. Stressor-response model for the spotted seatrout (*Cynoscion nebulosus*). Institute of Food and Agricultural Sciences, University of Florida.

Melancon, A. 2015. Personal Communication. Department of Oceanography and Coastal Sciences, Louisiana State University, Baton Rouge, LA, amela22@lsu.edu.

Moffatt and Nichol Engineers. 2010. Review and analysis of Pontchartrain estuary water quality as impacted by opening of the Bonnet Carre Spillway. US Arm Engineer District, New Orleans.

National Geodetic Survey. 2015. State Plane Coordinate (SPC) Utilities. Retrieved from: ‹http://www.ngs.noaa.gov/TOOLS/spc.shtml›

Nieland, D.L., R.G. Thomas, and C.A. Wilson. 2002. Age, growth, and reproduction of the spotted seatrout in Barataria Bay, Louisiana. Transactions of the American Fisheries Society 131:245-259.

Penland, S., A. Beall, and J. Waters, eds. 2002. Environmental atlas of the Lake Pontchartrain basin. Lake Pontchartrain Basin Foundation, New Orleans.

Roy, E.D., N.T. Nguyen, S. Bargu, and J.R. White. 2012. Internal loading of phosphorus from sediments of Lake Pontchartrain (Louisiana, USA) with implications for eutrophication. Hydrobiologia. 684: 69-82.

Salkind NJ. 2008. Statistics for People Who Think They Hate Statistics. Sage Publications, Inc. Thousand Oaks, California.

Smith, EA. 2014. Cyanobacteria Harmful Algal Blooms in South Louisiana Estuaries: A Synthesis of Field Research, Management Implications, and Outreach. Dissertation. Louisiana State University

Stachelek, J. and C.J. Madden. 2015. Application of inverse path distance weighting for high-density spatial mapping of coastal water quality patterns. International Journal of Geographical Information Science. 00:1-11.

Turner Designs. 2015. C6™ Multi-sensor Platform. Retrieved from: ‹http://www.turnerdesigns.com/products/submersible-fluorometer/c6-multi-%20sensor-%20platform›

Vemco. 2015. Range calculator. Retrieved from: ‹http://vemco.com/range-calculator/›

Wu, K. 2005. Long-term freshwater input and sediment from three tributaries to Lake Pontchartrain, Louisiana. Dissertation. Louisiana State University

Wuenschel, M.J., R.G. Werner, and D.E. Hoss. 2004. Effect of body size, temperature and salinity on the routine metabolism of larval and juvenile spotted seatrout. Journal of Fish Biology 64:1088-1102.

Xiaobo, C., J. Yafei, and A. K. M. Azad Hossain. 2013. Numerical Modeling of Flow and Sediment Transport in Lake Pontchartrain due to Flood Release from Bonnet Carré Spillway, Sediment Transport Processes and Their Modelling Applications. Chapter 11.

Xu, X.J., and K. Wu. 2006. Seasonality and interannual variability of freshwater inflow to a large oligohaline estuary in the northern Gulf of Mexico. Estuarine, Coastal, and Shelf Science. 68: 619-626.

CHAPTER 4: GENERAL CONCLUSIONS

With the ecological and economic importance of spotted seatrout in Louisiana, considering habitat complexity, ecological functions, environmental stressors, and overall estuarine stability are necessary for the long term success of this fishery. My research has focused on spotted seatrout in Lake Pontchartrain, with this in mind, by providing data on and interpretation of the complex supporting matrix of interconnected habitats and water quality regimes present in this estuary. Hot spots for fish were predominantly located in the center, center-north, and northeast areas of the lake while cold spots dominated the western edge. More importantly, however, it was the determination that representative receivers from each bottom type (and even in some instances the same receiver), were categorized as both hot spots and cold spots at different times in the assessment. In agreement with literature covering the life history of the species, spatial ecology assessments in other Louisiana coastal estuaries (Lake Calcasieu and Barataria Bay), and numerous Habitat Suitability Models, adult spotted seatrout do not exhibit strong habitat preferences. The lack of distinct bottom type preference provides supporting evidence for the species' adaptive use of every habitat type available in Lake Pontchartrain. This conclusion further strengthens the paradigm that ecosystem health is highly dependent on habitat heterogeneity.

In evaluating the water quality patterns and relationships in Lake Pontchartrain, it is clear that there are distinct patterns for all the water quality parameters assessed. Relationships between CDOM and hydrocarbons, CDOM and salinity, dissolved oxygen and temperature, and turbidity and chlorophyll *a* were all determined to be significant when considering their distribution, but only salinity and temperature stood out as the factors most influential when considering spotted seatrout distribution. Following the

generalized linear model produced, it is clear that when predicting the presence/absence of spotted seatrout, salinity was both the most influential and most perplexing factor. While the temperature range for the lake fell well within the species biological limits, salinities remained at the extreme low end of their respective range and would even be categorized as extremely stressful for the months used in building the model. With literature on the species detailing a highly adaptable physiology, it may be that the spotted seatrout in Lake Pontchartrain are either highly adapted to low salinities or make use of this estuary despite its salinity range due to other metabolically beneficial conditions.

Overall, this study demonstrated the effective use of acoustic telemetry, sonar imaging technology, Dataflow water quality sampling, ArcGIS mapping/spatial analysis, and statistical software for building a more complete understanding of the habitat preferences of adult spotted seatrout in one of the largest and most important estuaries in Louisiana. This approach demonstrated the flexibility of such a system in addressing the habitat trends for a highly mobile species across the spatial extent of the lake. In analyzing the resulting data through hot spot analysis, regions of high use within the lake could be determined not only for the number of unique individual fish visiting an area, but the intensity of use as well. Through these technologies, spotted seatrout habitat preferences for physical features and chemical conditions provided invaluable insight into the species' biology and spatial ecology. By expanding the scientific knowledge base for spotted seatrout in Lake Pontchartrain, this research can lend support to fisheries managers' decision-making and direct their initiatives towards an ecosystem-based management approach.

With building a more complete understanding of this species as a major goal of fisheries scientists, it is clear that many more research questions remain to be addressed.

Future work will need to broaden the ecological scope of this research to include biological considerations, including food web dynamics, predator/prey interactions, and inter/intra-species competition. New research into biological requirements must also expand to include not only adult spotted seatrout but also include juvenile and larval life history stages. Event-driven effects on the species to be researched include those resulting from hurricanes, Bonnet Carré Spillway openings, and algal blooms. Addressing the responses exhibited by spotted seatrout in Lake Pontchartrain to the abovementioned dynamics would enhance management and conservation initiatives. Paramount to any ecosystem-based management is the scientific understanding of a species' adaptive strategies to survive in its physical, chemical, and biological environment. Through the collaborative use of multiple technologies, this research serves as a fundamental database and toolset for researchers and managers in meeting the evolving challenges in managing this valuable recreational species.

APPENDIX A: LAKE PONTCHARTRAIN ESTUARY

INTRODUCTION

The Lake Pontchartrain Basin (LPB) is a 44,000 km^2 region encompassing sixteen Louisiana parishes and four Mississippi counties (Penland et al. 2002, Flocks et al. 2009a). Within the basin lie five river systems, including the Amite, Tickfaw, Tchefuncte, Tangipahoa, and Pearl. Three estuarine waterbodies in the basin include Lake Maurepas, Pontchartrain, and Borgne (Flocks et al. 2009a). With over 1.5 million people living in the immediate vicinity of Lake Pontchartrain alone, concerns over environmental quality have taken center stage for this lake through organizations that include LDWF, LSU, UNO, USGS, and the LPBF (Penland et al. 2002). Such organizations have enacted extensive work projects addressing the need for water and habitat quality assessments through the Coastal Wetland, Planning, Protection, and Restoration Act (CWPPRA), Pontchartrain Ecosystem Research and Education Project, Lake Pontchartrain Basin Restoration Act of 2000, and Coast 2050 Program (Penland et al. 2002). It is clear to natural resource managers that understanding the geological, environmental, and water quality conditions within the basin and especially those of Lake Pontchartrain, will allow them to effectively address the potential for both use and restoration of the lake and its surrounding watershed. A depiction of the watershed, feeding river systems, and waterbodies within is included in Figure A1 below.

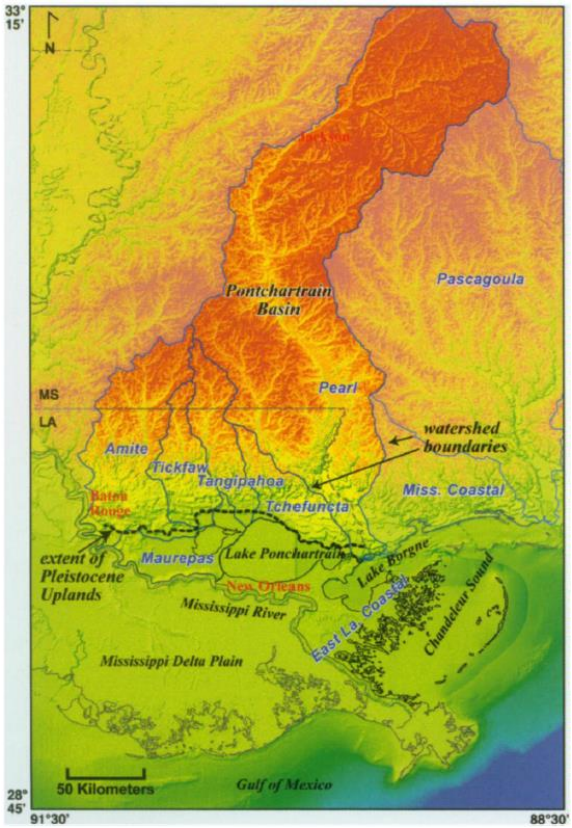

Figure A1 Lake Pontchartrain watershed outlined in grey, with feeding river systems noted in blue (Flocks et al. 2009a)

The major waterbody of the basin, as depicted in Figure A1 above, is Lake Pontchartrain, with Lake Maurepas to the west and Lake Borgne to the east. To the west of these lakes is the alluvial ridge of the Mississippi River (MSR) while to the east is the Pearl River Basin. To the north are the sloping uplands, and the region southeast of the lakes contains connections to Breton, Chandeleur, and Mississippi Sounds (Georgiou et al. 2009). Geomorphic regions, in relation to the lakes, include Pleistocene Terraces in the north, MSR Deltaic Plain in the south, and Marginal Deltaic Basin within which the lakes reside (Penland et al. 2002). Estuarine marshes, bottomland hardwood forests, swamps, and bayous are natural features within the basin. Natural stressors include wetland loss, subsidence, saltwater intrusion, shoreline erosion, hurricanes, and flooding (Penland et al. 2002). Anthropogenic stressors include pollution by agricultural, urban, and industrial runoff as well as intermittent openings of the Bonnet Carré Spillway have

had additional deleterious impacts on water quality. With a rich assemblage of estuarine species, a primary benefit of the lake has historically been fisheries, particularly commercial interests in brown shrimp (*Farfantepenaeus aztecus*), white shrimp (*Litopenaeus setiferus*), blue crabs (*Callinectus sapidus*), red drum (*Sciaenops ocellatus*), and spotted seatrout (*Cynoscion nebulosus*) (Penland et al. 2002; Hastings 2009). With so much ecological and economic value, it is especially important to understand the underlying geology responsible for shaping the region and Lake Pontchartrain.

GEOLOGY

The geological processes that shaped the LPB were noted as beginning around 60 million years ago, however, the most critical events took place beginning around 100,000 years ago (Flocks et al. 2009a). In a general view, the northern two-thirds of the basin consist of parallel terraces whose age increases with distance inland and whose sedimentary character includes undifferentiated sands and clays (Reed and FitzGerald 2009). The bottom third consists largely of more recently formed estuaries whose sedimentary character is primarily deltaic silts and clays (Reed and FitzGerald 2009). At the earliest point of interest lies the formation of the Gulf of Mexico during the early Mesozoic Era (Flocks et al. 2009a). Coastal plain river systems cut valleys in the terrain, creating a series of basins and deltaic deposits, interbedded with oxidized clays (strata of marine origin from glacio-eustatic sea level changes in the Cenozoic and Miocene) (Flocks et al. 2009a). These units effectively comprise the Plio-Pleistocene terraces in the northern region of the basin (Flocks et al. 2009a). The Pleistocene Epoch, which began approximately 22,000-18,000 years ago, contained the last glacial period, called the Wisconsin glaciation (Penland et al. 2002; Flocks et al. 2009a). During this period,

sea level was significantly lower (approximately 120 m) than modern day, allowing river systems to incise the Pleistocene sediments (Flocks et al. 2009a).

In the Holocene Period (18,000-4,000 years ago), rapid sea level rise resulted in the shoreline shifting landwards and the river valleys filling with deltaic and marine sediments (Penland et al. 2002; Flocks et al. 2009a). During this same period, subsidence along the Baton Rouge-Denham Springs fault system resulted in the earliest forms of Lake Maurepas, Pontchartrain, and Borgne as a shallow embayment (Flocks et al. 2009a). The large embayment had tidal flats, oyster shelves, and high salinities (polyhaline) trends up to 4,200 years ago. Additional faulting and subsidence drove the embayment further below sea level and the Pine Island Barrier system formed along the south shoreline (Penland et al. 2002; Flocks et al. 2009a). Around 4,000 years ago, the embayment became separated from the Gulf of Mexico, and the region was transformed by the progradation of MSR deltas, in particular the St. Bernard Delta within the southern basin (Flocks et al. 2009a). Under the influence of the MSR and its deltas, the open bay transformed into a mesohaline estuarine system with the northern boundary of the St Bernard complex burying the Pine Island Barrier trend (Penland et al. 2002; Flocks et al. 2009a). During the Quaternary period, (around 2,900 years ago), the modern forms of the lakes emerged. Figure A2 below provides the geological picture of the formation of Lake Pontchartrain.

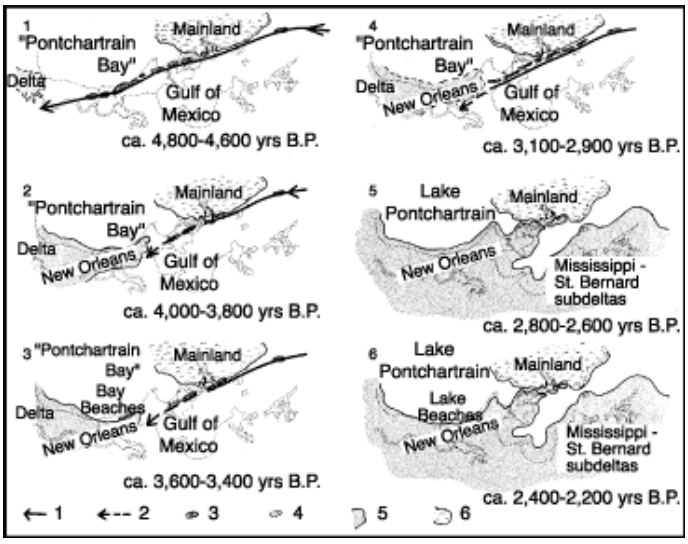

Figure A2 Timeframe and visual depiction of the geological evolution of Lake Pontchartrain from original form as Pontchartrain Bay (Penland et al. 2002)

A comprehensive understanding of the geology beneath the lake provides a natural framework from which to understand the present influences over the lake's sediment and physical form (Flocks et al. 2009a). The modern form of the lake is of an oval, approximately 66 km from east to west and 40 km from north to south, covering 1,630 km^2 (Penland et al. 2002, Bargu et al. 2011, O'Connell et al. 2013, Xiaobo et al. 2013). As a quasi-enclosed waterbody, tidal influence is now far less influential than previously in its history, with connections to the Gulf of Mexico limited to the Rigolets Pass and via Lake Borgne through the Chef Menteur Pass. As both connections are narrow tidal channels, the diurnal tide is provided only a small range (0.6 m at most) of influence over water depth (Penland et al. 2002; Xiaobo et al. 2013). Regarding freshwater connections, the lake maintains a connection to Lake Maurepas by way of Pass Manchac (Xiaobo et al. 2013). In the modern day the same geological processes that have shaped the lake, including fault-related subsidence, compaction, and sea level change continue to be the primary forces altering the basin's bathymetry, shifting it

further below sea level by an estimated 5.6-29 mm/year and a cumulative range of subsidence over 50 years of 0.25-1.25 m (Flocks et al. 2009a; Flocks et al. 2009b).

BOTTOM TYPES

The waterbodies within the LPB are very shallow embayments, with an average depth of 3m in Lake Maurepas, 2.7 m in Lake Borgne, and 6m in Lake Pontchartrain (Miller et al. 2005). While Lake Pontchartrain is the largest in extent, Lake Maurepas and Lake Borgne are far smaller at 241 km^2 and 550 km^2, respectively (Miller et al. 2005). As the centerpiece, Lake Pontchartrain exhibits sediment characteristics typical of such shallow coastal waters. According to bathymetric surveys, Lake Pontchartrain exhibits a flat bottom trend with the shorelines encompassing the most relief (Flocks et al. 2009b). Sediment cores provide a window into the history of the lake, with stratigraphic records including high concentrations of shell materials from marine species below 3 m evidencing the past conditions of an open embayment, barrier island sands typically as thin (<10cm) layers, deltaic silts and clays along the southern and eastern shorelines, and the weathered grey of hardened silty-clay terraces along the northern shores (Flocks et al. 2009b).

Since the Pleistocene, the majority of sediments accumulating within the lake are similar silts and clays, with approximately 70% of recent sediment samples having grain sizes <63 μm (Flocks et al. 2009b; Hastings 2009). The accumulation of such fine sediment deposits is due in large part to the shallow nature (3-5 m average depth) and low-energy environment of the lake (Flocks et al. 2009b; Hastings 2009). Lacking a major river's influence/sediment load, the sediment reaching the lake is from lower-energy riverine sources or from overland flow (Flocks et al. 2009b).

Soft Bottom

The topmost meter of the lake is characterized by brown-grey mud, highly altered through bioturbation and resuspension, the former largely as a result of wind forcings (Flocks et al. 2009b; Reed and FitzGerald 2009). As such, the lake center exhibits sediment containing a high proportion of silt (58%) and clay (34%), with low organic content (3-9%) (Roy and White 2012). Due to the dynamics of circulation, which will be discussed in more detail later, silts concentrate on the periphery while clays are concentrated in the center (Reed and FitzGerald 2009). Sediment deposition around the channels (Pass Manchac, Chef Menteur, Rigolets) and the Bonnet Carré Spillway, however, are more dependent on the interplay of tidal and fluvial forces, typically exhibiting a larger proportion of coarse sediments as a result (Flocks et al. 2009b; Reed and FitzGerald 2009). The character of Lake Pontchartrain's sediment is not limited to natural factors alone.

Historically, large shell beds were found along the lake bottom, but historical shell dredging left only very restricted, remnant patches (Flocks et al. 2009b). In addition, hydraulic dredging for fill has left four large holes in the lake's floor along the New Orleans shoreline (between Lakefront Airport and West End), two of which were 10m deep and lie parallel to shore (Penland et al. 2002; Hastings 2009). These two have since filled in with sediment to just 6m in depth (Hastings 2009). The other two dredge holes lie at the mouth of the Inner Harbor Navigation Channel (IHNC) and remain at a depth of 12-16 m due to tidal scouring (Penland et al. 2002). A bathymetric map is included in Figure A3 below, indicating bathymetry of the lake and important hydrological connections

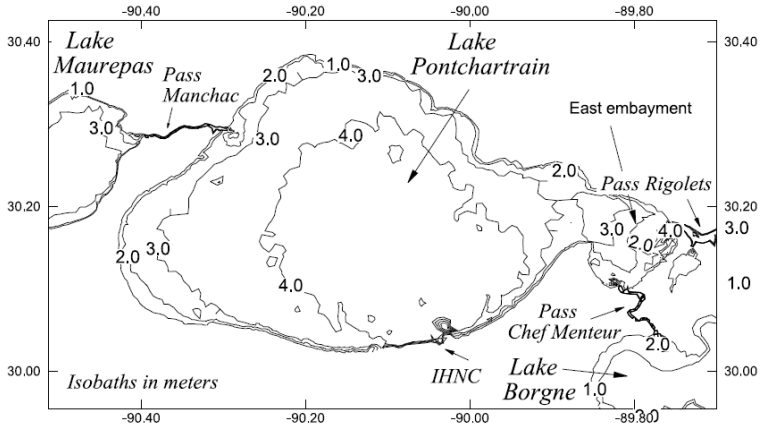

Figure A3 Bathymetry of Lake Pontchartrain with bottom depth marked in meters and hydrologic connections to Lake Maurepas via Pass Manchac and Lake Borgne via Pass Chef Menteur (McCorquodale and Georgiou 2004)

Hard bottom

Soft bottom sediments, which make up the majority of the lakebed, provide not only habitat but also food for the various benthic, burrowing, and demersal species inhabiting the lake (Hastings 2009). While this particular bottom type is the most common, it was historically the shell beds, that is, hard substrate, which provided the most dynamic and beneficial bottom habitat (Lopez 2004; Whitmore 2006; Hastings 2009). Past shell reefs were extensive across the lakebed, consisting largely of the clam *Rangia cuneata*. Hard substrates like the reefs provide attachment sites for sessile organisms, most notably filamentous algae (*Cladophora*, *Oedogonium*, and *Rhizoclonium*) (Hastings 2009). As a food base for benthic crustaceans and invertebrates (amphipods, isopods), it is the availability of hard substrates that has long been held as a major ecological food web driver (Lopez 2004; Whitmore 2006; Hastings 2009). It was along this paradigm that the Lake Pontchartrain Artificial Reef Working Group organized in 2009 to have five artificial reefs built within the lake (Lopez 2004). Five former oil and gas drilling sites were chosen, specifically, those having a remnant shell pad around which restoration materials might be placed (Whitmore 2006). Materials for the

restoration of the reefs included crushed limestone and two forms of concrete ReefBalls^{TM}, 3-ft tall "pallet balls" and 2-ft tall "bay balls" (Lopez 2004; Whitmore 2006). The first site (L1) was completed in 2001 and consisted of 3,200 yards of crushed limestone placed near Lakefront Airport in 2001(Lopez 2004). In 2003, sites H1, H4, and H3 were completed with 180, 208, and 212 reef balls, respectively (Lopez 2004). Site N1 was the final site, completed in 2004 with 80 reef balls. Each site is approximately one acre in size. Images of the reef sites and materials are provided below in Figure A4 and Figure A5.

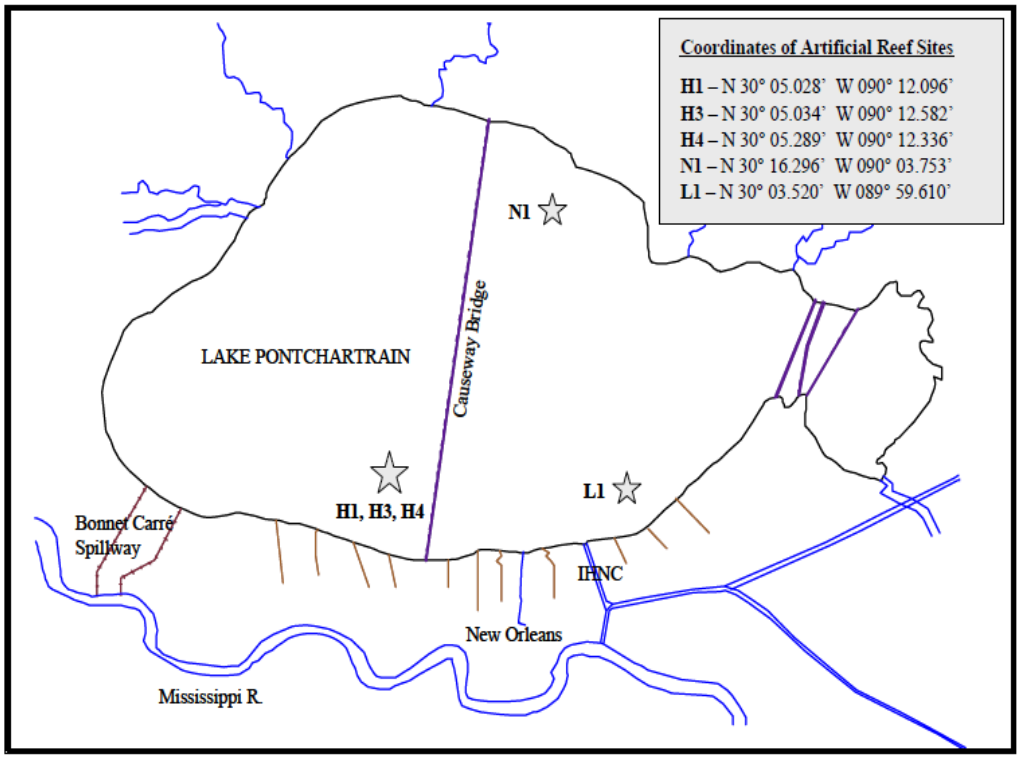

Figure A4 Geographic locations of reef sites with latitude and longitude provided and depicted within Lake Pontchartrain as grey stars (Whitmore 2006)

Figure A5 Image of limestone reef balls being deployed for the purpose of building of artificial reefs in Lake Pontchartrain (Lopez 2004)

While man-made reefs have been used to modestly recreate the historically occurring shell beds, other manmade structures have inadvertently been providing hard substrates around the lake as well (Hastings 2009). Crab traps, posts for docks/piers, and rock piles are such structures, however, the most notable man-made additions to the lake are the Pontchartrain Causeway and Interstate-10 bridges, each with an extensive set of supporting concrete pilings (Hastings 2009). Significant alterations to the shoreline have occurred as well. Defining "shoreline type" as a "homogenous length of coastline with uniform geological and ecological attributes," the extensive Lake Pontchartrain shoreline (125 mi) includes both natural and man-made types (Penland et al. 2002).

Natural shorelines include marshes, cypress swamps, and lakeshore camps along the western and eastern boundaries (Hastings 2009). Man-made shoreline protection materials including riprap, bulkhead, and concrete seawalls have been installed along the southern boundary and mixed with natural shoreline types along the northern boundary (Flocks et al. 2009b; Hastings 2009). Overall, at least 30% of the lake's shoreline has been converted to hard substrate with the development of urban regions (New Orleans, Metairie, Kenner, Slidell, and Mandeville) and 70% remains as natural shoreline

(Hastings 2009). Regions by the shoreline not only provide hard substrate for organisms at the base of the food chain but also secondary habitat for valuable fish species including Gulf menhaden (*Brevoortia patronus*), bay anchovy (*Anchoa mitchilli*), Atlantic croaker (*Micropogonias undulatus*), striped mullet (*Mugil cephalus*), and hardhead catfish (*Ariopsis felis*) (Hastings 2009). Large beds of submerged aquatic vegetation (SAV) were also widespread historically, providing habitat to the same species that utilize the shoreline regions today.

Submerged Aquatic Vegetation

Historically, SAV was abundant along the entire shoreline of Lake Pontchartrain, and largely consisted of native species including American eelgrass (*Vallisneria Americana*), widgeongrass (*Ruppia maritima*), southern naiad (*Najas guadalupensis*), and clasping leaf pondweed (*Potamogeton perfoliatus*) (Duffy and Baltz 1998; Poirrier et al. 2009). According to the earliest description in 1954, V. Americana and *R. maritima* dominated much of the shoreline, including the north shore from the Tchefuncte River east to the Rigolets, and along the south shore from Indian Beach east to South Point (Poirrier et al. 2009). The spatial extent which is available for colonization by these species is largely limited by water clarity, which can change with water depth (1-2 m) and wind mixing (Poirrier et al. 2009). With increasing municipal and agricultural runoff, water quality in the lake suffered and the SAV beds declined by 90% from 1950 to 1985 (Duffy and Baltz 1998). Additional declines have been evidenced in lake surveys conducted in 1980, 1986, and 1991-1992 (Poirrier et al. 2009). Researchers saw a decline of 74% following Hurricane Andrew in 1992 and a 95% decline after a severe winter storm in 1993 (Poirrier et al. 2009). Changes in species composition have also been noted. For example, following a severe drought which increased both salinity and

clarity, *R. maritima* extended to reach depths of 2 m and surpassed *V. Americana* as the dominant macrophyte from 1999-2000 (Penland et al. 2002; Hastings 2009). In 2000, a lakewide survey from shoreline to the 2-m depth mark was conducted indicating abundant and continuous beds along the northshore with *R. maritima* and *V. Americana* as the most abundant species and scattered patches from Lincoln beach west to Jahncke Canal along the southshore (Penland et al. 2002). From this survey scientists estimated the total coverage of SAV to be around 450 ha, with 150 ha consisting of *R. maritima*, and 12 ha comprised of *V. Americana* (Penland et al. 2002). Figure A6 and Figure A7 below provide a map of the SAV species distribution and the average annual abundance by species.

Figure A6 Locations of submerged aquatic vegetation along the near-shore areas of Lake Pontchartrain, depicted as abundant, common, or infrequent (Penland et al. 2002)

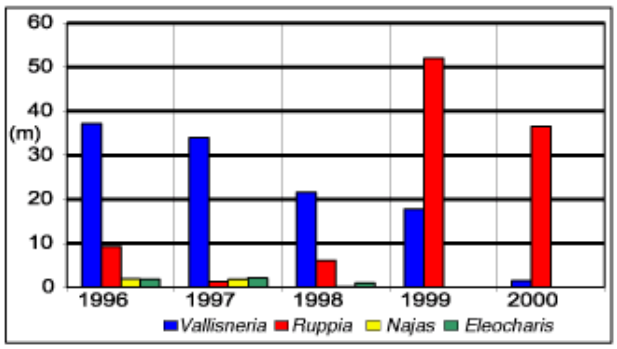

Figure A7 Shifting annual area of submerged aquatic vegetation species from 1996 to 2000, including American eelgrass (*Vallisneria Americana*), widgeongrass (*Ruppia maritima*), southern naiad (*Najas guadalupensis*), and clasping leaf pondweed (*Potamogeton perfoliatus*) (Penland et al. 2002)

V. Americana previously dominated the SAV of Lake Pontchartrain in part due to its affinity for freshwater, a characteristic shared by *N. guadalupensis* and *P. perfoliatus* (Duffy and Baltz 1998; Poirrier et al. 2009). In addition to being a freshwater macrophyte, clusters of ribbonlike blades defines its form and makes it less susceptible to wave damage (Duffy and Baltz 1998). This species' distribution, however, has been reduced by 50% since it was first studied in 1953 and supplanted by *R. maritima* in 1999 (Poirrier et al. 2009). *R. maritima* is a euryhaline species capable of tolerating a broad range of salinities, colonizing marine, estuarine, and even freshwater habitats (Cho and Poirrier 2005). Its slender branching stems with slim, flat leaves can be found in beds on the northeast, east and southeastern shorelines (Cho and Poirrier 2005). The species has rapid shoot/root/rhizome growth and seed production from May-November with growth rates peaking in late summer and dense beds by the late fall (Cho and Poirrier 2005). From December to April biomass of the species declines, particularly as the wind and waves of winter storms tear away at the bushy, branching plant (Cho and Poirrier 2005). With a better tolerance to salinity changes and a robust seed bank, as compared to its competition, this species can very quickly recover and has demonstrated such resilience following Hurricane Andrew in 1992, Hurricane Georges in 1998, and Hurricane Katrina

in 2005 (Poirrier et al. 2009). It should be noted that SAV beds, when present, provide a significant barrier to wave energy, significantly decreasing erosion especially important when high wind and wave events threaten the stability of shoreline sediments (Shaffer et al. 2009).

Unlike the simple, soft-bottom type found in most littoral and deeper portions of the lake, grass beds provide structural complexity, a refuge from predators, and foraging food resources to young fish species (Duffy and Baltz 1998). Grassbeds are of particular importance for juvenile blue crabs, brown shrimp, and spotted seatrout (Hastings 2009). As one of the most highly sought after sportfish, spotted seatrout juveniles move into the lake from June-September and exclusively occupy these regions (Hastings 2009). Grass shrimp (*Palaemonetes spp*.), a common food item for the growing fish, occupy both freshwater regions (species *P. paludosus* and *P. kadiakensis*) and brackish areas (species *P. pugio, P. intermedius*, and *P. vulgans*) (Hastings 2009).

Researchers from 1991-1993, seeking to quantify the difference in distribution and abundance of fish species between unvegetated substratum, native SAV, and patches of the invasive *M. spicata* determined that community diversity was highest in beds of *V. Americana*, intermediate in mud bottom, and lowest with either *R. maritima* or *M. spicatum* (Duffy and Baltz 1998). In addition, fish species were determined to be more abundant in vegetated areas when compared to adjacent regions consisting of mud bottom (Duffy and Baltz 1998). The replacement of native populations with *M. spicatum* has also influenced population dynamics of the lake's fish, as the finely branched leaves spread thickly across the water surface, significantly affecting dissolved oxygen and water clarity (Duffy and Baltz 1998). With grassbeds declining, natural resource managers have taken steps towards the restoration of the native estuarine plants in order to benefit fisheries production (Cho and Poirrier 2005).

WATER QUALITY

Major water quality issues within the Pontchartrain estuary stem from the increasingly deleterious land-use changes, hydrological alterations with control structures, sand and gravel mining, sewage treatment plant discharges, and rapid population growth in the region (Kansheng and Xu 2007; McCorquodale et al. 2009). With land being converted from natural marsh and forests into cropland and urban developments, stormwater runoff is as a major contributor of pollution to the waterbody, flushing heavy metals, wastewater, agricultural products, pathogens, sediment, pesticides, oils, and chemicals into the estuarine waters (Kansheng and Xu 2007; Hastings 2009; Moffatt and Nichol Engineers 2010; O'Connell et al. 2013). In addition, high salinity influx through the IHNC (when it was operational) produced a 250 km^2 dead zone through salinity stratification (McCorquodale et al. 2009). An analysis of LPB estuary waters using EPA indices for water quality was completed in 2010 and evidenced to the fact that of the ten watersheds within the basin, eight were designated as having serious water quality problems (Moffatt and Nichol Engineers 2010).

According to the EPA indices, all of the watersheds were ranked a poor for aquatic and wetland species at risk, wetland loss, four common pollutants, and water quality data (Moffatt and Nichol Engineers 2010). For the lake itself, the northwest region experiences the highest freshwater input and has the least modified hydrology while the northeast region is highly impacted by agricultural and urban runoff (Lane et al. 2001). The southwest region's largest influence are the Bonnet Carré Spillway and industrial runoff from oil refineries while the southeast region is most impacted by extensive reaches of artificial shoreline, high urban runoff and (previous to their closing) the marine water influx from the Gulf of Mexico through the IHNC and Mississippi River

Gulf Outlet (MRGO) (Lane et al. 2001; O'Connell et al. 2013). Figure A8 provided below provides a visualization of these regions as designated by researchers.

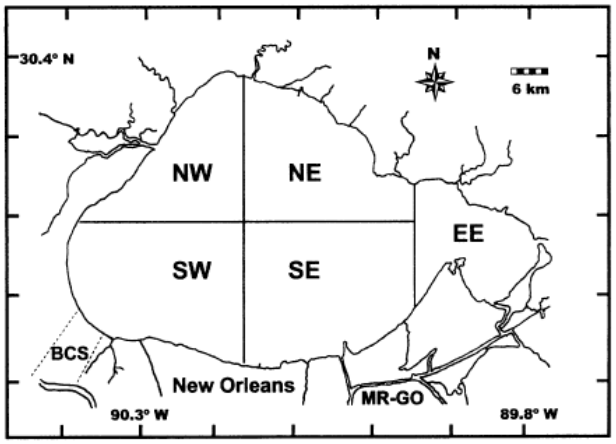

Figure A8 Regional delineation of Lake Pontchartrain for assessing influential forces on water quality (O'Connell et al. 2004)

Plankton Blooms

Phytoplankton are the most widespread of the autotrophs in Lake Pontchartrain. Green algae (*Chlorophyceae*: e.g. *Chlamydomonas*, *Phacotus*, and *Sphaerocystis*) and diatoms (*Chrysophyceae*: e.g. *Chaetoceros*, and *Coscinodiscus*) typically dominate the phytoplankton community, which can include freshwater, brackish, and euryhaline taxa (Hastings 2009). Blue green algae (cyanobacteria) species have a significant role in the lake, as they are often responsible for blooms appearing in late summer/early autumn within the western half of the lake (Hastings 2009). While *Oscillatoria*, *Microcystis*, *Lyngbya*, and *Anabaena* dominate this group, each genus within the group has a set of particular characteristics that can provide an advantage and thus affect its distribution in the lake (Hastings 2009). *Anabaena* is a freshwater cyanobacteria intolerant of salinities above 1ppt, but *Microcystis* can survive in salinities from 0 ppt to 10 ppt (Moffatt and Nichol Engineers 2010; Roy et al. 2013). *Cylindrospermopsis*, however, has an upper salinity limit of just 4 ppt (Moffatt and Nichol Engineers 2010). *Microcystis* does not

have the biological ability to fix atmospheric nitrogen, but *Anabaena* and *Cylindrospermopsis* are capable of supplementing this nutrient in this manner (Moffatt and Nichol Engineers 2010). Cloudy conditions and high turbidity are more favorable to *Microcystis* than either of these two species (Moffatt and Nichol Engineers 2010). Conditions beneficial for the growth of all blue-green algae species, however, are calm, warm (>25^{o}C), eutrophic waters (Moffatt and Nichol Engineers 2010; Roy et al. 2013).

Eutrophication

As a predominant influence, eutrophication is a serious concern for The Lake Pontchartrain Basin Foundation, whose SAVE OUR LAKE campaign is dedicated to improving the lake's water quality (Hastings 2009; Moffatt and Nichol Engineers 2010). Nutrients of most concern are nitrogen and phosphorus. Major dissolved forms of nutrients include ammonia (NH_2), nitrates (NO_2), nitrites (NO_3), total phosphorus, and phosphate compounds (PO_4) (Hastings 2009). Typically, nutrient levels are controlled by season, with high values in the spring occurring with maximum river input and low values in the summer due to biological uptake. Spring waters are P-limited and in the summer and autumn the waters are N-limited (Hastings 2009). It has been estimated that land-use changes have increased the annual N-loading by 10 times the historic amounts, and even in years without a spillway opening the average N-load falls around 24 million pounds (Hastings 2009). N-loading totals were derived by researchers to include 17 million pounds due to river discharge, 2.8 million due to atmospheric deposition, 2.2 million from urban runoff, and 1.1-3 million from leakage through the spillway (Hastings 2009). Should the Bonnet Carre spillway be opened, MSR water (containing up to four times the lake's concentration of total-N and total-P) can add 35-53 million pounds more to the system (Hastings 2009). High nutrient fluxes from these outflows are dangerous

not only due to the harmful algal blooms that can result, but also the potential development of hypoxic/anoxic conditions (Hastings 2009).

Looking at the Redfield ratio of carbon to nitrogen and phosphorus is also often used an indication of the nutrient conditions in a waterbody. Under ideal conditions, the ratio (C:N:P) falls as 106:16:1 for coastal regions, but should the ratio for N:P be smaller than seven or larger than seven the system is either nitrogen limited or phosphorus limited, respectively (Moffatt and Nichol Engineers 2010). Spillway water from the 2008 opening was notably P-limited with a N:P ratio of 11.7 and a nitrate to phosphate ratio of 21.7 (Moffatt and Nichol Engineers 2010). With 97% of the sediment carried by the water also being fine-grained, the plume water was highly turbid, with total suspended solids (TSS) at 144 mg/L (Moffatt and Nichol Engineers 2010). A pattern of succession for the phytoplankton was documented, from diatom dominance initially, green algae following, and cyanobacteria (blue-green) in the main bloom (Moffatt and Nichol Engineers 2010). Chlorophyll *a* concentration is typically used to define a bloom. Data from midlake samples indicated chlorophyll *a* concentrations as high as 855 μgL^{-1} for the earlier 1997 release but less pronounced in 2008 at 16.48 μgL^{-1} (Moffatt and Nichol Engineers 2010). With blooms, oxygen depletion often results from benthic decomposition taking place in warm, calm waters, as well as toxin production (Moffatt and Nichol Engineers 2010). The primary toxin producing blue-green algae in Lake Pontchartrain include *Anabaena*, *Aphanizomenon*, *Microcystis*, *Cylindrospermopsis*, *Planktothrix* and *Nodularia* which can in turn produce hepatotoxins that block protein synthesis and neurotoxins that attack the nervous system (Moffatt and Nichol Engineers 2010; Bargu et al. 2011).

Biological oxygen demand (BOD) is the term used to define the relationship between the organic material available in the water column and the oxygen demands of

the bacteria as a result of decomposition (Hastings 2009). Surface dissolved oxygen (DO) for the lake typically ranges from 5.6-10.3 mgL^{-1}, but in warmer months bottom water concentrations can drop to 1.4 mg/L (Hastings 2009). While the long term average air temperature is 19^{o}C, colder temperatures (12^{o}C) experienced in the winter (January) influence water temperatures, allowing higher levels of DO (Xu and Wu 2006; Kansheng and Xu 2007). With the far warmer temperatures (28^{o}C) experienced in the summer months (July), DO saturation can be exceptionally reduced (Xu and Wu 2006; Kansheng and Xu 2007). As an example, the DO saturation point is reached at just 7.8 mgL^{-1}in water with a salinity of 10 ppt and temperature of 25^{o}C (Hastings 2009). Adding increased BOD to this equation can very quickly drive DO levels to the deadly range of hypoxic (2-3 mgL^{-1}) and even anoxic (0 mgL^{-1}) conditions (Hastings 2009). Like DO, pH can also have a critical influence on the chemical and biological processes in the lake, with most aquatic species preferring values between 6.5 and 8 (McCorquodale et al. 2005). Should the pH fall outside of this range, organisms begin experiencing stress on their physiological systems, which in time will decrease the diversity of species capable of surviving under such conditions and the success of reproduction (McCorquodale et al. 2005). Unlike DO, however, with a pH range of 6.84 to 7.99, water quality in Lake Pontchartrain does not present stressful chemical conditions along this parameter (McCorquodale et al. 2005).

Salinity and Freshwater

Salinity is a critical factor in determining the lake's chemical character. The lake exhibits a rather narrow salinity range, typically from 0-8 ppt, with lower values (1.2 ppt) in the west and higher values (up to 15.2 ppt) in the east (Hastings 2009). While the major salts dissolved in the lake water, including chloride, sodium, sulfate, magnesium,

calcium, potassium, and bicarbonate, are also those found in marine waters, the lake is classified as oligohaline due to their concentration (Hastings 2009). With a volume of 6 km^3, the residence time for this low salinity water within the lake falls between 57 and 60 days (Bargu et al. 2011; Roy et al. 2013). The challenges salinity poses for estuarine species are twofold. In order to balance the osmotic pressure from the lake's water with its own body fluids, species must have physical control over the body's salt and water balance, also called osmoregulation (Hastings 2009). The second challenge that salinity levels present is in the form of stratification-induced hypoxia (Brammer et al. 2007) (Hastings 2009). When the MRGO and IHNC outlets allowed a direct connection between the lake and the Gulf of Mexico, strong salinity gradients developed as marine waters entered the relatively fresh southeastern quadrant of the lake (Poirrier 2013). As density differences prevented mixing within the water column, the bottom most layers became hypoxic, producing a 250 km^2 dead zone (Hastings 2009). In Lake Pontchartrain, the magnitude and timing of saltwater water influxes have varied throughout its history, and still define the salinity patterns within the environment today.

Previously there were three channels through which saltwater could flow into Lake Pontchartrain, including the IHNC, Chef Menteur Pass, and Rigolets Pass (Poirrier 2013). Lake Pontchartrain's tidal cycle operates on a diurnal pattern, one high tide and one low tide per 24 hour cycle (Hastings 2009). The peak tidal range of 0.15 m to 0.6 m occurs during the spring ebb and flow tides, which can bring as much as 7,800 m^3s^{-1} of water collectively through the IHNC (previously open), Chef Menteur Pass, and Rigolets (Georgiou et al. 2009; McCorquodale et al. 2009; Li et al. 2010). The proportion of tidal flow for these canals was determined to be 10%, 30%, and 60% respectively (Hastings 2009). Prior to its closing, the IHNC was a man-made canal located in the southeast corner of the lake, connecting it to the MRGO and thus the Gulf of Mexico (Li et al.

2010; Xiaobo et al. 2013). The Chef Menteur Pass is a naturally occurring, meandering channel located in the eastern side of the lake, connecting it to the southwest corner of Lake Borgne (which is connected to the coastal ocean) (Li et al. 2010). Finally, the Rigolets is another natural channel on the eastern end of the lake connecting it to Lake Borgne (Li et al. 2010). Figure A9 below details the bathymetry and points of water exchange in Lake Pontchartrain as well as salinities based on average conditions over a ten year period.

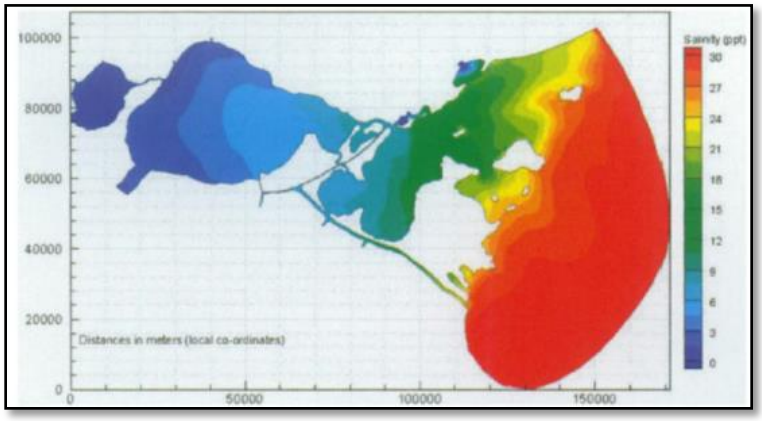

Figure A9 Long term salinity patterns for Lake Maurepas, Lake Pontchartrain, Lake Borgne, and eastward to the marine environment of Chandeleur Sound (McCorquodale et al. 2009)

The Tchefuncte, Tangipahoa, Amite, Tickfaw, and Pearl Rivers are the direct sources of freshwater, nutrients, and sediment to the lake (Xiaobo et al. 2013). Freshwater and sediment are credited with not only maintaining environmental integrity but also restoring surrounding wetlands (Kansheng and Xu 2007). With respect to water quality, the riverflow, specifically the quantity, timing, and duration have profound influences on salinity, temperature, turbidity, and DO within the lake (Xu and Wu 2006). Long term annual precipitation in the region ranges from 1,108 to 2,178 mm, with the highest amount in July (159 mm) and lowest in October (86 mm) (Xu and Wu 2006;

Kansheng and Xu 2007) . As the largest contributors to the lake, the Amite, Tickfaw, and Tangipahoa Rivers present average daily discharges of 59 m^3s^{-1}, 10.9 m^3s^{-1}, and 32.9 m^3s^{-1}, respectively (Kansheng and Xu 2007). In assessing annual yield, these three waterways add a total of 5.04 km^3/yr of freshwater, consisting of 2.76 km^3/yr, 1.01 km^3/yr, and 1.27 km^3/yr, respectively from each river (Kansheng and Xu 2007). Large variations in annual yield have been found across 60 years of data, with the flow for the Amite from 0.58-3.58 km^3/yr, Tickfaw with 0.09-0.58km^3/yr, and the Tangipahoa with 0.45-1.94 km^3/yr (Wu 2005). Researchers have determined that over 80% of the variation in annual freshwater flow could be explained by changes in annual precipitation (Wu 2005). With 74%, 73%, and 69% of each rivers total annual yield (respectively) being reached between December and May, the rivers follow a seasonal pattern of high discharge in the winter/spring and lower in the summer/autumn (Kansheng and Xu 2007).

The abovementioned river systems also contribute sediment critical for aquatic ecosystems (Kansheng and Xu 2007). Rivers flowing through the uplands pick up eroded silts and clays, predominantly from soil types Tangi-Ruston-Smithdale, Tala-Tangi, and Maytt-Guyton (Xu and Wu 2006). As with salinity, TSS fluctuations occur seasonally, with high fluxes in the spring due to limited vegetative cover and increasing agricultural disturbances, and low fluxes in the summer due to heavy vegetation cover (Wu 2005). In addition, The average annual TSS runoff from the Amite, Tickfaw and Tangipahoa River systems is approximately 29 tons/km^2, 10 tons/km^2, and 25 tons/km^2, respectively (Wu 2005; Kansheng and Xu 2007). As a result of seasonal influences, there is a very strong relationship between annual TSS yield and total precipitation, especially the precipitation recorded for Jan-April (Kansheng and Xu 2007). These differences occur both seasonally and interannually, resulting in an annual difference in TSS concentration as great as six times higher for the Amite alone (Wu 2005). Overall annual TSS loading

resulting from the three major river systems are approximately 141,074 tons/yr, 18,278 tons/yr, and 51,008 tons/yr (Kansheng and Xu 2007). Figure A10 below details the long term TSS loading for these three rivers. It should be noted that as the soil-laden waters mix with the more saline lake water, ionic reactions increase the settling out of the sediment particles, but with its shallow bathymetry and fine-grained sediment, the influence of winds must also be taken into account for the lake (Hastings 2009).

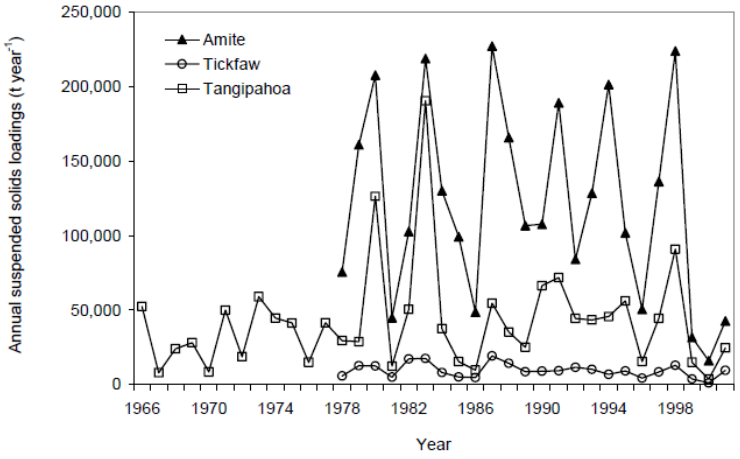

Figure A10 Annual average contribution of suspended solids from the Amite, Tickfaw, and Tangipahoa Rivers into Lake Pontchartrain (Kansheng and Xu 2007)

Turbidity

Lake Pontchartrain is far more turbid than freshwater lakes or marine waters due primarily to continual re-suspension of sediments, a product of bioturbation to a small degree and to water turbulence produced through wind stress to a far greater degree (Flocks et al. 2009b). By definition, turbidity relates to a decrease in the transparency of water, specifically the decreasing depth at which light attenuates due to scattering and reflection by suspended inorganic sediments, phytoplankton, and detritus (Cho 2007). Due to the lake's wide fetch (1630 km^2) and shallow depths (3.7 m), it only requires a wind speed of 6.8 ms^{-1} (15 mph) to mix the bottom sediments throughout the water

column (Cho 2007). Typical turbidity values for the surface waters of the lake are between 5.8 and 9.3 nephelometric turbidity units (NTU**)** (Xu and Wu 2006). In the past, shell dredging reduced the secchi depth (another measure of clarity) to only 24-31in while in the 90's the depth of clarity reached 50-60in (Hastings 2009). Large-scale turbidity changes, even in a wide coastal waterbody, are primarily due to the direction, duration, and strength of the prevailing winds (Cho 2007). As a result of wind direction, turbidity increases in the northeast region with south and westerly winds while west winds increase turbidity in the eastern region (Cho 2007). The southern region, it follows, is most turbid when the wind is out of the north (Cho 2007). Along the shoreline, waves create turbulence, scoring unstable bottom sediments (Cho 2007). Winds of just 10 knots substantially increase turbidity while winds of 15 knots create bottom orbital velocities of 10 cms^{-1} and TSS concentrations in excess of 100 mgL^{-1} (Flocks et al. 2009b). It is the orbital currents generated by local waves that are attributed with bottom sediment resuspension and the prevailing winds and tides that most influence circulation within the estuary (Penland et al. 2002). Figure A11 below depicts the lake and regions of resuspension potential (grey) with increasing winds out of the northeast.

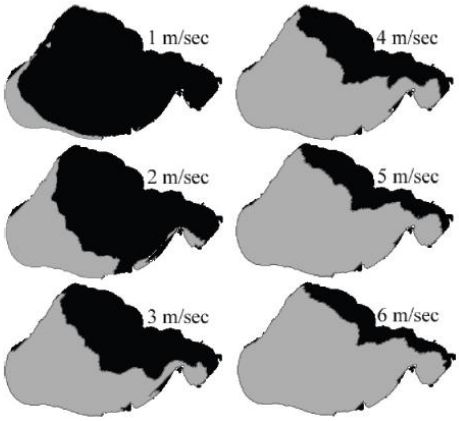

Figure A11 Regions of resuspension potential (grey) with increasing wind speeds from the northeast (Miller et al. 2005)

Circulation

Large scale water circulation patterns within Lake Pontchartrain are largely dependent upon tidal fluctuations and wind-generated waves (Flocks et al. 2009b). The tidal range within the lake is small, only 10-20 cm, but water levels are further increased with easterly and southerly winds which can drive water into the estuary (Cho 2007). Winds from the west and north, however, increases the outward movement of waters from the lake (Cho 2007). For windspeeds of 2 ms^{-1} or less, the lunar tide dominates the water levels, with the strongest currents produced in the immediate areas around the Rigolets and Chef Menteur Pass (Penland et al. 2002; Wu 2005). With winds of 3 ms^{-1} or more, the winds are the controlling factor and override the minor tidal changes (Wu 2005). As a result of friction, surface and shoreline currents are predominantly in the direction of the wind while deeper, and central regions of the lake display flow in the opposite direction (Penland et al. 2002; McCorquodale and Georgiou 2004). Overall, the prevailing circulation pattern found in the lake and as determined by three-dimensional hydrodynamic models is a two gyre system consisting of strong shoreline currents with weaker centrally located currents (McCorquodale and Georgiou 2004, Flocks et al. 2009b). Northerly and southerly winds produce and strengthen this two-gyre system but easterly and westerly wind forcings produce a single gyre in the shallow northern end of the lake (Penland et al. 2002; McCorquodale and Georgiou 2004). In addition, cold fronts, common in the autumn and winter, effectively alter the low-speed wind pattern associated with stationary high pressure systems to the fast-speed changeable winds (typically from south to north) (Miller et al. 2005). The patterns of wind-driven circulation are displayed in Figure A12 below.

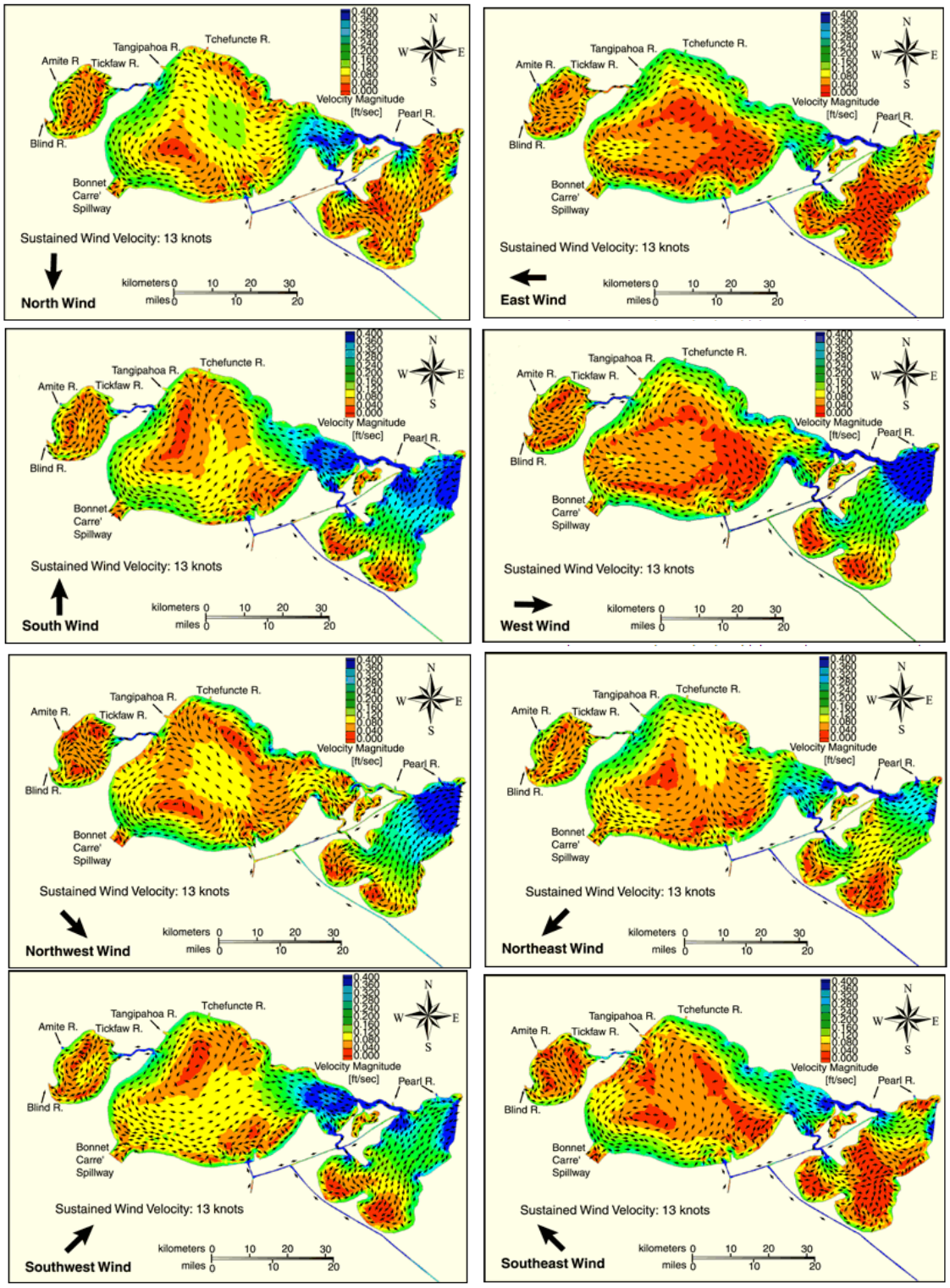

Figure A12 Changing circulation patterns with prevailing wind directions (Penland et al. 2002)

SPECIAL ENVIRONMENTAL CONSIDERATION

Bonnet Carré Spillway

Following the Great Flood of 1927, the Bonnet Carré Spillway (BCS) was constructed in 1931 within the southwest corner of Lake Pontchartrain and approximately 19 km west of New Orleans (Roy et al. 2013; Xiaobo et al. 2013) . Its purpose was to provide an outlet for flood waters from the MSR to protect New Orleans should the river reach a flood stage of 5.2 m (Roy et al. 2013; Xiaobo et al. 2013). The BCS has been opened ten times in its history and while the timing, duration, and volume vary for each event, any opening has profound effects on the lake and its biota (Roy et al. 2013). Traditional circulation patterns in the lake depend on wind and tidal forces that typically produce strong currents along shorelines and tidal passes where high rates of sediment transportation and resuspension occur (Xiaobo et al. 2013).

A BCS event, in contrast to typical flow patterns, can produce a massive plume of sediment-laden freshwater flowing from the southwest corner northwards and eastwards (Xiaobo et al. 2013). In fact, after only three weeks the floodwaters can be distributed throughout the entire lake and it can take two to three months after the spillway is closed for suspended sediment within the lake to return to normal conditions (Xiaobo et al. 2013). With a wind-dominated estuary, it is also of note that the speed and extent of the plume's movement depends more on the magnitude of the spillway event (Roy et al. 2013). Large-scale diversions have even been proposed for coastal restoration, particularly as they can provide sediments to rebuild wetlands, freshwater to control salt-water intrusion, and nutrients for productivity (McCorquodale et al. 2009). Table A1 below details each spillway event.

Year	Date opened	Date Closed	Days opened	Max. discharge m^3/s
1937	Jan28	Mar 16	48	5975
1945	Mar 23	May 18	57	9005
1950	Feb 10	Mar 19	38	6315
1973	Apr 8	Jun 21	75	5522
1975	Apr 14	Apr 26	13	3115
1979	Apr 17	May 31	45	5409
1983	May 20	Jun 23	35	7589
1997	Mar 17	Apr 18	31	6881
2008	Apr 11	May 8	28	4531
2011	May 9	June 20	42	8892

Figure A13 History of Bonnet Carré Spillway openings including date of opening, closing, and maximum rate of discharge (Xiaobo et al. 2013)

At its peak performance, the Bonnet Carré Spillway can release 250,000 ft^3/s, approximately 17% of the MSR flood of 1.5 million ft^3/s (Roy et al. 2013). As the three most recent openings (1997, 2008, and 2011) evidence, this far surpasses any other naturally occurring freshwater source to the lake. Based on long term daily flow patterns, the average annual inflow from the LPB is 6.1 km^3, but for these release years, spillway releases amounted to 11.7 km^3, 7.5 km^3, and 21.9 km^3, respectively (Roy et al. 2013). These volumes constituted 176%, 113%, and 303% of the total lake volume, respectively (Roy et al. 2013). With each release a plume of sediment-rich MSR water is discharged into Lake Pontchartrain and travels along the southern edge, driven by the Coriolis Effect. Travel time for the plume across the lake is largely controlled by the wind, with the plume reaching the eastern outlets in 6 days for 1997, 18 days for 2008, and less than 14 days for 2011 (Roy et al. 2013). Considering the typical residence time for water in the lake is 60 days, these speeds are three to ten times faster than normal freshwater inputs.

In the most recent release, researchers determined that the plume produced drastically reduced water clarity, with secchi depths dropping from 0.9±0.2 m before the

release to 0.3±0.1 m during the event (Roy et al. 2013). In addition, previous salinity ranges along an east-west transect were 2.6-4.9 ppt dropped during the release to ≤0.15 ppt except in the sampling sites farthest from the spillway (Roy et al. 2013). With the influx of freshwater and nutrients, surface chlorophyll *a* concentrations jumped from a mean of 3.6±1.1 µg/L to 35 µg/L (Roy et al. 2013). The most obvious biological impacts from such releases include the loss of SAV due to vastly increased turbidity and the blooms of phytoplankton.

While there are no documented major blooms during its early operation (1937-1983), the 1997 BCS event which occurred from March 17-April 18 produced significant deleterious effects on the water quality and benthic environment (Brammer et al. 2007; Roy et al. 2013). Sampling sites across the lake indicated to researchers secchi depth was reduced from a range of 1-5.5 m to 0.2-0.3 m, remaining low (0.6-2.4) for the rest of the year (Brammer et al. 2007). In addition, salinity ranged initially from 1.5-5.1 ppt in bottom waters but shifted to a much lower range of 0.2-0.8 ppt during the event, remaining low (1.68 ppt maximum) through May 1998 (Brammer et al. 2007). DO concentration during the release ranged from 6-9 mgL^{-1} in surface waters and 3-8 mgL^{-1} in the bottom waters (Brammer et al. 2007). Anytime a BCS event occurs a pulse of N-rich water enters, shifting the limiting nutrient to phosphorus, and spurring a release of soluble reactive phosphorus from the sediment to restore the normally occurring N-limited conditions (Roy et al. 2012).

The initial response by photosynthetic biota to a BCS event typically includes a large bloom of diatoms, especially *Skeletonema costatum*, which prefers rich oligohaline waters (Mize and Demchek 2009). As nutrient levels drop, the secondary response is the rise in biomass of blue-green algae like *Anabaena* sp., *Aphanizomenon* sp., and *Cylindrospermopsis raciborskii* capable of N-fixation and P storage (Mize and Demchek

2009; White et al. 2009; Bargu et al. 2011; Roy et al. 2012). The resulting bloom in 1997 was larger than 2008 due to the earlier timing of the release, greater discharge from feeding tributaries, less cloud cover (30% vs 68%), and less turbulent hydrologic flows (Moffatt and Nichol Engineers 2010). The 1997 bloom primarily consisted of *Anabaena* spp and *Microcystis* spp. while species diversity in 2008 was far greater and included the centric diatom *Melosira*, chlorophyte *Klebsormidium*, blue-green algae species named above, pennate diatoms, and flagellates (Moffatt and Nichol Engineers 2010; Bargu et al. 2011; Roy et al. 2013) . In contrast, SAV beds declined abruptly in 1997 (Penland et al. 2002). Beds of *R. maritima* and *M. spicatum* (2,000 m^2 area) displayed significant decline as a result of the light-prohibitive turbidity, phytoplankton blooms, and the epiphytic growth of green filamentous *Cladophora* spp. (Penland et al. 2002; Poirrier et al. 2009).

CONCLUSION

It is the overall resilience of the system and its species that is of concern to natural resource managers for Lake Pontchartrain, especially in light of the cumulative impacts of both natural and human stresses on this dynamic system. The geology of the region is one of great change, including riverine systems, deltaic systems, and even open embayments. Now, the same geologic processes that make up the lake's history continue to shape the modern lake, most notably through subsidence and sea level rise. While most of the lakebed is characterized by the soft silts and clays from its most recent geologic past, restoration projects for the renewal of reef beds and SAV are being undertaken to renew the past ecological functions and productivity of economically valuable estuarine species. Across approximately 136 species, the biological resources of the lake include a myriad of fish and crustaceans, from the *Rangia cuneata* clam to

shrimp, blue crabs, black drum, red drum, spotted seatrout, and many more. With so many species to manage effectively and a waterbody so impacted by human influences, improvements to water quality are underway with restoration projects, awareness/outreach programs, and monitoring through citizen groups like the Lake Pontchartrain Basin Foundation, Louisiana universities, and state organizations.

LITERATURE CITED

Bargu, S., J.R. White, C. Li, J. Czubakowski, and R.W. Fulweiler. 2011. Effects of freshwater input on nutrient loading, phytoplankton biomass, and cyanotoxin production in an oligohaline estuarine lake. Hydrobiologia. 661: 377-389.

Brammer, A.J., Z.R. del Rey, E.A. Spalding, and M.A. Poirrier. 2007. Effects of the 1997 Bonnet Carre Spillway opening on infaunal macroinvertebrates in Lake Pontchartrain, . Journal of Coastal Research. 23: 1292-1303.

Cho, H.J. and M.A. Poirrier. 2005. Seasonal growth and reproduction of Ruppia Maritima in Lake Pontchartrain, Louisiana, USA. Aquatic Botany. 81:37-49.

Cho, H.J. 2007. Effects of prevailing winds on turbidity of a shallow estuary. International Journal of Environmental Research and Public Health. 4: 185-192.

Duffy, K.C., and D.M. Baltz. 1998. Comparison of fish assemblages associated with native and exotic submerged macrophytes in the Lake Pontchartrain estuary, USA. Journal of Experimental Marine Biology and Ecology. 223: 199-221.

Flocks, J., M. Kulp, J. Smith, and S.J. Williams. 2009a. Review of the geologic history of the Pontchartrain Basin, Northern Gulf of Mexico. Journal of Coastal Research. 54: 12-22.

Flocks, J., J. Kindinger, M. Marot, and C. Holmes. 2009b. Sediment characterization and dynamics in Lake Pontchartrain, Louisiana. Journal of Coastal Research. 54:113-126.

Georgiou, I., J.A. McCorquodale, J. Schindler, A.G. Retana, D.M. FitzGerald, Z. Hughes, and N. Howes. 2009. Impact of multiple freshwater diversions on the salinity distribution in the Pontchartrain estuary under tidal forcing. Journal of Coastal Research. 54: 59-70.

Hastings, R.W. 2009. The Lakes of Pontchartrain. University Press of Mississippi.

Kansheng, W., and Y.J. Xu. 2007. Long-term freshwater inflow and sediment discharge into Lake Pontchartrain in Louisiana, USA. Hydrological Sciences Journal. 52: 166-180.

Lane, R.R., J.W. Day, Jr., G.P. Kemp, and D.K. Demcheck. 2001. The 1994 experimental opening of the Bonnet Carre Spillway to divert Mississippi River water into Lake Pontchartrain. Ecological Engineering. 17: 411-422.

Li, C., E. Weeks, and B.M. Blanchard. 2010. Storm surge induced flux through multiple tidal passes of Lake Pontchartrain estuary during Hurricanes Gustav and Ike. Estuarine, Coastal, and Shelf Science. 87: 517-525.

Lopez, J. 2004. The Lake Pontchartrain artificial reef program. Lake Pontchartrain Basin Foundation with the Louisiana Department of Wildlife and Fisheries.

McCorquodale, J.A., and I. Georgiou. 2004. Modeling freshwater inflows in a shallow lake. Archives of Hydro-Engineering and Environmental Mechanics. 51:3-12.

McCorquodale, J.A., I. Georgiou, C. Chilmakuri, and M. Martinez. 2005. Lake hydrodynamics and recreational activities in the south shore of Lake Pontchartrain, Louisiana. University of New Orleans.

McCorquodale, J.A., R.J. Roblin, I. Georgiou, and K.A. Haralampides. 2009. Salinity, nutrient, and sediment dynamics in the Pontchartrain estuary. Journal of Coastal Research. 54: 71-87.

Miller, R.L., C.E. del Castillo, and K.A. McKee. 2005. Remote sensing of coastal aquatic environments: Technologies, Techniques and Applications. Dordrecht: Springer.

Mize, S.U., and D.K. Demchek. 2009. Water quality and phytoplankton communities in Lake Pontchartrain during and after the Bonnet Carre Spillway opening, April to October 2008, in Louisiana, USA. Geological Marine Letters. 29: 431-440.

Moffatt and Nichol Engineers. 2010. Review and analysis of Pontchartrain estuary water quality as impacted by opening of the Bonnet Carre Spillway. US Arm Engineer District, New Orleans.

O'Connell, M.T., R.C. Cashner, and C.S. Schieble. 2004. Fish assemblage stability over fifty years in the Lake Pontchartrain estuary; Comparisons among habitats using canonical correspondence analysis. Estuaries. 27: 807-817.

O'Connell, M.T., A.M.U. O'Connell, and C.S. Schieble. 2013. Response of Lake Pontchartrain fish assemblages to Hurricanes Katrina and Rita. Estuaries and Coasts. 37: 461-475.

Penland, S., A. Beall, and J. Waters, eds. 2002. Environmental atlas of the Lake Pontchartrain basin. Lake Pontchartrain Basin Foundation, New Orleans.

Poirrier, M.A., E.A. Spalding, and C.D. Franze. 2009. Lessons learned from a decade of assessment and restoration studies of benthic invertebrates and submerged aquatic vegetation in Lake Pontchartrain. Journal of Coastal Research. 54: 88-100.

Poirrier, M.A. 2013. Effects of closure of the Mississippi River Gulf Outlet on saltwater intrusion and bottom water hypoxia in Lake Pontchartrain. Gulf and Caribbean Research. 25: 105-109.

Reed, D.J., and D. FitzGerald. 2009. Introduction. Journal of Coastal Research, 54: vii-xi.

Roy, E.D., N.T. Nguyen, S. Bargu, and J.R. White. 2012. Internal loading of phosphorus from sediments of Lake Pontchartrain (Louisiana, USA) with implications for eutrophication. Hydrobiologia. 684: 69-82.

Roy, E.D., and J.R. White. 2012. Nitrate flux into the sediments of a shallow oligohaline estuary during large flood pulses of Mississippi River water. Journal of Environmental Quality. Technical Report.

Roy, E.D., J.R White, E.A. Smith, S. Bargu, and C. Li. 2013. Estuarine ecosystem response to three large scale Mississippi River flood diversion events. Science of the Total Environment, 458-460: 374-387.

Shaffer, G.P., J.W Day, Jr., S. Mack, G.P. Kemp, I. Van Heerden, M.A. Poirrier, K.A. Westphal, D. FitzGerald, A. Milanes, C.A. Morris, R. Bea, and P.S. Penland. 2009. The MRGO navigation project: A massive human-induced environmental, economic, and storm disaster. Journal of Coastal Research. 54: 206-224.

Whitmore, K.A. 2006. Artificial reef performance in Lake Pontchartrain, Louisiana. Thesis. University of New Orleans.

Wu, K. 2005. Long-term freshwater input and sediment from three tributaries to Lake Pontchartrain, Louisiana. Dissertation. Louisiana State University.

Xiaobo, C., J. Yafei, and A. K. M. Azad Hossain. 2013. Numerical Modeling of Flow and Sediment Transport in Lake Pontchartrain due to Flood Release from Bonnet Carré Spillway, Sediment Transport Processes and Their Modelling Applications. Chapter 11.

Xu, X.J., and K. Wu. 2006. Seasonality and interannual variability of freshwater inflow to a large oligohaline estuary in the northern Gulf of Mexico. Estuarine, Coastal, and Shelf Science. 68: 619-626.

APPENDIX B: BIOLOGY OF THE SPOTTED SEATROUT (*CYNOSCION NEBULOSUS*)

DISTRIBUTION, FEEDING HABITS, GROWTH

While spotted seatrout is the common name endorsed by the American Fisheries Society, the species may also be referred to as specks, speckled trout, trucha del mar, truite gris, or spotted weakfish (Bortone and Wilzbach 1997; Blanchet et al. 2001). With respect to physical features, the spotted seatrout has an elongated fusiform body shape with silver grey coloration (Hill 2005). The upper body consists of a darker grey-blue tone with black spots above the lateral line and extending to the caudal fin. The dorsal fin consists of 12 spines and 25-28 soft rays, and the caudal fin is truncate in shape. Large, ctenoid scales cover the body surface except the soft dorsal and anal fins. The head is concave when viewed in profile and the lower jaw projects further than the upper jaw (Hill 2005). Figure B1 provides a picture for reference.

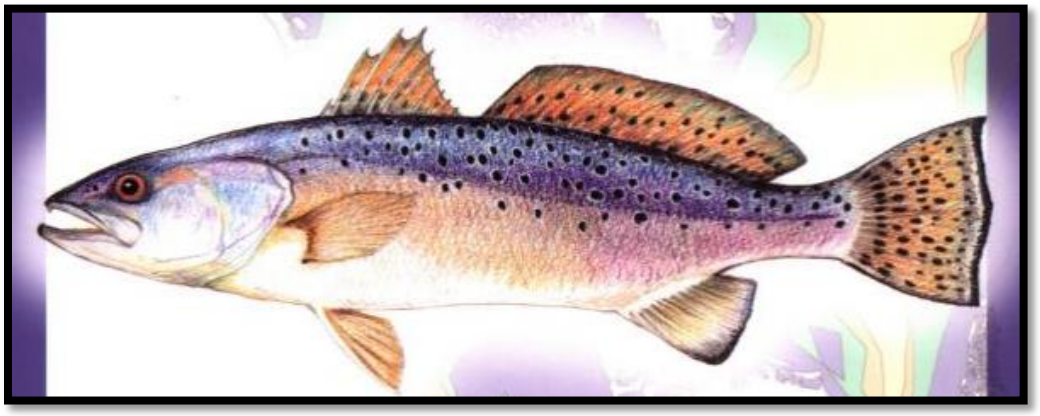

Figure B1 Image of spotted seatrout (Bortone 2003)

Spotted seatrout have a wide geographic range, extending from Cape Cod, MA southward along the Atlantic Coast, and across the Gulf Coast to Campeche, Mexico (Lassuy 1983; Blanchet et al. 2001). Figure B2 below features their distribution and

locations of abundance along the Gulf of Mexico. At all life stages, spotted seatrout are closely associated with the estuarine environment, however, the growth and feeding habits are specific to each point in the life history (Bortone and Wilzbach 1997). As larvae, spotted seatrout utilize grassbed nurseries within their natal estuaries, specifically for ample food resources as well as physical cover providing protection from predators (Bortone and Wilzbach 1997).

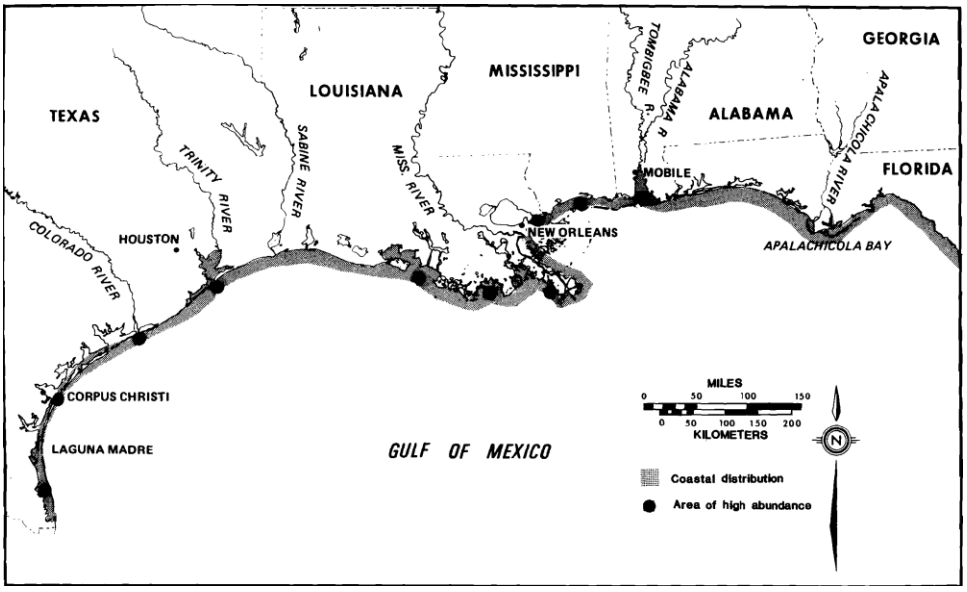

Figure B2 Spotted seatrout distributions around Gulf of Mexico (Lassuy 1983)

As an "opportunistic carnivore whose food changes with size," spotted seatrout prey choices are distinctly different among life stages (Lassuy 1983). In general, larvae between 20 and 50 mm in standard length (SL), are planktivorous, feeding largely on copepods in fresh, brackish, and salt waters (Darnell 1961; Hill 2005). From 40 to 150mm SL, a dietary shift is evident as the fish change to juveniles and the prey choices expand to include penaeid shrimp (*Penaeidae* family), caridean shrimp (*Palaemonidae* family), small fish, crabs, benthic invertebrates, and mysids (Hill 2005) . Between 150 and 250 mm, penaeid shrimp become the predominant prey choice, but adult spotted seatrout (>350 mm) are largely found in surface waters targeting fish including anchovy (*Anchoa* spp), silversides (*Atheriniformes*), mullets (*Mugil* spp), pinfish (*Lagoden*

rhomoides), Atlantic croaker (*Micropogonias undulatus*), menhaden (*Brevoortia patronus*), and sheepshead minnows (*Cyprinodon variegatus*) (Kostecki 1984; Blanchet et al. 2001; Nieland et al. 2002; Hill 2005). It should also be noted that ontogenic shifts and associated prey choice are also due in large part to the structure of the surrounding ecological community (Lassuy 1983).

In Lake Pontchartrain, quantitative studies of the dietary habits of the lake's inhabitants have been made by other researchers including those from Tulane University and Louisiana Department of Wildlife and Fisheries (Darnell 1958). It was noted that calanoid copepods (*Acortia tonsa*) and adult schizopods (*Mysidopsis*) were the major prey of young spotted seatrout and thus held a critical trophic position for the species (Darnell 1961). When the young reached 40-99 mm, small crustaceans made up 44% of their food material, specifically isopods (*Isopoda*), schizopods, amphipods (*Amphipoda*), and chironomid larvae (*Chironomidae*) (Darnell 1958; Darnell 1961). These micro-bottom species are abundant due to high turbidity conditions, large regions of mud-bottom, and the sparse distribution of grassy flats found in Lake Pontchartrain (Darnell 1958). Deviations from accepted food patterns typical to the spotted seatrout also occurred when researchers analyzed the feeding habits of adults. Due to the near absence of panaeid shrimp, caridean shrimp, or pinfish, adult spotted seatrout were found to be targeting anchovies, a species ubiquitous throughout the lake. Not only do spotted seatrout in the lake bypass the panaeid shrimp phase to enter adult feeding patterns, but do so much earlier in life, at a TL of 100mm (Darnell 1958). In contrast, Florida spotted seatrout were observed to have four feeding stages consisting of copepods for fish up to 30 mm TL, schizopods for fish 20-70 mm, caridean shrimp for those 50-80 mm, anchovies for fish up to 150 mm, and adult diets of panaeid shrimp at 150 mm and greater (Darnell 1958). The distribution of spotted seatrout, however, is likely not only

"tied to the availability of a food web that meets their needs" but also "suitable salinity and temperature regimes" that can influence their growth rate (Lassuy 1983).

In general, spotted seatrout growth occurs in distinctive patterns throughout their lives. The first year of life is marked by the fastest growth, with a growth rate of 0.4 mm per day, allowing fish age-1 to reach approximately 200-350 mm TL (Nieland et al. 2002; Bortone 2003). After the rapid growth rate in early life, spotted seatrout then grow less than 100 mm in the second year, and less than 75 mm per year in the time following (Bortone 2003). The energetic costs incurred by basic metabolic processes are dominated by mass scaling, shifting as an individual spotted seatrout grows in size (Post and Lee 1996). The early life history is marked by rapid growth in mass with a proportionate increase in metabolic rates, but since adults have significantly slower growth, the metabolic rate increases disproportionately to size. Growth has also been found to differ significantly on both broad regional scales (along latitudes) and finer scales (specific estuaries) (Smith et al. 2008). With a wide geographic range, the leading theory for latitudinal differences relies on a principle of countergradient growth. As an example, spotted seatrout in Chesapeake Bay have been found to exhibit faster growth in the time leading to maturity than those in Florida as a direct result of a significantly reduced growing season (Smith et al. 2008). In addition to the broad effects at the regional scale, a suite of features influence spotted seatrout more directly. Habitat features including temperature regimes, salinity ranges, dissolved oxygen, turbidity, and habitat type directly influence a species' ability to meet the metabolic cost of growth, reproduction, and activity (Post and Lee 1996). Thus understanding these elements is critical for those responsible for the species' management.

ECOLOGICALLY IMPORTANT HABITAT TRAITS

Along the US, the Gulf of Mexico encompasses over 200 estuaries from the coast of Florida to the Lower Laguna Madre in Texas and, according to the Cooperative Gulf of Mexico Estuarine Inventory, over 5.2 million hectares (ha) have been designated as estuarine habitat (Blanchet et al. 2001). Spotted seatrout are considered an estuarine species rarely traveling farther than 30 km from the estuary where they were spawned (Smith et al. 2008). The distribution of fish within the estuary is likely driven by water quality, specifically those which effect relative fitness (Neahr et al. 2010). Generally, adult spotted seatrout prefer shallow, brackish waters up to 10 meters deep with shallow marsh edges adjacent to open water (Bortone 2003). In the winter, spotted seatrout make use of the shallow warm bays and in the summer travel to cool deep-water channels (Blanchet et al. 2001; Hill 2005). While the adults utilize a wide variety of habitats within the estuary, including seagrass beds, oyster reefs, sand/mud bottom, or manmade structures, the juveniles are more limited to the marsh edge/backwaters and the larvae solely to the seagrass beds (Hill 2005). The concept of the estuary as a nursery for spotted seatrout stems from the species' entire life cycle occurring within a single estuary and each life stage occupying a particular territory whose chemical and physical traits optimize net energy gain for the individual (Baltz et al. 1993; Beck et al. 2001).

Dissolved Oxygen

The metabolic activity of fish is impacted by the oxygen concentration of water in which the species lives, thus dissolved oxygen (DO) can be a controlling factor in the distribution of juvenile and adult spotted seatrout within the estuarine system (Blanchet et al. 2001). It should also be noted that DO and the level of metabolic demand is in part controlled by temperature and salinity. For the Gulf region, DO demand has been

determined specifically for spotted seatrout. At an optimum temperature of 28^{o}C and salinity of 20 parts per thousand (ppt), the hourly demand on oxygen can range from 214-574 mg of O_2 per kg of fish body weight (Hill 2005). Minimum metabolic demands at this same temperature, however, were observed to change depending on the salinity. Researchers observed the minimum demand to be 210 mg/kg/hr at 10 ppt, 125 mg/kg/hr at 20 ppt, and 230 mg/kg/hr at 30 ppt (Lassuy 1983). At high summer temperatures of 30^{o}C, the hourly demand ranged from 148-502 mg O_2/kg (Hill 2005). As a result of water stratification during the summer and eutrophication (increase in nutrient concentrations), however, detrimental hypoxic conditions within the Gulf region are a serious concern to fisheries management (Goodman and Campbell 2007).

Large areas (1.82 million ha) of hypoxic bottom waters are produced in the Gulf of Mexico as a result of nutrient rich freshwater from overland flow entering the estuarine/coastal systems of the region (Blanchet et al. 2001). In the Louisiana province, 5.2-29.3% of the total estuarine regions were affected by such conditions between 1991 and 1994 (McDonald et al. 2013). During a similar timeframe (1993-1999) the continental shelf region shared by Texas and Louisiana the hypoxic zone encompassed an area large as New Jersey (McDonald et al. 2013). In assessing the species' limitations, researchers conducted 24 and 48 hour tests on spotted seatrout juveniles (45.0±3.7 mm TL) acclimatized for 10 days to an environment 28^{o}C and with a salinity of 28 ppt (Goodman and Campbell 2007). It was determined for these spotted seatrout that a lethal dose for 50% of the fish (LD50) occurred at a DO level of 1.88 to 1.89 mgL^{-1} while the LD90 occurred at 1.58 mgL^{-1} (Goodman and Campbell 2007). In aquaculture ponds used for spotted seatrout stocking in Texas, lethal DO levels for larval stages were noted to be <4 mgL^{-1} (Hill 2005). While spotted seatrout are considered moderately susceptible to hypoxia in their estuarine habitat, it is the younger juvenile and larval stages that are the

most susceptible (Blanchet et al. 2001). Adult spotted seatrout, utilize less energy for growth than either of these two earlier life stages, and are capable of leaving areas with low DO (Blanchet et al. 2001).

Salinity

"Salinity and temperature are considered the most important physio-chemical factors influencing fish distributions between and within estuary systems (Bortone 2003)." For spotted seatrout, age-dependent patterns of tolerance are evident from the egg stage through to adult (Blanchet et al. 2001). The optimum salinity for eggs is 28.1ppt and 100% survival has been reported eggs in waters with salinities from 18.6-37.5 ppt (Banks et al. 1991). A critical minimum below which no survival is expected has been noted at 0 ppt and the critical maximum at 50 ppt (Banks et al. 1991; Blanchet et al. 2001; Wuenschel et al. 2004). In using the estuary for feeding, spawning, and nursery grounds, spotted seatrout are noted as being euryhaline, but are fully capable of adapting to salinities as low as 0.2 ppt and as high as 70 ppt (Banks et al. 1991).

Spotted seatrout encountering a broad range of salinities require competent osmoregulatory mechanisms in order to balance the fish's internal osmotic concentration to that of the environment (Banks et al. 1991; Wuenschel et al. 2004). Adults and juveniles capable of this process exhibit similar preferences for salinities of 15-35 ppt (Banks et al. 1991; Wuenschel et al. 2004). To detail the salinity preferences of spotted seatrout in coastal Louisiana, the LDWF conducted over 9,000 monthly seine hauls between 1986 and 2000 across Louisiana's coastal estuaries (Bortone 2003). Size classes for juveniles included class I (<25 mm TL), II (>25-50 mm TL), III (>50-100 mm TL) and IV (>100-150 mm TL) (Bortone 2003). Mean salinity values for juveniles within these size ranged were determined by researchers to be 13 ppt, 11.1 ppt, 11.3 ppt, and

11.1 ppt, respectively. In analyzing the salinity preferences, researchers further concluded that only size I used significantly lower salinities (Bortone 2003).

Adult spotted seatrout were also assessed as a component of LDWF's sampling program (Bortone 2003). Adult size classes were determined to be class I (≤149 mm TL), II (≥150 mm and ≤304 mm TL), III (≥305 mm and ≤449 mm TL) and IV (≥450 mm TL). For adult spotted seatrout in Terrebonne Bay, Louisiana, the highest abundance of individuals occurred within the marine salinity zone (> 25 ppt) when compared to either the mixing zone (0.5-25 ppt) or tidal fresh zones (0-0.5 ppt). While the preferred range for adults appeared to be 15-28 ppt, researchers noted seasonal considerations were critical to understanding temporal differences in salinity preferences. The range of salinities utilized by adult spotted seatrout indicated that specific preferences may be due not only to season (discussed in later sections on spawning and habitat suitability models), but also the estuarine habitat to which the native population is adapted (Bortone 2003).

It is through the processes of osmoregulation that such adaptability is possible for the species, and in turn, defines habitat limitations (Wuenschel et al. 2004). One mechanism utilized is the reduction in gill membrane permeability should the pressure difference between internal and external fluids increase (Wuenschel et al. 2004). In doing so, the individual also limits oxygen transfer, decreasing their capacity to meet metabolic energy demands. While the optimum salinity (by swimming preference) is between 20 and 25 ppt, the extreme tolerances where decreased oxygen supplies make maintaining swimming difficult are salinities below 10 ppt or above 45 ppt (Blanchet et al. 2001; Hill 2005). In fact, such levels provide for "no excess available energy beyond ecological maintenance requirements (Lassuy 1983)." Typically salinities below 5 ppt are noted by researchers as "intolerable" and likely to lead to mass mortalities, especially

if such conditions result from a rapid freshening (Lassuy 1983). Changing salinity over a short period of time causes hydromineral imbalances in a fish's blood, which becomes diluted as salinity drops or concentrated when it rises drastically; either condition can be lethal (Serafy et al. 1997).

Salinity Changes within an Estuary

Salinity shifts in estuaries is a common phenomenon and a function of river discharge volumes and tidal prisms (Sklar and Browder 1998). Variations in salinity are often seen as shifts in the location of isohalines, the lines of uniform salinity. High freshwater input relative to a small tidal prism will result in lower salinities within the estuary by effectively shifting the isohalines seaward (Sklar and Browder 1998). In shallow estuaries, seawater inflow during dry seasons can be significantly higher in volume that that contributed by inflowing river systems, shifting isohalines up the estuary. Freshwater pulses, by comparison, can create rapid salinity changes and high stress environments to fish species (Sklar and Browder 1998). As an example, the United States Army Corps of Engineers developed extensive systems of canals, locks, and other flood control structures in south Florida (Sklar and Browder 1998). Biscayne Bay is a hypersaline lagoon connected to this canal system, which when opened, can cause a precipitous salinity drop of 25 ppt within one hour in receiving waters (Serafy et al. 1997). The Caernarvon Freshwater Diversion is a similar structure, directing waters from the Mississippi River into the Breton Sound Estuary (Rozas et al. 2005). Capable of diverting 226 m^3s^{-1} of Mississippi River water, researchers in 2000 and 2001 assessed changes to the macrofauna within the brackish and intermediate zones in response to a prolonged release. Salinity gradients shifted with the pulse event. With in-flowing water at a salinity of $\leq$5 ppt, the average salinity in the receiving region dropped from 8.6 ppt to

5.9 ppt. While the inflow region did experience a drop in salinity, the community structure was unaffected, changing only in species density and biomass (Rozas et al. 2005). While freshwater pulses can effectively alter the salinity regime in an estuary, these pulses have historic patterns of influence.

Temperature

Environmental stressors experienced by spotted seatrout also include the effects of water temperature changes within their estuaries (Hill 2005). For larval spotted seatrout in the Gulf of Mexico the optimum temperature lies between 23^{o}C and 33^{o}C. Being the most vulnerable of stages, larvae are also susceptible to changes in water temperature, failing to metamorphose at temperatures ≤ 23.5^{o}C (Hill 2005). Juveniles and adults from the region, however, display similar temperature tolerances. Juvenile growth is optimal at temperatures ≥28^{o}C and survive throughout a range of 11.5-32^{o}C (Hill 2005). Through over 9,000 seine hauls across coastal Louisiana, LDWF determined that the mean temperature preferences for size class I (<25mm TL), II (>25-50mm TL), III (>50-100 mm TL) and IV (>100-150mm TL) were 27.6^{o}C, 27.3^{o}C, 24.6^{o}C, and 23.4^{o}C respectively (Bortone 2003). While the preference of size class I and II did not differ significantly, any other comparison yielded a significant difference in temperature preference (Bortone 2003).

Adults spotted seatrout have the widest temperature tolerance range from 4-33^{o}C in which they can live and feed, but typically have a preferred range dependent on their region (Kostecki 1984). In Florida, the preferred range is 16-27^{o}C and in Louisiana waters the species' preferred range is 20-32^{o}C (Kostecki 1984; MacRae and Cowan 2010). Optimum temperatures for spotted seatrout across the Gulf of Mexico region appear to be within the range of 25-30^{o}C (Lassuy 1983). Since the spawning season

constitutes the largest timeframe for adult spotted seatrout and the preferences around it, spawning is discussed in a following section. For spotted seatrout in Louisiana's coastal waters, the post spawning period (September) and overwintering season (October-March) are when adult spotted seatrout contend with cooling temperatures, and in the northern regions of their distribution, decreasing fall temperatures prompt the fish to emigrate from their estuaries and into the deeper waters of the coastal shelf (Bortone 2003) (Lassuy 1983). Individuals return when the water temperature reaches 10-12^{o}C in North Carolina, 17^{o}C in Georgia, and 21^{o}C in Texas (Lassuy 1983). Within the Gulf of Mexico, such movements are less pronounced as the fish seek out deep channels and holes within the estuary to overwinter (Arnoldi 1984). In Lake Calcasieu (LA), research conducted by LDWF from 1976-1983 using gillnets determined that during extreme heat or cold, deeper and more thermally stable bay channels, specifically Calcasieu Pass and Calcasieu Ship Channel, were utilized by the species as a direct shift in distribution in response to seasonal temperature changes (Arnoldi 1984).

Spawning

In Louisiana waters, spawning schools have been documented in many estuarine systems, including Barataria Bay, Breton Sound, Callilou Bay, and Terrebonne Bay (Saucier and Baltz 1993). Gillnet surveys were conducted from 1988 to 1990 within these bays to determine if salinity significantly correlated with spawning site selection (Helser et al. 1993). Natural salinity groupings/zones were evident in each waterbody and ranged from the upper oligohaline region (0-9 ppt), to the intermediate mesohaline region (10-14 ppt) and finally the lower polyhaline region (15-30 ppt) (Helser et al. 1993). For both recruits and adults, the greatest variation in location of abundance was found to be a result of a zone by season interaction. During the spawning season (May-

August), adult and recruit abundance were significantly and positively related to salinity, with both groups found most often in the lower polyhaline region. In the post-spawning season (September-December), however, adults displayed a uniform distribution across all salinities. Recruit abundance also changed, becoming significantly negatively related to salinity and therefore found most often in the upper oligohaline region (Helser et al. 1993). Researchers found that abundance was not only significantly related to salinity, but also current velocity (Helser et al. 1993). Along these bays, spawning aggregations were often found in barrier island passes, including those adjacent to Grand Isle, Timbalier Island, and Grande Terre (Saucier and Baltz 1993). Currents flowing between the islands provide an effective mechanism for the transportation/dispersion of eggs into inshore environments, where the offspring are most likely to find the salinity and temperature ranges that will improve overall survival (O'Connell et al. 2005, Callihan 2011). In addition, researchers evaluated the physical characteristics of habitats occupied by each successive life stage.

PHYSICAL CHARACTERISTICS

In many estuaries in Louisiana, seagrass beds are sparse and typically spotted seatrout adults will preferentially choose spawning locations near marsh edges as a result. Louisiana estuaries contain extensive marsh areas, each with dominant species of emergent vegetation (Bortone 2003). Over 163,000 ha of salt marsh areas are dominated by smooth cordgrass, blackrush (*Juncus roemerianus*), and saltgrass (*Distichlis spicata*) (Bortone 2003). Around 308,700 ha constitute brackish marsh areas containing wiregrass (*Spartina patens*), and around 147,470 ha constitute intermediate marsh areas containing wiregrass and sawgrass (*Cladium jamaicense*) (Bortone 2003). With respect to bottom type, adult spotted seatrout were found by researchers to display little habitat selection,

choosing to spawn over rubble, sand/shell reefs, pilings, and soft bottom uniformly (Bortone 2003). In addition, once spawning is complete, adult spotted seatrout have shown little physical habitat preference (MacRae and Cowan 2010).

Through dietary analysis, acoustic imaging of habitat types, and gillnetting, researchers from LDWF and Louisiana State University (LSU) working throughout Barataria Bay determined that spotted seatrout, as a highly mobile species, changed habitat use often while engaging in foraging activities (MacRae and Cowan 2010). In fact, data clearly indicated that adult spotted seatrout displayed no consistent pattern of selection between the marsh edge, soft-bottom, and oyster shell reef (MacRae and Cowan 2010). Researchers determined that in general spotted seatrout were to be found in open water, independent of the bottom habitat structure. The researchers assessing presence/absence of spotted seatrout adults determined their habitat use was most likely dependent on food availability provided a suitable salinity and temperature regime were present, a finding in agreement with additional research (Perret et al. 1980; Harding and Mann 2001; MacRae and Cowan 2010). Despite these findings, anecdotal evidence on the value of structural complexity and vertical relief has been used to initiate artificial reef projects in order to mimic natural oyster shell beds that can presumably provide habitat supportive of more diverse and abundant fish species (MacRae and Cowan 2010, Callihan 2011).

Turbidity

The least detailed feature of fishery production and preferred habitat patterns by spotted seatrout is the influence of turbidity (Bortone 2003). It is considered beneficial to early life stages in that increased turbidity enhances survival by providing physical cover to the smallest and most vulnerable life stages. With the shallow, microtidal (<2 m)

estuaries of Louisiana dominated by storm events and fine sediments from the Mississippi River, the abundance of small fish is estimated to be higher in those nearshore shallow environments with a turbidity over 10 nephlometer turbidity units (NTU) (Bortone 2003). Excessively turbid waters are often produced as a result of rapidly inflowing, sediment-laden waters during and following severe storm events (hurricanes/cyclone/tropical storm) (Blanchet et al. 2001). These flows can result in spotted seatrout mortalities as a result of suffocation. As suspended sediment clogs gills, oxygen exchange with surrounding waters is severely restricted and death is possible (Blanchet et al. 2001).

Algal Blooms

Harmful algal blooms are a common occurrence in most coastal estuaries, including those of Maryland, Virginia, North Carolina, Florida, Louisiana, and Texas (Fleming et al. 1999). As a result, spotted seatrout are often exposed within their estuaries to such blooms and the detrimental effects that may result (Fleming et al. 1999). Algae are microscopic photosynthetic cells that form the base of the aquatic food chain and typically come in the form of dinoflagellates, diatoms, or cyanobacteria. They are present in all water types, from marine to brackish and even freshwater. Being so ubiquitous, when the particular chemical and physical conditions are present, an overgrowth of the cells can occur quickly. A toxic algae bloom, as opposed to a nuisance bloom, occurs when one or more of the 80 toxic species proliferate, creating a deadly environment for fish and shellfish (Fleming et al. 1999).

Conditions within an estuary are often conducive to the overproduction of these microscopic cells, especially when the estuary receives high concentrations of nutrients (nitrogen and phosphorus) into shallow, warm, slow-moving waters. These nutrients are

often contributed by runoff from the surrounding watershed, the sources including human/animal waste products, fertilizers, and industry by-products. In using estuarine environments, spotted seatrout are particularly vulnerable to these blooms that can develop quickly within the estuary, often resulting in a massive loss of life. While the majority of fish kills produced as a result of harmful algae blooms were historically attributed to the subsequent low dissolved oxygen conditions, the species and the toxins produced may in fact have played a larger role in the massive fish mortality events (Fleming et al. 1999).

HABITAT SUITABILITY MODELS

In predicting spotted seatrout distribution and abundances related to habitat preferences, Geographic Information Systems (GIS) technology provides an invaluable tool for managers in integrating spatial and ecological information into a single database (Bortone 2003). Models specifically focused to a single species and its habitat preferences are known as Habitat Suitability Models (HSM) (Bortone 2003). A subset of HSM are Habitat Suitability Index models (HSI), which rely on mathematical expressions that calculate habitat suitability for a species depending both on the environmental data available and on those variables with the greatest influence on the species distribution. The HSI can incorporate changing values, allowing for seasonal/event-driven changes as well as the unique limitations of the species and its particular life stages. The driving assumption is the positive relationship between the assigned index value and the species abundance (Bortone 2003). In order for such a model to be developed, however, comprehensive data and research must be incorporated to identify the specific environmental variables necessary. Modern models have become sophisticated to the point of including not only commonly considered variables (salinity, temperature, DO,

bottom substrate, submerged aquatic vegetation (SAV) but also ecological variables including species interaction, predation, and prey availability (Bortone 2003). HSI's have already been developed by managers through The Center for Coastal Monitoring and Assessment Biogeography Program, US Fish and Wildlife Services Habitat Evaluation Procedures Program, and BP's Estuarine Living Marine Resources Database Program (Bortone 2003).

Researchers working in Pensacola Bay, FL developed a qualitative HSI for the bay area, incorporating the chemical variables of salinity, water temperature, and DO (Bortone 2003). Physical features included in the model were bottom substrate, SAV, and emergent macrophytes (Bortone 2003). Mapping the entire bay, researchers separated zones of salinity in 5 ppt increments, temperature by 2^{o}C isotherms, and DO in 1 mg/L portions. With aerial photography, the extent of SAV and emergent vegetation were determined. Matrices allowed researchers to organize data for abundance/distribution according to these increments with critical values (and their associated suitability index values) established under the assumption all other variables were to be held constant. Suitability index values included unsuitable (0), low (0.01-0.33), moderate (0.34-0.66), high (0.67-0.99), and optimal (1.0) (Bortone 2003). The optimum condition occurred within a cell only when all the environmental variables were optimum, but if a single variable emerged as unsuitable, the entire cell would be designated unsuitable (Bortone 2003). Values and ranges for juvenile and adult spotted seatrout are available in Figure B3 below.

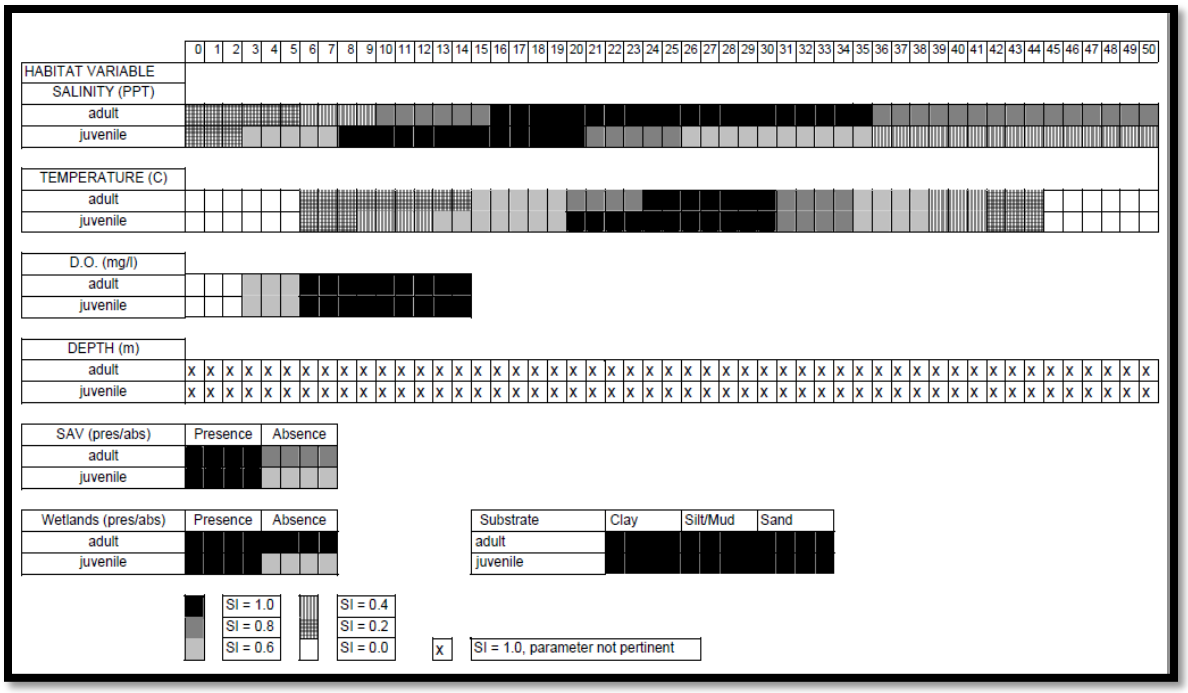

Figure B3 Suitability by age as determined for HSI (Bortone 2003)

According to the suitability index values, adult spotted seatrout encounter optimal salinity between 16 and 35 ppt, high suitability from 9-50 ppt, moderate suitability from 6-9ppt, and low suitability from 0-5 ppt (Bortone 2003). Regarding temperature regions, adults and juveniles appear to share similar preferences, with a combined high and optimal range from 20-34^{o}C. Moderate temperature ranges were also similar, extending down to 13^{o}C for juveniles and 15^{o}C for adults. Both age classes shared an upper limit of moderate suitability at 38^{o}C. With respect to bottom substrate, the age classes were designated as having optimal conditions with clay, mud/silt, or sand bottom conditions (Bortone 2003). Regions with the highest suitability values for juvenile and adult spotted seatrout were determined to be those with SAV and emergent vegetation, particularly from May to August wherein the species encountered optimum water temperatures for growth (25-30^{o}C) and increasing salinities. Nonvegetated regions were determined to have medium to low suitability, particularly during the period from December to January with decreasing salinity values and temperatures (to 10-14^{o}C). With their increased

capacity to manage metabolic demands, adult spotted seatrout overall were depicted as having more extensive high-suitability zones as compared to the juveniles (90% of the bay from May-August). In addition, suitable habitat for adults extended into deeper water portions of the bay, which is appropriate for adult spotted seatrout as they exhibit piscivorous feeding patterns within mid-waters. A similar HSI developed by the Florida Department of Environmental Protection revealed similar measures of suitability for spotted seatrout in Tampa Bay and Charlotte Harbor, Florida (Bortone 2003).

CONCLUSION

In general, the species prefers large regions of shallow (3-6 m), brackish (15-28 ppt for growth, maturation, spawning, and survival of larvae) water with an abundance of crustaceans and fish of a suitable size for consumption and a stable temperature regime (16-27^{o}C) (Kostecki 1984, Mazzotti et al. 2008). While highly adaptable to a wide range of both salinity and temperature, spotted seatrout have proven uniquely adapted to their natal estuary, characterized by its own water quality regimes (Bortone 2003). It is the seasonal/event-driven variability in dissolved oxygen, salinity, and temperature that have been noted to be the most influential physiochemical variables on spotted seatrout distribution. Secondary/complicating variables, specifically bottom type, turbidity, and algal blooms, however, are also important features in shaping the suitability of estuarine zones for this species (Bortone 2003). Over the course of their life history, spotted seatrout exhibit different habitat preferences and physical capacities to adapt metabolically to meet these environmental instabilities.

LITERATURE CITED

Baltz, D.M., C. Rakocinski, and J.W. Fleeger. 1993. Microhabitat use by marsh-edge fishes in a Louisiana estuary. Environmental Biology of Fishes 36:109-126.

Banks, M.A., G.J. Holt, and J.M. Wakeman. 1991. Age-linked changes in salinity tolerance of larval spotted seatrout (*Cynoscion nebulosus*). Journal of Fish Biology 39:505-514.

Beck, M.W., K.L. Heck Jr., K.W. Able, D.L. Childers, D.B. Eggleston, B.W. Gillanders, B. Halpern, C.G. Hays, K. Hoshino, T.J. Minello, R.J. Orth, P.F. Sheridan, and M.P. Weinstein. 2001. The identification, conservation, and management of estuarine and marine nurseries for fish and invertebrates. Bioscience 8:633-341.

Blanchet, H. M.VanHoose, L. McEachron. B. Miller, J. Warren, J. Gill, T. Waldrop, J. Waller, C. Adams, R.B. Ditton, D. Shively, and S. Vanderkooy. 2001. The spotted seatrout fishery of the of Mexico, United States: A regional management plan. Gulf States Marine Commission.

Bortone, S.A. and M.A. Wilzbach. 1997. Status and trends of the commercial and recreational landings of spotted seatrout (*Cynoscion nebulosus*) South Florida. Florida Center for Environmental Studies. Technical Series 2:1-47.

Bortone, S.A. 2003. Biology of the Spotted Seatrout. CRC Press, Boca Raton, Florida.

Callihan, J.L. 2011. Spatial ecology of adult spotted seatrout, *Cynoscion nebulosus*, in Louisiana Coastal Waters. PhD Diss. Louisiana State University. Baton Rouge.

Darnell, R.M. 1958. Food habits of fish and larger invertebrates of Lake Pontchartrain, Louisiana, an estuarine community. Institute of Marine Science 5:353-413.

Darnell, R.M. 1961. Trophic spectrum of an estuarine community, based on studies of Lake Pontchartrain, Louisiana. Ecology 42:553-568.

Fleming, L.E., J. Easom, D. Baden, A. Rowan, and B. Levin. 1999. Emerging harmful algae blooms and human heath: *Pfiesteria* and related organisms. Toxicology Pathology 5: 573-581.

Goodman, L.R. and J.G. Campbell. 2007. Lethal levels of hypoxia for Gulf coast estuarine animals. Marine Biology 152:37-42.

Harding, J.M. and R. Mann. 2001. Diet and habitat use by bluefish, *Pomatomus saltatrix*, in Chesapeake Bay estuary. Environmental Biology 60:401-409.

Helser, T.E., R.E. Condrey, and J.P. Geaghan. 1993. Spotted seatrout distribution in four Coastal Louisiana estuaries. Transactions of the American Fisheries Society 1:99-111.

Hill, K. 2005. Spotted seatrout (*Cynoscion nebulosus*). Smithsonian Marine Station at Fort. Retrieved from ‹http://www.sms.si.edu/irlspec/Cynosc_nebulo.htm›

Kostecki, P.T. 1984. Habitat suitability index models: Spotted Seatrout. Washington DC: Fish and Wildlife Service US Department of the Interior.

Lassuy, D.R. 1983. Species profiles: Life histories and environmental requirements (Gulf of Mexico) spotted seatrout. National Coastal Ecosystems Team.

MacRae, P.S.D. and J.H. Cowan, Jr. 2010. Habitat preferences of spotted seatrout, *Cynoscion nebulosus*, in coastal Louisiana: A step towards informing spatial management in estuarine ecosystems. The Open Fish Science Journal 3:154-163.

Mazzotti, F.J., L.G. Pearlstine, T. Barnes, S.A. Bortone, K. Chartier, A.M. Weintstein, and D. DeAngelis. 2008. Stressor-response model for the spotted seatrout (*Cynoscion nebulosus*). Institute of Food and Agricultural Sciences, University of Florida.

McDonald, D.L., P.D. Cason, B.W. Bumguardner, and S. Bonnot. 2013. Critical thermal maximum of juveniles spotted seatrout (*Cynoscion nebulosus*) reared for summer stocking in Texas. Journal of Applied Aquaculture 25:308-319.

Neahr, T.A., G.W. Stunz, and T.J. Minello. 2010. Habitat use patterns of newly settled spotted seatrout in estuaries of the north-western Gulf of Mexico. Fisheries Management and Ecology 17:404-413.

Nieland, D.L., R.G. Thomas, and C.A. Wilson. 2002. Age, growth, and reproduction of the spotted seatrout in Barataria Bay, Louisiana. Transactions of the American Fisheries Society 131:245-259.

O'Connell, M.T., C.D. Franze, E.A. Spalding, and M.A. Poirrier. 2005. Biological resources of the Louisiana coast: Part 2. Coastal animals and habitat association. Journal of Coastal Research 44:146-161.

Perret, W.S., J.E. Weaver, R.O. Williams, P.L. Johansen, T.D. McIlwain, R.C. Raulerson, and W.M. Tatum. 1980. Fishery profiles of red drum and spotted seatrout. Gulf States Marine Fisheries Commission Report 6.

Post, J.R. and J.A. Lee. 1996. Metabolic ontogeny of teleost fishes. Canadian Journal of Aquatic Science 53: 910-923.

Rozas, L.P., T.J. Minello, I. Munuera-Fernandez, B. Fry, and B. Wissel. 2005. Macrofaunal distributions and habitat change following winter-spring releases of freshwater into the Breton Sound estuary of Louisiana (USA). Estuarine, Coastal, and Shelf Science 65: 319-336.

Saucier, M.H. and D.M. Baltz. 1993. Spawning site selection by spotted seatrout, *Cynoscion nebulosus*, and black drum, *Pogonias cromis*, in Louisiana. Environmental Biology of Fishes 36:257-272.

Serafy, J.E., K.C. Lindeman, T.E. Hopkins, and J.S. Ault. 1997. Effects of freshwater canal discharge on fish assemblages in a subtropical bay: Field and laboratory observations. Marine Ecology Progress Series 160:161-172.

Sklar, F.H. and J.A. Browder. 1998. Coastal environmental impacts brought about by alterations to freshwater flow in the Gulf of Mexico. Environmental Management 22:547-562.

Smith, N.G., C.M. Jones, and J. Van Montfrans. 2008. Spatial and temporal variability of juvenile spotted seatrout *Cynoscion nebulosus* growth in Chesapeake Bay. Journal of Fish Biology 73:597-607.

Wuenschel, M.J., R.G. Werner, and D.E. Hoss. 2004. Effect of body size, temperature and salinity on the routine metabolism of larval and juvenile spotted seatrout. Journal of Fish Biology 64:1088-1102.

APPENDIX C: WATER QUALITY AND THE DATAFLOW SYSTEM

INTRODUCTION

The social, economic, and scientific importance of coastal environments have sparked intense interest in developing both a better understanding and management systems under the principle of sustainable development (Figure C1). Many countries have established water-related laws with distinct aims, including establishing baseline monitoring data for water quality parameters, identifying regions at risk for eutrophication/plankton blooms, evaluating environmental integrity and the influence of human-induced nutrient/climate changes, environmental thresholds, and assessment of restoration efforts (Hart et al. 1993; Gagnon et al. 2007). At the heart of any and all regulatory or planning actions for coastal zone management, therefore, is water quality data collection.

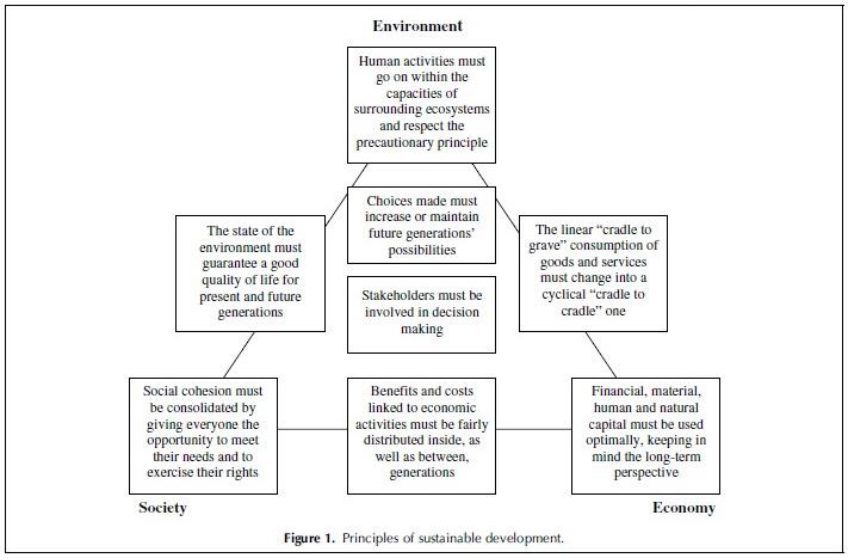

Figure C1 Sustainable development principles and links between social, environmental and economic sectors (Gagnon et al. 2007)

Through scientific research into the processes that define the physical and chemical character of rivers, estuaries, and wetlands, it is clear that not only are aquatic systems exceptionally vulnerable to the effects of human activity, both directly (destruction) and indirectly (overland flow), but also that individual system's unique heterogeneity across these parameters makes each a challenge for assessment (Zambrano et al. 2009). Spatial heterogeneity is largely considered a positive attribute, linked to the health, biodiversity, and sustainable functioning of each coastal system (Zambrano et al. 2009). In the collection of water quality data, both spatial and temporal dimensions must be considered in order to achieve a comprehensive understanding of the environment to be managed. Traditional methods of sampling at stations, however, place severe restrictions on the number of samples that can be collected (limited sites/spatial data), on the number of diagnostics that can be run (limited chemical data), and on the number of research cruises that can be taken to collect such samples (limited temporal data) (Hart et al. 1993). As a result, such methods are very limited and costly (Peterson et al. 2011).

Fixed site monitoring/sampling also fails to resolve the dynamic spatial complexity inherent to coastal systems and is therefore inadequate for evaluating biogeochemical changes due either to management actions or to significant events (freshwater pulses, plankton blooms, hypoxia, oil spills, etc.) (Hart et al. 1993). Working without a complete picture leads to growing uncertainty among managers and scientists. Portable underway flow-through systems, including Dataflow, have been developed by integrating off-shelf water quality instruments that can, as a unit, provide comprehensive, synoptic, and spatially referenced water quality data (Hodge et al. 2005). In addition, these systems can be operated by a single person either on a small research vessel for special focus assessments or on large ships of opportunity for regional scale evaluations. In the most basic description, flow-through systems are "devices containing the primary

sensing element, signal amplification and filtering system, and dedicated software for data processing and compensation (Charef et al. 2000)." As such, these "smart sensors" provide scientists and managers with a powerful tool for assessing heterogeneity both within and across coastal systems while managing the costs of such assessments (Charef et al. 2000).

INSTRUMENTATION AND USE

The Dataflow system is a portable flow-through system that can be transported on almost any vessel for the purpose of collecting high quality biogeochemical data, effectively producing a "snap-shot" of water quality across a region (Madden and Day Jr. 1992). The system itself uses the forward momentum of a vessel to force surface waters through an intake pipe, a debubbler for the removal of entrained oxygen bubbles, a pump to control flow, a sensor array, and finally overboard through an outlet hose (Madden and Day Jr. 1992; Madden 2013). The sensors within the array can be chosen to meet specific research needs, but for this study included an YSI 600XL multi-parameter probe for reading water temperature, dissolved oxygen (DO), and salinity (Madden and Day Jr. 1992). A Turner Designs C6 unit was also a component of the system, providing additional instrumentation in the form of fluorometers which utilized the properties of light absorbance and scattering to determine concentrations of specific phytoplankton pigments (chlorophyll *a*, phycocyanin, phycoerythrin), oils, colored dissolved organic matter (CDOM), and suspended sediments (Madden and Day Jr. 1992). Please see Figure C2 for a detailed diagram of the first edition of the Dataflow system.

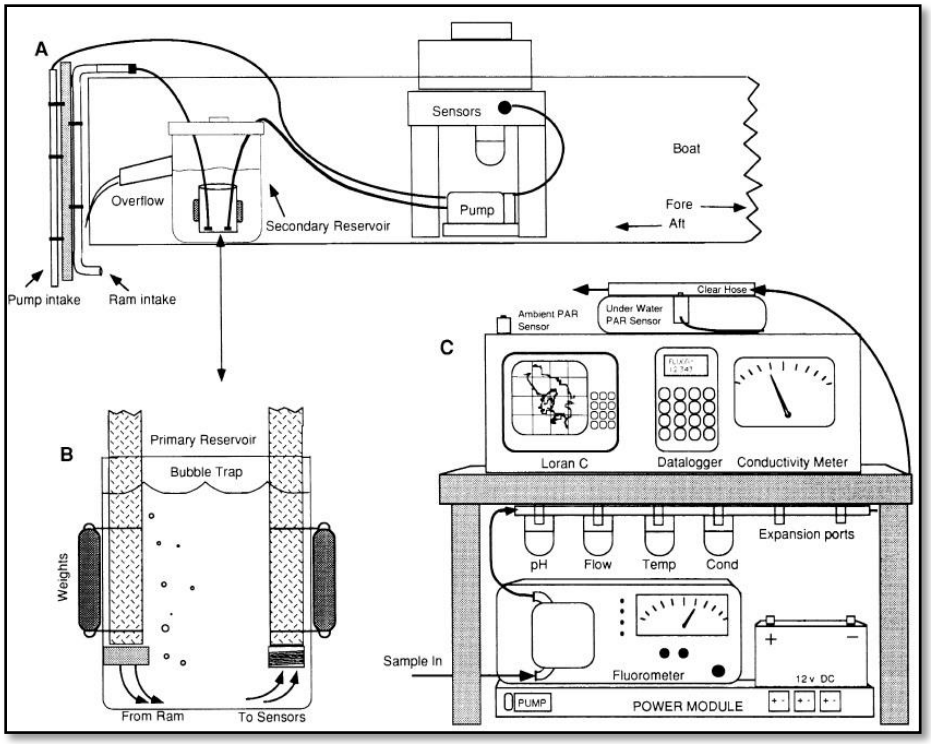

Figure C2 Diagram of the organization and instrumentation of Dataflow system (Madden and Day Jr. 1992)

Regarding the Dataflow's physical housing, it is composed of a vertical tower containing the instrumentation, approximately 60 cm high, 100 cm wide, and 50 cm deep (Madden and Day Jr. 1992). Travel time of a sample through the Dataflow is around 3 seconds, with sampling conducted as quickly as every 0.5 seconds. This system is both effective and accurate even at fast rates of travel ($30 km h^{-1}$). As the sensors are interfaced with a data logger, specialized software has been developed that is capable of communicating/coordinating all the sampling instruments and recording data within a period of milliseconds. All data recorded from the sensors are then geo-referenced through a global positioning device (GPS) and aggregated into a single dataset for analysis/mapping with a specialized software package (Madden and Day Jr. 1992; Hodge et al. 2005; Madden 2013). Discussed below is a case study for Louisiana that highlights

the utility of the Dataflow system as well as a following section discussing its specialized uses.

DATAFLOW: LOUISIANA

The Mississippi River has been the focus of many research teams in evaluating its influence on coastal dynamics (Day et al. 2009). Considering the river's influence, researchers specifically focused on Breton Sound estuary for assessing the influence of river flow through the Caernarvon diversion (Lane et al. 2007). The 25,000 km^2 estuary system consists of low level uplands, wetlands, and open water regions. In efforts to protect such ecosystems, restoration initiatives have included the use of river diversions for salinity regulation and estuary maintenance (Lane et al. 2007). Monitoring changes in temperature, salinity, total suspended sediments (TSS), and chlorophyll *a* were classic water quality parameters to consider within such a system and so were included in the assessment (Lane et al. 2007).

Freshwater pulses have been known to influence both primary and secondary productivity in estuaries by increasing nutrient concentration (Lane et al. 2007). Maintaining salinity gradients is also a critical element to estuary health as it controls stresses experience by plants and animals and therefore habitat quality and biodiversity (Lane et al. 2007). Breton Sound receives regular river pulses through the Caernarvon diversion, typically in seasonal fluxes (Day et al. 2009). Research has been largely focused on water quality parameters discussed above as well as the net movement and export of freshwater and sediment with normal diversions over 1-2 months and 2 week high-water pulses. Situated at mile 81.5 on the Mississippi River, the Caernarvon diversion can pass up to 225 m^3s^{-1} of water, but as it is most often gravity-fed, river water

is only diverted when the stage height has reached 1.2 meters above sea level (Day et al. 2009).

From 1999-2004 it was estimated that discharge at Caernarvon varied from 0-213 m^3s^{-1} (Day et al. 2009). During this time, additional parameters needed for a focused assessment included nitrate and nitrite (NOx), ammonia and ammonium (NHx), dissolved inorganic nitrate (DIN) total phosphorus (TP), and dissolved silica (DSi) (Day et al. 2009). From fall 2000 to 2002, the Dataflow system was used to collect this data in Breton Sound. Twenty-seven tracks were established and including 16 calibration stations. The flow-through system collected data every 5 seconds from surface waters as the vessel carrying it traversed the estuary at 50 kmh^{-1}, effectively sampling every 70 meters (Lane et al. 2007). Transects were completed within 4-6 hours and covered 210 km total distance (Lane et al. 2007). Discrete samples were collected to verify/validate data and an acoustic Doppler current profiler was used to determine the water budget. These data were then collectively incorporated into a numerical modeling system, specifically, a finite element modeling grid (Day et al. 2009).

The resulting data indicated that river-derived sediment arrived in the estuary after passing through either the eastern route (Bayou Mandeville, Lake Leary, Bayou Terra aux Boeufs) or the western route (Delacroix Canal, Manvel's Canal, River aux Chene) and carrying only 10-20% of the initial sediment load (Day et al. 2009). This result displays the expected pattern of decreased deposition with increased distance from the source (river). Water temperature was found to display a strong seasonal/spatial pattern, with the coldest temperature at $<12^oC$ in winter and the warmest during the summer at $>30^oC$. In addition, it was determined that while river water entering the system was typically colder than the waters of the estuary, it quickly equilibrated to ambient conditions within a few kilometers. The pattern for salinity in the estuary was

visible with mapping as a constantly fresh upper region following a gradient to between 14 and 30 practical salinity units (PSU) along the western and eastern routes. River diversions could even force out all saline waters for almost a month, following a 2 week lag behind a large release (Day et al. 2009). Figure C3 below provides a map of the sampling area.

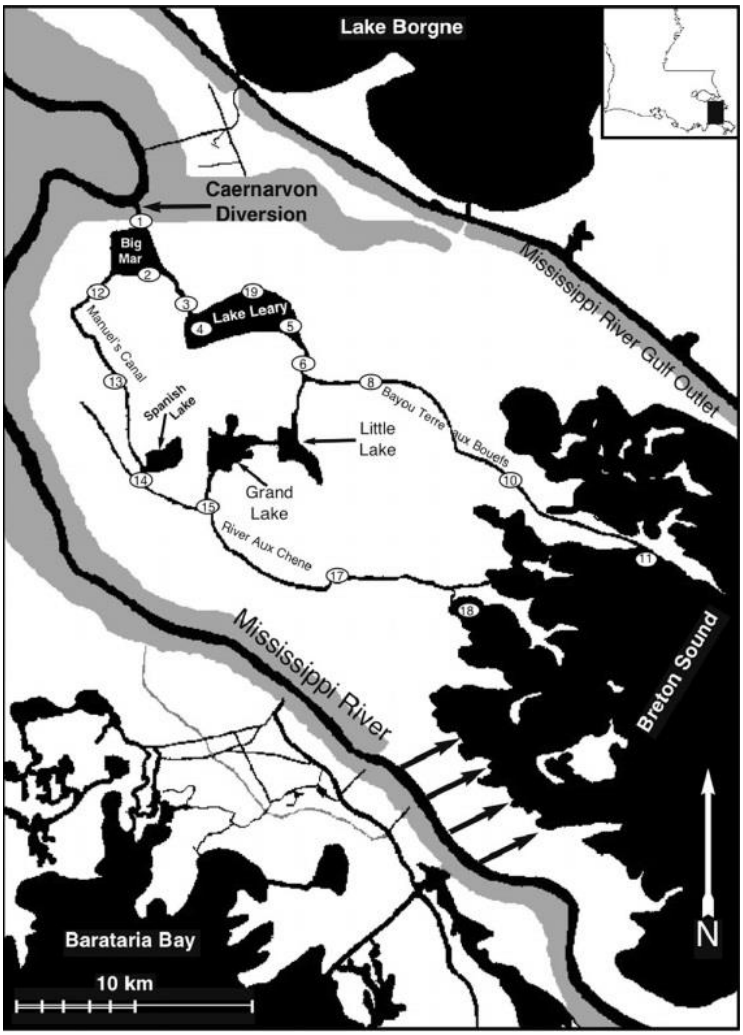

Figure C3 Sampling transect for freshwater diversion to Breton Sound (Lane et al. 2007).

Total suspended solids (TSS) indicated that suspended materials were carried 10-15 km through the estuary at concentrations of 40-252 mgL^{-1} (Day et al. 2009). Within the estuary, however, large fluctuations were found during the winter/spring and certainly

following resuspension due to a frontal passage. Along with the large flush of river water in the late winter/early spring, large fluxes of DIN were found as NOx rates dropped along the eastern and western routes (nutrient sinks). Phosphate followed a similar pattern with higher rates during winter discharge; however, unique zones of high concentration were found toward either the diversion or the marine end of the estuary. For chlorophyll *a*, it was determined that the highest concentrations occurred within the mid estuary in the summer due to low discharge and strong stratification. While chlorophyll *a* concentrations in the upper reach were around 10 μgL^{-1}, the highest values occurred in the center region of the estuary at 20-30 μgL^{-1}. Finally, the concentration diminished from the middle towards the mouth (Day et al. 2009).

The flow-through system was determined to be a critical tool in mapping physio-chemical variables, enhancing the resolution of data, and providing natural resource managers with accurate visualizations of a highly dynamic system (Lane et al. 2007). It was concluded that the diversion could be utilized as an effective tool for coastal restoration and that it served as the most important source of nutrients to the estuary. The diversion was also determined to be the driving force behind the prevention of salt water intrusion or bloom formation via its flushing potential, which can effectively replace all the freshwater in the estuary within 12.6 days (269 million m^3 discharged) (Day et al. 2009). Maps of the water quality parameters are provided below in Figure C4. Similar assessments into the effects of freshwater pulses have also been conducted within the subtropical estuaries of Florida (Buzzelli et al. 2013). In 2012 releases within the Caloosahatchee River Estuary were recorded in a similar manner from January to April by the South Florida Water Management District with similar water quality patterns (Buzzelli et al. 2013).

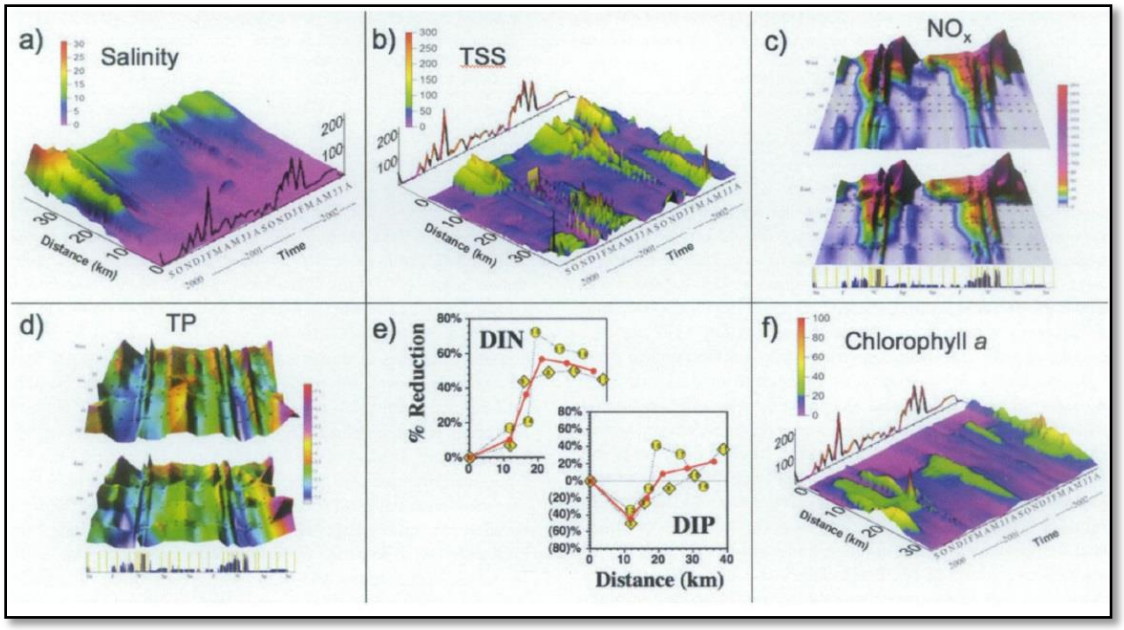

Figure C4 Flow-through transects displaying water quality patterns of Breton Sound (Day et al. 2009).

SPECIALIZED USE

Nutrient Dynamics

In the coastal zone of Louisiana, seasonal loading of nitrogen (N) likely produces phosphorus (P) limitation over the continental shelf, providing a prime area for testing the fast repetition rate fluorescence mapping system (FRRF) (Sylvan et al. 2011). In order to assess nutrient limitation in real time, research was conducted from June to July 2002 covering the Louisiana continental shelf and Mississippi River plume. From Southwest pass west along Terrebonne Bay and the Atchafalaya delta, a system using flow-through underway sampling produced maps of surface distributions of NO_3^-,NO_2^-, NH_4^+, PO_4^{3-}, chlorophyll *a*, and alkaline phosphatase activity (AP) through fluorescence. While traditional sampling indicated that there was widespread P-limitation stemming from the Mississippi River plume westward, the FRRF system demonstrated a more complex picture, with phytoplankton physiology driven by the rapidly changing surface conditions. These alterations would ultimately result in shifting phytoplankton

community structure. In addition, high DIN concentrations and DIN/P ratios provided supporting evidence to P-limitation as being caused by surplus DIN production in combination with low P rather than simply low levels of P. Using the FRRF system enabled researchers to sample on very fine spatial/temporal scales as well as assessing nutrient stress and type (Sylvan et al. 2011).

Tracking Phytoplankton Blooms

The detrimental effects of algal blooms are known to extend beyond the simple visual results and include ecological damage, toxicity, and mortality of aquatic biota (Morse et al. 2011). Of particular importance to natural resource personnel responsible for waters that exhibit these seasonal blooms is determining the water quality factors at play, especially prior to bloom formation. Research of this nature has been undertaken in Chesapeake Bay, specifically for the dinoflagellate *Cochlodinium polykrikoides* Margalef in the James River by the Hampton Roads Sanitation District and the Virginia Institute of Marine Science (Mulholland et al. 2009; Morse et al. 2011). This species regularly blooms from August to September throughout the lower Chesapeake Bay and its tributaries (Mulholland et al. 2009). These blooms are lethal to juvenile fish and even (in 1992) have the capacity to extend out into the Atlantic Ocean (Mulholland et al. 2009).

It was found from 2007 to 2008 that the bloom initiation (3 cells/mL) began in the upper Lafayette River in late July when there was little freshwater input to the system except through rainfall or runoff (Morse et al. 2011). Following a long summer drought, intense rainfall strengthened the already established water column stratification. In addition, the timing coincided with a neap tide, with conditions favoring little tidal energy to disperse either incoming nutrients from overland flow or the algal cells in the surface waters. It was predicted and found that chlorophyll *a* concentrations were at their

highest values in waters with the lowest salinities. Through this research, the timing of the bloom was determined to be controlled by a combination of spring-neap modulation and precipitation events. By understanding the algal bloom dynamics, actions to moderate such blooms or predict such blooms through modeling will be more effective (Morse et al. 2011).

Managing SAV Beds

Along tributaries of the Chesapeake Bay, geographical information systems (GIS) mapping has revealed SAV communities exhibiting large declines, with invasive species taking over many regions (Shields et al. 2012). Since habitat conditions affect the establishment and retention of such beds, numerous studies have focused their attention to determining which water quality parameters are the most important. To help in this effort, researchers utilized the Dataflow system to assess temperature, salinity, chlorophyll *a* concentration, total dissolved N, total dissolved P, and light attenuation along the several tributaries of the lower Chesapeake Bay, Virginia (Shields et al. 2012). Of all the habitat conditions explored, the researchers determined that salinity and TSS displayed the most seasonal and spatial trends, with salinity at its highest in August at the mouth of the estuary and TSS at its highest in May. Chlorophyll *a* varied substantially from 8.7 μgL^{-1} to 49 μgL^{-1}. Having observed the effects of short term salinity stress on freshwater SAV distribution (losses from 1998 to 2002 being attributed to salinities over 7 for 1-2 months), the researchers determined that salinity and light were the most critical factors in determining the potential species distribution and abundance (Shields et al. 2012).

SAV beds are highly valued as coastal habitats, serving as both a refuge and food source for benthic and pelagic species (Gruber et al. 2011). They also aid in nutrient

retention and biogeochemical recycling. Perhaps the most critical attribute of all is their capacity for modifying local hydrodynamics. This feedback loop generated by SAV presence results in improved water quality conditions for the growth and survival of species dependent on such habitats. The goal of researchers in 2007 and 2008 was to describe the fine-scale spatial patterns of water chemistry associated particularly with the canopy-forming species *Stuckenia pectinata* and *Ruppi maritima* in the Choptank and Henga River estuaries (both part of the Maryland portion of Chesapeake Bay). Assessment included the influence of canopy height, shoot density, or size (Gruber et al. 2011).

With its compact design, the Dataflow system was loaded onto a small boat and drifted/poled over the beds (Gruber et al. 2011). By not using the motor and having the sampling hose directed ahead of the vessel, researchers made every effort to reduce resuspension of particles. As a result, sampling tracks were highly irregular and at times the intake valve was clogged with plant material. A paddle wheel flow sensor was adapted for the hose to sound an alarm if the flow was reduced to <3L/minute. In addition, event-influenced turbidity due to the influence of shellfish dredging and cow-nose ray feeding were noted and the data removed from the analysis (Gruber et al. 2011). The resulting data gave evidence to the significant influence of large, dense, tall, canopy-forming beds, which had a prominent impact on reducing turbidity as well as controlling temperature, DO, and chlorophyll *a*. This effect produced a quiescent state within the beds significantly different from surrounding areas of water. These results may also serve as guidelines for restoring self-sustaining beds of the species most successful at surviving hydrographic modifications (Gruber et al. 2011).

ISSUES OF BIAS AND PERFORMANCE

While flow-through systems allow researchers on individual vessels to achieve rapid, synoptic surveys at speed and their use on ships of opportunity provide observations of surface water properties along set routes at low cost, there are several important issues to consider with the use of such systems (Rudnick and Klinke 2007). Issues specific to the unit itself include standardized use and operation, calibration, performance criteria, and maintenance (Hart et al. 1993; Hodge et al. 2005; Slade et al. 2010). Issues specific to use in the field include temporal considerations, biofouling, wind/wave energy, and transects that provide coverage adequate to represent the region of focus (Hart et al. 1993). When considering the final step of data use through mapping, complications include accuracy of GPS units, resolution between sampling points, and interpolation assumptions. It is apparent with so many "moving parts" that associated with each is the bias that will collectively affect the resulting data. It is always recommended that the researcher not only take into account such impediments to robust and reliable data, but also supplement the flow-through system with additional technologies that can validate and verify data collected (Hart et al. 1993).

With a system capable of real-time data collection from in-line instrumentation, it is essential that such data be analyzed for accuracy, precision, selectivity, and sensitivity (Hart et al. 1993). All these measures, but accuracy (truthfulness in data to real conditions) and precision (refinement in measurement) in particular, can be influenced by many outside sources. Field sources of error include biofouling, clogging of sampling pipes with vegetation/sediment, and resuspension of sediment/air entrainment through wind/wave energy. Though not discussed in depth, time of sampling is also critical to detailing the true conditions of a region, and researchers must take into account not only large-scale considerations (season/year), but also time of day or night will also likely

present variability in water quality parameters (Hart et al. 1993). In order to improve data reliability, researchers consistently utilize stationary monitoring posts/buoys. Consisting of sampling stations in fixed locations, most have been in operation longer than flow-through systems have been available and can provide valuable data regarding historical conditions. They have also been used in nearly every example discussed previously as a check for flow-through system's accuracy (Peterson et al. 2011).

In considering the flow-through sensors separately from outside influences, other limitations to data collection are apparent. The simplest issue is the analytical detection limits of the equipment itself (Hodge et al. 2005). Figures C5 presented below details detection potential for the YSI 600XL, specifically the lowest and highest possible detectible readings from the sensors, resolution, and accuracy. Figures C6 presented below details detection potential for the Turner Designs C6 sensors, specifically the lowest and highest possible detectible readings from the sensors and minimum detectible level. Should conditions exist outside these ranges, the sensors will be unable to detect them. When sensors drift, optical or electrical systems will significantly vary within these limits (Slade et al. 2010). Drift, however, can often be managed through frequent calibration. Offsets in calibration, which increase variability in data, are often already calculated by the manufacturer (Slade et al. 2010).

YSI 600XL & 600XLM Sensor Specifications			
	Range	Resolution	Accuracy
Dissolved Oxygen % Saturation ET 6562 Rapid Pulse™ Sensor*	0 to 500%	0.1%	0 to 200%: ±2% of reading or 2% air saturation, whichever is greater; 200 to 500%: ±6% of reading
Dissolved Oxygen mg/L ET 6562 Rapid Pulse™ Sensor*	0 to 50 mg/L	0.01 mg/L	0 to 20 mg/L: ± 0.2 mg/L or 2% of reading, whichever is greater; 20 to 50 mg/L: ±6% of reading
Conductivity* ET 6560 Sensor*	0 to 100 mS/cm	0.001 to 0.1 mS/cm (range dependent)	±0.5% of reading + 0.001 mS/cm
Salinity	0 to 70 ppt	0.01 ppt	±1% of reading or 0.1 ppt, whichever is greater
Temperature ET 6560 Sensor*	-5 to +50°C	0.01°C	±0.15°C
pH ET 6561 Sensor*	0 to 14 units	0.01 unit	±0.2 unit

Figure C5 Detection limitations for YSI 600XL (YSI 2007)

Application	MDL	Dynamic Range
CDOM/FDOM	0.15 ppb** 0.5 ppb***	0-1250 ppb** 0-5000 ppb***
Chl *in vivo* (Blue Excitation)	0.025 µg/L	0-500 µg/L
Chl *in vivo* (Red Excitation)	0.5 µg/L	>500 µg/L
Fluorescein Dye	0.01 ppb	0-500 ppb
Oil - Crude	0.2 ppb***	0-2700 ppb ***
Oil - Fine	10 ppb* 10 ppm****	>10,000 ppb * >100 ppm****
Optical Brighteners for Wastewater Monitoring	0.6 ppb ***	0-15,000 ppb ***
Phycocyanin (Freshwater Cyanobacteria)	2 ppb^{PC}	0-40,000 ppb^{PC}
Phycoerythrin (Marine Cyanobacteria)	0.15 ppb^{PE}	0-750 ppb^{PE}
Rhodamine Dye	0.01 ppb	0-1000 ppb
Tryptophan for Wastewater Monitoring	3 ppb	>20,000 ppb
Turbidity	0.05 NTU	0-3000 NTU

Figure C6 Detection limitations for Cyclops-7 Submersible sensors of the C6 unit, including minimum detection level (MDL) (Turner Designs 2015)

One variable that can present widely variable readings both due to complications within the sensory array and influences in the natural environment is chlorophyll *a*, and therefore is worthy of a much closer examination. Chlorophyll *a* is a photosynthetic pigment found in both eukaryotic (algae) and prokaryotic (cyanobacteria) organisms and is therefore often used as a proxy for their concentrations (Gregor and Marsalek 2004).

Standard laboratory methods use discrete filtered (100-150 mL) samples with chlorophyll *a* extracted with ethanol and finally concentration determination by spectrophotometry. Flow-through systems, on the other hand, enable rapid readings of the pigment through fluorescence. Chlorophyll *a* can be highly variable, however, as it is largely dependent on the plankton's physiological condition, which in turn is subject to environmental factors of nutrient availability, history of light exposure, and presence of pollutants (Althuis et al. 1994). In addition, pigment type and concentration varies among species (Althuis et al. 1994). As an example, the excitation band of light found for eukaryotic algae is 440 nanometers (nm) and emission at 680 nm. The excitation band for phycocyanin (cyanobacteria) is 620 nm and emission at 645 nm (Gregor and Marsalek 2004).

Solar irradiance serves as both a source of energy for the plankton and a source of damage to the cells if too high, altering chlorophyll *a* readings substantially (University of Maryland 2000). Typically, a basic unit of solar energy is the 15- gram-calorie, a term used to describe the amount of heat needed in order to raise 1 g of water 1^{o}C (Halverston and Smith 1979). Applying this value to a unit of area, the measurement will become the Langley (ly), or 1g cal/cm2 (Halverston and Smith 1979). Thresholds of inhibition have been determined for some species as between 0.1 and 0.2 ly/mm (University of Maryland 2000). With respect to chlorophyll *a*, plankton fluorescence was found to be reciprocally related to irradiance, with maximum numbers at night and minimum at midday (Kiefer 1973). Adjustments using field-sourced chlorophyll *a* discrete samples often help to alleviate this variability and calibrate the instrumentation for use in a specific hydrographic region (University of Maryland 2000).

As a last step to water quality research, each system utilizing a flow-through system has an accompanying software/technology for geo-referencing sample points

(Hodge et al. 2005). While GPS units provide this critical link for managers seeking to map out and assess patterns across regions, each unit varies in data output. The frequency/rate at which a unit can determine and output coordinates can be dependent on the rate the GPS receives satellite data (Hodge et al. 2005). In addition, the number of available satellites for triangulating position may change and thus affect accuracy and speed of coordinate retrieval. Once data is collected and placed into a spatial framework via software (ArcGIS, Surfer), interpolation between data points is necessary to complete the map. Interpolation is a technique that converts point data into region data and relies heavily on the influence of surrounding points to fill in the gaps (Zambrano et al. 2009). Bias inherent to mapping is the assumption that the image displays the true nature of the water body and thus needs to be recognized as a 'snapshot' of surface water conditions according to the sampling equipment used, the specific time of sampling, and the software used to fill in areas lacking sampling points (University of Maryland 2000). Figure C7 below details the results of these mapping techniques.

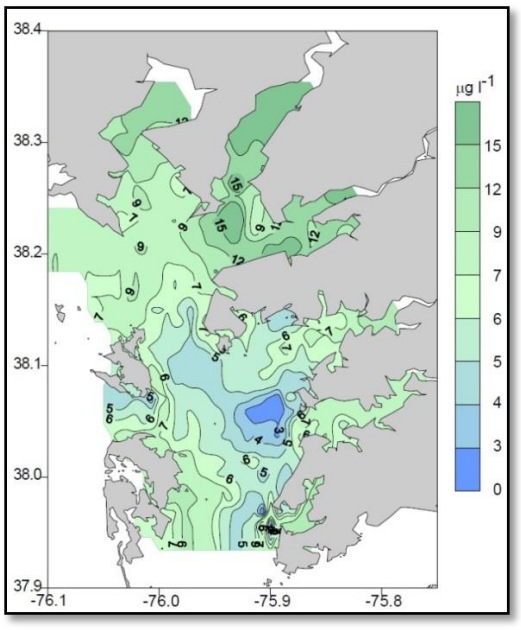

Figure C7 Spatial interpolation of chlorophyll *a* (University of Maryland 2000).

CONCLUSION

Flow-through systems have demonstrated incredible flexibility in meeting research initiatives. Being compact, the system allows for easy transportation and rapid data collection while its modular design provides researchers the capability to select instrumentation specific to the region/biogeochemical parameter of interest. Such systems have been used across the globe, from small tributaries to expanses as large as the North Sea. Advanced performance criteria for have already been proposed as an industry-wide standard in the UK, including "easy care instrumentation, on-site maintenance, modular construction, internal diagnostics, stay-clean properties, and hardware/software flexibility (Hart et al. 1993). " Finally, data collection through this method can be complemented in a manner that effectively manages bias. It is abundantly clear that in combining the expertise of researchers (set research/management initiatives, sampling tracks, maintenance, calibration schedules), the stability of fixed sampling stations (historical data collection and validation), the flexibility of the flow-through system (modular capacity and compact design) and the GIS positioning that bias with any one component will be moderated effectively by another and provide high quality data maps to natural resource managers.

LITERATURE CITED

Althuis, I.J.A., W.W.C. Gieskes, L. Villerius, and F. Colijn. 1994. Interpretation of fluorometer chlorophyll registrations with algal pigment analysis along a ferry transect in the southern North Sea. Netherlands Journal of Sea Research 33:37-46.

Buzzelli, C., B. Boutin, M. Ashton, B. Welch, P. Gorman, W. Yongshan, and P. Doering. 2013. Fine-scale detection of estuarine water quality with managed freshwater releases. Estuaries and Coasts 37:1134-1144.

Charef, A., A. Ghauch, P. Baussand, and M. Martin-Bouyer. 2000. Water quality monitoring using a smart sensing system. Measurement 28:219-224.

Day, J.W., J.E. Cable, J.H. Cowan, Jr., R. Delaune, K. de Mutsert, B. Fry, H. Mashriqui, D. Justic, P. Kemp, R.R. Lane, J. Rick, S. Rick, L.P. Rozas, G. Snedden, E. Swenson, R.R. Twilley, and B. Wissel. 2009. The impacts of pulsed reintroduction of river water on a Mississippi delta coastal plan. Journal of Coastal Research 54:225-243.

Gagnon, B., G. Marcoux, R. Leduc, M.F. Pouet, and O. Thomas. 2007. Emerging tools and sustainability of water quality monitoring. Trends in Analytical Chemistry 26:308-314.

Gregor, J., and B. Marsalek. 2004. Freshwater phytoplankton quantification by chlorophyll *a*: A comparative study of *in vitro, in vivo,* and *in situ* methods. Water Research 38: 517-522.

Gruber, R.K., D.C. Hinkle, and W.M. Kemp. 2011. Spatial patterns in water quality associated with submersed plant beds. Estuaries and Coasts 34:961-972.

Halverston, H.G. and J.L Smith. 1979. Solar radiation as a forest management tool: a primer of principles and application. Gen. Tech. Rep. PSW-33. Pacific Southwest Forest and Range Exp. Stn. Forest Serv. US Dep. Agriculture, Berkeley, CA.

Hart, B.T., I.D McKelvie, and R.L. Benson. 1993. Real time instrumentation for monitoring water quality: An Australian perspective. Trends in Analytical Chemistry 12:403-412.

Hodge, J., B. Longstaff, A. Steven, P. Thornton, P. Ellis, and I. McKelvie. 2005. Rapid underway profiling of water quality in Queensland estuaries. Marine Pollution Bulletin 51:113-118.

Kiefer, D.A. 1973. Fluorescence properties of natural phytoplankton populations. Marine Biology 22:263-269.

Lane, R.R., J.W. Day Jr., B.D. Marx, E. Reyes, E. Hyfield, and J.N. Day. 2007. The effects of riverine discharge on temperature, salinity, suspended sediment and chlorophyll *a* in a delta estuary. Estuarine, Coastal and Shelf Science 74:145-154.

Madden, CJ and J.W. Day Jr. 1992. An instrument system for high speed mapping of chlorophyll *a* and physiochemical variables in surface waters. Estuaries 15:421-427.

Madden, C. 2013. Personal communication. South Florida Water Management District. West Palm Beach, Florida, cmadden@sfwmd.gov.

Morse, R.E., J. Shen, J.L Blanco-Garcia, W.S. Hunley, S. Fentress, M. Wiggins, and M.R. Mulholland. 2011. Environmental and physical controls on the formation and transport of blooms of the dinoflagellate *Cochlodinium polykrikoides* Margalef in the lower Chesapeake Bay and its tributaries. Estuaries and Coasts 34:1006-1025.

Mulholland, M.R., R.E. Morse, G.E. Boneillo, P.W Bernhardt, K.C. Filippino, L.A. Procise, J.L. Blanco-Garcia, H.G. Marshall, T.A. Egerton, W.S Hunley, K.A. Moore, D.L. Berry, and C.J. Gobler. 2009. Understanding causes and impacts of the dinoflagellate Cochlodinium polykrikoides blooms in the Chesapeake Bay. Estuaries and Coasts 32: 734-747.

Peterson, W., F. Schroeder, and F.D. Bockelmann. 2011. FerryBox application of continuous water quality observations along transects in the North Sea. Ocean Dynamics 61:1541-1554.

Rudnick, D.L., and J. Klinke. 2007. The underway conductivity-temperature-depth instrument. Journal of Atmospheric and Oceanic Technology 24:1910-1923.

Shields, E.C., K.A. Moore, and D.B. Parrish. 2012. Influences of salinity and light availability on abundance and distribution of tidal freshwater and oligohaline submerged aquatic vegetation. Estuaries and Coasts 35:515-526.

Slade, W.H., E. Boss, G. Dall'Olmo, M.R. Langner, J. Loftin, M.J. Behrenfeld, C. Roesler, and T.K. Westberry. 2010. Underway and moored methods for improving accuracy in measurement of spectral particulate absorption and attenuation. American Meteorological Society 27:1733-1746.

Sylvan, J.B., A. Quigg, S. Tozzi, and J.W. Ammerman JW. 2011. Mapping phytoplankton community physiology on a river impacted continental shelf: Testing a multifaceted approach. Estuaries and Coasts 34:1220-1233.

Turner Designs. 2015. Optical Specification Guide Cyclops-7 Submersible Sensors. Retrieved from ‹http://www.turnerdesigns.com/t2/doc/spec-guides/998-2181.pdf›

University of Maryland Center for Environmental Science. 2000. Chesapeake Bay water quality monitoring program. Maryland Coastal Bay: Ecosystem Health Assessment.

YSI Incorporated. 2007. YSI 600XL and 600XLM Sondes Specification Sheet. Retrieved from ‹https://www.ysi.com/600XLM›

Zambrano, L., V. Contreras, M. Mazari-Hiriart, and A.E. Zarco-Arista. 2009. Spatial heterogeneity of water quality in a highly degraded tropical freshwater ecosystem. Environmental Management. 43:249-263.

APPENDIX D: OVERVIEW OF THE HUMMINBIRD® SYSTEM

INTRODUCTION

The Humminbird® imaging system used to visualize the bottom types of Lake Pontchartrain operates using sonar. While general SONAR (Sound and Navigation Ranging) systems were developed in the early 1900s's, side scanning capabilities were not developed until 1960 (Kaesar and Litts 2013). In 2005 Humminbird® produced a recreational fish-finding system capable of side-scan imaging, producing two dimensional images of the benthic environment (Kaesar and Litts 2013). The system accomplishes this through a series of steps. First, a transducer converts electrical energy into sound energy through the expansion and contraction of internal piezo electric disks (Humminbird 2012). Then these vibrations produce a beam (cone-shaped) of sound waves which travel through the water (Humminbird 2012). These precision soundwaves, or "pings," collide with the bottom of the waterbody and reflect off features. Finally, the returning sonar energy is translated back into electrical energy, and produces a thin cross-sectional image of the bottom based on travel time (distance) and strength (amplitude) of the return signal (Humminbird 2012). As the vessel to which the Humminbird® is attached progresses along each transect, consecutive strips of shaded pixels produce an image of the benthic environment (Humminbird 2012). The process of producing these images, however, is much more detailed and highly dependent on both the sonar system's characteristics and the aquatic environment in which it is operated.

FUNTIONING OF SONAR

Sonar generates sound waves, which are in fact transient pressure fluctuations in the water acting within the ambient hydrostatic pressure (Clarke 2010). A wave propagates through the medium as regions of compression, seen as the oscillation of the particles. This movement is parallel to the wave's direction (Clarke 2010). The frequency of a sound signal defines the number of sound waves per cycle, with higher frequencies producing better resolution (ability to discern two adjacent features) but limited depth performance and lower frequencies offering lower resolution but greater depth potential (Humminbird 2012). Frequencies of 455 kHz and 800 kHz are available with the Humminbird® system for side-scan imaging. To balance high quality imaging (target separation is 2.5 inches along-track) with depth range (150ft), 455 kHz was the chosen frequency for use in the lake (Humminbird 2012). The power, or amount of energy produced by the transducer, also improves the capability of the system to discern targets at distance, overcome "noise" in the environment, and reach greater depths (Humminbird 2012). Peak-to-peak power, or the power put out at the highest points for this system is 4,000 Watts while Root Mean Square, or the power put out over the entire transmit cycle, is 500 Watts (Humminbird 2012). The measurement for sound intensity (a ratio of ambient pressure with that generated by the transducer or reflected back) is the decibel (dB). Operating at 455 kHz, this system operates at -10db (Humminbird 2012). Figure D1 below depicts how the system functions below the vessel, including coverage.

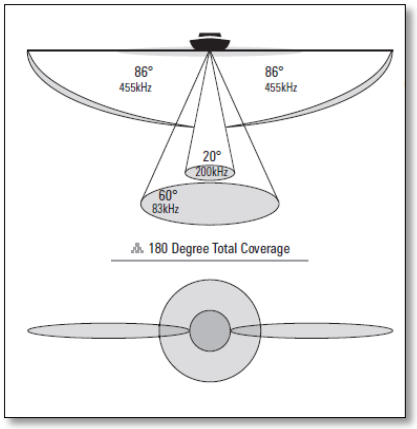

Figure D1 Humminbird® 1198c sonar system coverage (Humminbird 2012).

Once sound is produced, its movement through water is influenced by a myriad of factors. Surface waves which lift the transducer out of the water produce clear errors, including black lines across the resulting imagery and false undulation patterns in the bottom contouring (Humminbird 2012). Scattering, or deviation for the sound energy from its trajectory, below the surface due to water column turbulence, debris, air bubbles, or salinity/density fluctuations can also increase error, while attenuation can also occur as the acoustic wave expands in a spherical manner, decreasing in intensity (amplitude^2) with depth (Humminbird 2012; Kim 2012). For these reasons, side-scan mapping was attempted under calm water conditions and a boat speed appropriate to reduce turbulence produced by the propeller (Humminbird 2012). A rule-of-thumb used by field researchers to determine an appropriate depth for imaging purposes is 10-20% of the range used (Kaesar and Litts 2013). For this research, the range chosen was 75ft (22.86m), producing optimal depths between 2.28 and 4.57m. While some nearshore regions are very shallow (0.5) this general range for the lake is appropriate.

The water characteristics considered to have the most influence over the speed of sound are salinity, temperature, and pressure (depth). Models predicting sound speed have been generated encompassing these overarching influences. In general, increasing

temperature, salinity, and pressure increases the speed of sound through water (Rouse 2013; University of Rhode Island 2015; Tucholski 2015). When stratification of the water column is present, the speed of sound through the layers illustrates the complex relationship between these factors and sound speed (Rouse 2013). Of special note under these conditions, is the region where the rapid change in temperature (thermocline) produces a sharp decline in sound speed despite increasing water pressure (Rouse 2013). Provided below is an equation used to determine the approximate speed of sound through water (m/s represented as "c") as a simple assessment of these relationships. Figure D2 and Figure D3 detail how these chemical and physical features of the aquatic environment affect sound speed in the water column are also provided (Tucholski 2015).

$$c(t,z,S) = 1449.2 + 4.6t - 5.5x10^{-2}t^2 + 2.9x10^{-4}t^3 + (1.34 - 10^{-2}t)(S-35) + 1.6x10^{-2}z$$

with the following limits:

$0 \le t \le 35°$ C

$0 \le S \le 45$ p.s.u.

$0 \le z \le 1000$ meters

Figure D2 Speed of sound in water in relation to salinity, temperature, and depth (Tucholski 2015).

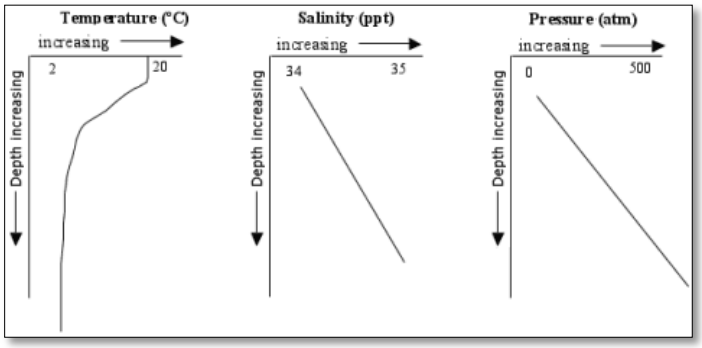

Figure D3 The influence of salinity, temperature, and depth on the speed of sound (Rouse 2013, University of Rhode Island 2015).

With side-scanning sonar, sound waves are directed at right angles from the boat's path, generating thin coverage front to back, but very wide from left to right (Humminbird 2012). As the sound wave reaches the bottom it can be deflected. The angle of incidence, or grazing angle, can produce a weak signal as a result of the bottom orientation sloping away from the transducer rather than a change in hardness (Humminbird 2012; Kaesar and Litts 2013). Darkened pixel tone in this instance signifies a change in elevation (darker for deeper) (Humminbird 2012; Kaesar and Litts 2013). In general, however, varying shades of gray (grayscale) represent the range of densities for bottom types. Dense bottom types (rock or compacted sediment) strongly reflect the sonar signals, producing lighter tones while weaker signals and darker tones are returned by soft-bottom types (mud, sand, vegetation) (Humminbird 2012; Kaesar and Litts 2013). Objects standing off the bottom may even produce a sonar shadow, resulting from a lack of reflected sonar behind the object and providing an indication of height (longer shadow = taller object) (Humminbird 2012; Kaesar and Litts 2013). In addition, some portion of the sonar signal may also be absorbed by the bottom of the waterbody. All bottom types are to some extent absorptive and typically occur according to the following equation: a = kfn. "A" represents the absorption coefficient (decibels) with "f" as the frequency of the sound wave, "n" as a variable shared by sand/silt/clay at a value of 1.12, and "k" a variable dependent upon porosity (open space in sediment) (Kim 2012). It should be noted that taking into account the bottom features encountered and the frequencies available, sonar speed traveling from the transducer to the bottom and back is very fast for the Humminbird® system. The number of times per second a transducer can send and receive sonar signals is referred to as the sonar update rate (Humminbird 2012). In shallow waters (<10ft), this rate can peak at 60 times per second,

but more generally, the cycle can be completed in less than 0.25 seconds (Humminbird 2012).

SONAR EQUATION

Considering all the details regarding the use of sonar for bottom typing is the sonar equation: SN = SL -2TL – NL + BS + DI (Clarke 2010). "SN" represents the signal to noise ratio (decibels), wherein the returning sonar sound waves must be stronger than the background noise level (Clarke 2010). "SL" represents the source sound level (dB) typically noted by the manufacturer, while "TL" represents the transmission losses. These losses occur due to spherical spreading of the sound signal and its return signal, absorption, and scattering (Clarke 2010). "NL" represents the noise level of the background environment encompassing the noise density at the center of the cone and bandwidth. In general, a narrower bandwidth is preferred to reduce noise energy. "BS" represents background scatter strength due to sediment type, grazing angle, pulse length, and beam width (Clarke 2010). In general backscatter strength weakens with increasing angle of incidence (weaker performance with distance). Finally, "DI" stands for directivity index, or the intensity of the beam held in one direction by the sonar system as compared to the intensity of spherically shaped output (Clarke 2010). This final equation brings together all the main components discussed previously in understanding the use of a Humminbird system, and other similar SONAR systems operated for the purposes of mapping bottom habitat types and thus incorporating important features into an ecosystem-based management approach.

LITERATURE CITED

Clarke J.E.H. 2010. Submarine Acoustic Imaging Methods: GGE 3353 Imaging and Mapping II. University of New Brunswick. Retrieved from ‹http://www.omg.unb.ca/GGE/SE_3353.html›

Humminbird. 2012. Operations Manual. Johnson Outdoors Marine Electronics, Inc. Retrieved from: ‹http://www.humminbird.com/Category/Support/Product-Manuals/›

Kaeser, A.J. and T.L. Litts. 2013. An Illustrated Guide to Low-cost, Side Scan Sonar Habitat Mapping. Continuing Education Workshop. Retrieved from: ‹http://www.fws.gov/panamacity/resources/An%20Illustrated%20Guide%20to%20Low-Cost%20Sonar%20Habitat%20Mapping%20v1.1.pdf›

Kim Y.J. 2012. The Underwater Propagation of Sound and Its Application. Dartmouth Undergraduate Journal of Science Retrieved from: ‹http://dujs.dartmouth.edu/winter-2012/the-underwater-propagation-of-sound-and-its-applications#.VaPvDvlVhBd›

Rouse, L.J. 2013. Speed of Sound: OCS 4170 Physical Oceanography. Louisiana State University.

Tucholski E. 2015. Speed of Sound in the Sea: SP411 Underwater Acoustics and Sonar. United States Naval Academy. Retrieved from: ‹http://www.usna.edu/Users/physics/ejtuchol/documents/SP411/Chapter4.pdf›

University of Rhode Island. 2015. Discovery of Sound in the Sea. Retrieved from: ‹http://www.dosits.org/tutorials/sciencetutorial/speed/›

VITA

Noelle Bramer was born in December of 1984 in Boston, Massachusetts. She was raised alongside a brother and sister in Brewster, Massachusetts and graduated from Nauset Regional High School in 2003. From 2009 to 2011 she attended the University of Vermont where she earned a Bachelor of Science in Environmental Science with a focus on water resources. After graduation, Noelle spent two years working as a professional environmental consultant. For four months she worked aboard research vessels as a part of the science crew responsible in part for completing the Natural Resource Damage Assessment under the National Oceanic and Atmospheric Administration and in response to the BP Deepwater Horizon Spill. After working alongside LSU professors in this endeavor, she joined LSU as Dr. James Cowan Jr.'s graduate student with a Board of Regents Fellowship. At LSU she served two years as the Secretary for the Coast and Environment Graduate Student Organization (CEGO) participating in numerous outreach events including Ocean Commotion and Earth Day Outreach. She is currently a candidate for the degree of Master of Science in the Department of Oceanography and Coastal Sciences.